ERASMUS MUNDUS MSC PROGRAMME

COASTAL AND MARINE ENGINEERING AND MANAGEMENT
COMEM

TIDAL MORPHODYNAMIC MODELLING IN THE DEE ESTUARY, UK

University of Southampton
June 2010

Karunya Ramachandran
22913394

The Erasmus Mundus MSc Coastal and Marine Engineering and Management is an integrated programme organized by five European partner institutions, coordinated by Delft University of Technology (TU Delft).
The joint study programme of 120 ECTS credits (two years full-time) has been obtained at three of the five CoMEM partner institutions:

- Norges Teknisk- Naturvitenskapelige Universitet (NTNU) Trondheim, Norway
- Technische Universiteit (TU) Delft, The Netherlands
- City University London, Great Britain
- Universitat Politècnica de Catalunya (UPC), Barcelona, Spain
- University of Southampton, Southampton, Great Britain

The first year consists of the first and second semesters of 30 ECTS each, spent at NTNU, Trondheim and Delft University of Technology respectively.
The second year allows for specialization in three subjects and during the third semester courses are taken with a focus on advanced topics in the selected area of specialization:

- Engineering
- Management
- Environment

In the fourth and final semester an MSc project and thesis have to be completed.
The two year CoMEM programme leads to three officially recognized MSc diploma certificates. These will be issued by the three universities which have been attended by the student. The transcripts issued with the MSc Diploma Certificate of each university include grades/marks for each subject. A complete overview of subjects and ECTS credits is included in the Diploma Supplement, as received from the CoMEM coordinating university, Delft University of Technology (TU Delft).

Information regarding the CoMEM programme can be obtained from the programme coordinator and director

Prof. Dr. Ir. Marcel J.F. Stive
Delft University of Technology
Faculty of Civil Engineering and geosciences
P.O. Box 5048
2600 GA Delft
The Netherlands

ABSTRACT

Process-based morphological models are widely recognised as a valuable tool for predicting coastal and estuarine morphological developments. However, long-term morphodynamic models are still considered to be in the process of development. Considerable uncertainty is therefore anticipated when these models are being applied in long-term estuarine problems. Hence, evaluation of the performance of such models against observations becomes crucial in establishing their credibility.

The aim of this dissertation is to assess the performance of a morphodynamic model, PISCES, developed by HR Wallingford, quantitatively against the observations by using assessment method such as Brier Skill Score (BSS). The Dee Estuary has been chosen to model, since the availability of comprehensive repeat bathymetric datasets (2003-2006) covering the entire estuary and showing significant morphological changes during that period. Morphological modelling starting from 2003 for a three-year period will allow detailed comparison with the 2006 datasets.

Much effort has been taken to apply various input reduction and morphological acceleration techniques to reduce the simulation time. However, there were serious issues been identified when applying morphological factor in the model. Also, the Dee Estuary consists of complex bathymetry with the huge intertidal area making the system challenging one to model. Due to various uncertainties and failure of the model, modelling was only being carried out partially. The results are therefore a measure of whether the model performs in right direction in achieving the observed morphology.

Overall model performance was poor, although quantitatively reasonable agreement was obtained in deeper and some of the shallower regions. In addition, several modelling scenarios were performed and results were compared in order to assess the model performance for the morphological tide, and different morphological factors and morphological time steps. The overall morphological patterns were unchanged, but they varied in magnitudes.

This study concludes that, the present morphodynamic model consists of several uncertainties and cannot reproduce the observed morphological behaviour, thus further research is required to remove the inconsistencies and improve the model performance.

ACKNOWLEDGEMENTS

This thesis is the outcome of my MSc placement that I have had at HR Wallingford.

I would like to express my heartfelt appreciation and sincere gratitude to Tim Chesher (Group Manager, Coasts and Estuaries) for offering me a placement opportunity at HR Wallingford to carry out my Master's Dissertation, and also for giving me invaluable suggestions and supporting me throughout my placement.

I would like to gratefully and sincerely thank to my school supervisor, Professor Robert Nicholls (University of Southampton) for arranging my MSc placement with HR Wallingford, and also giving me valuable advice and suggestions during the course of this study.

I owe to my deepest gratitude to HR Wallingford supervisors, Dr. Jort Wilkens and Dr. Michiel Knaapen, whom without their continuous assistance and invaluable advice, this study would not have been possible. And I would like to gratefully and sincerely appreciate them for their patience and giving me all the necessary supports throughout my study period.

I am also very grateful to Dr. Tom Benson and Stephen Wells for assisting me in graphical processing of the model outputs, Dr.Yohama Gunawardena for helping with the sediment transport model (SANDFLOW), Dr. Michael Turnbull for the assistance in retrieving data and Jennifer Semmence for introducing me mesh processor (JANET).

And I would like to express my sincere thank all the staff at HR Wallingford for being friendly and supporting me in various ways, and making my stay very pleasant and enjoyable during my placement.

Last but not least, I am thankful to my family and friends who have shown their care and patience towards me during the course of this study.

Table of Contents

LIST OF FIGURES

LIST OF TABLES

LIST OF ABBREVIATIONS

ASMITA	Aggregated Scale Morphological Interaction between a Tidal basin and the Adjacent coast
BSS	Brier Skill Score
CD	Chart Datum
HAT	Highest Astronomical Tide
HW	High Water
LAT	Lowest Astronomical Tide
LiDAR	Light Detection and Ranging
LW	Low Water
MF	Morphological factor
MHWN	Mean High Water Neap
MHWS	Mean High Water Spring
MLWN	Mean Low Water Neap
MLWS	Mean Low Water Spring
MSC	Mean Square Error
OD	Ordinary Datum
RAM	Rapid Assessment Methodology
RMS	Root Mean Square
SCI	Site of Community Importance
SPA	Special Protection Area
SSSI	Site of Special Scientific Interest

LIST OF SYMBOLS

α	Advection factor to recover the true sediment flux from the product of depth-averaged quantities
(s,n)	Natural co-ordinates (parallel with and normal to mean flow) (m)
(x,y)	Cartesian co-ordinates in horizontal plane (m)
C_x	Bed celerity in x direction
C_y	Bed celerity in y direction
q_x	Sediment transport rate in the x-direction (m3/m/s)
q_y	Sediment transport rate in the y-direction (m3/m/s)
ΔT_m	Morphodynamic time step
Δt_{hyd}	Hydrodynamic time step
Δt_{mor}	Morphological time step
a	Off-shore M_2 tidal amplitude
B	A set of J baseline predictions (b_1, b_2, ...b_J)
c_s	depth-averaged concentration when the flow is saturated with sediment (kg/m3)
d	Water depth (m)
D_n	Lateral (turbulent) diffusivity (m^2/s)
D_s	Longitudinal (shear flow) dispersion coefficient (m^2/s)
H	Average depth of estuary below means sea-level
N	Filtering coefficient
h	Bed-level relative to a fixed datum
S	Erosion from or deposition on the bed ($kg/m^2/s$)
$ß_s$	Profile factor to compensate for integrating out the vertical profile of suspended sediment
t	Time (sec)
u	Depth-averaged horizontal component of velocity
v	Depth-averaged vertical component of velocity (m/s)
X	A set of J observations (x_1, x_2, ...x_J)
Y	A set of J predictions (y_1, y_2, ... y_J)
ω_s	Representative settling velocity (m/s)
P	Porosity of the bed
δ	Measurement error

1. INTRODUCTION

1.1 Background

Estuaries are areas of interaction between the fresh and saline coastal water that form a highly valuable unique environment. They are tidally driven, but partially sheltered from the full force of ocean waves (Karunarantha and Reeve, 2008). Estuaries often form most dynamic part of the coastal system as they subject to both marine and terrestrial influences (Moore, 2008). Estuaries are important to mankind as places of navigation, recreation and commerce as well as habitats for wildlife. Therefore, understanding and prediction of estuarine morphological behaviour is crucial part of their management in sustainable manner.

Estuarine environments constitute of complex and often non-linear hydrodynamic and morphological processes controlled by various forcing factors such as hydrodynamic conditions and sedimentary environment, sediment supply and underlying geology. The forcing acts at different time and space scales often through complicated interaction (Karunarathna et al., 2008). As a result of this, morphological evolution of estuaries takes place over a range of interacting time and spatial scales (Cowell et al., 2003a). Combination of these varying time scale and non-linear interaction has made morphological evolution of estuaries a complex phenomenon to predict.

Much of the effort has been taken during the last couple decades in developing coastal area numerical models. The concept behind the costal morphodynamic modeIlling and the state-of-the-art are given by Roelvink (2006). Morphodynamic models are indispensable tools for coastal managers to study and analyze the erosion and accretion problems and assess the morphological changes due to human interference natural factors. Whereas process-based hydrodynamic models are being widely applied and successfully validated against field measurements, sediment-dynamic and morphodynamic models are still considered to be in the process of development (Davies et al., 2002).

Over the recent past years morphological modelling has made significant progress, such models now have shown the capability of accurate prediction (Elias et al., 2006), but not yet on time scales as long as decades and centuries. Evaluating the performance of such models against observations is an essential part of their development process. In the past, this validation often been done by comparing the model prediction with observed behaviour in subjective manner (Sutherland et al., 2004). However, qualitative assessment becomes important for models that need to be used as an engineering tool.

Hence, this study aims to examine the morphological model developed by HR Wallingford in more objective manner. This study therefore involves in intensive morphological modelling and then comparing the model prediction with the measured dataset in quantitative and qualitative manner. Dee estuary has been chosen for the above investigation as it is a data rich environment that gives qualitative input for such detailed process based numerical modelling.

1.2 Problem Description

HR Wallingford has been in progress of developing morphological model for the coastal and river applications since last couple of decades. Recent further research at HR Wallingford into long-term morphodynamic modelling has led to the development of bed updating techniques which allow simulations of the order of months and years. This state-of-the-art of the morphological model is recognized as a key tool for understanding and predicting morphological developments of coastal and estuarine environment. However, evaluating the performance of such numerical model against comprehensive dataset becomes crucial in establishing its credibility and further development.

1.3 Aim and Objectives

Aim:

The aim of this study is to evaluate the performance of a morphological model, PISCES (Chesher et al., 1993), developed by HR Wallingford which could be applied in studying of long-term estuaries morphological problems.

Objectives:

- To carry out morphodynamic modelling for the period of three years and perform detailed quantitative and qualitative comparison between the model predictions against the measured dataset at 2006

- To assess the model performance for the morphological/ representative tide against the real tide (spring-neap tide)
- To assess the model performance for different morphological acceleration factor and different morphological time steps

1.4 Limitations

In order to make the above objectives achievable within the given time frame for this study, following limitations were set at the initial stage.

- The sediment transport model used in this study only simulates the non-cohesive sands which mainly move in suspension. Thus, movement of cohesive sediment transport is not considered.
- Tide is considered to be as the main forcing factor for the estuarine morphological development. The effect of waves on the sediment transport processes were investigated in the previous study (HR Wallingford, 2005), and it was concluded that wave effects have only minor effect on the sediment transport pattern, and therefore waves are not included in the modelling process.
- The effect of wind is simply ignored in this modelling study.
- Model does not capture any seasonal effects during the study period since the tidal conditions considered in this study are representing an equinoctial tides, which gives the largest spring tidal ranges.

1.5 Structure of report

Chapter 2 provides the background information about the study area Dee Estuary including brief historical development, hydrodynamic and morphological characteristics and ecological importance of the site. Chapter 3 intend to provide theoretical background of the estuarine processes which includes hydrodynamics, sediment transport and morphological development, and reviews numerical modelling and techniques applied in long term morphological simulations with the evaluation method of the model results. Numerical models those involved during this study are described in Chapter 4.

Chapter 5 explains the methodology that reviews the data used in this study, bathymetry preparation, boundary conditions, model setup etc. Chapter 6 presents the results obtained from the morphological modelling and detail quantitative comparisons of model results with measured dataset and including scatter plots, bed level changing trends, Brier Skill Score assessment. Chapter 7 derives conclusions regarding the overall model performance based on the model results and analyses that have been presented in Chapter 6 and also provides recommendations for future work.

2. STUDY AREA

2.1 Introduction

The Dee is a funnel-shaped, macrotidal estuary located on the border of north-west England and north Wales, drains into Liverpool Bay in the northern half of the Irish Sea (Figure 2.1). The Dee estuary is known as one of the most active and dynamic estuaries in the UK, with range of physical features such as channels, mud banks and tidal flats. The modern-day estuary has an effective length of 30 km compare to its natural length of 35 km and the maximum width of 8.5 km at the estuary mouth.

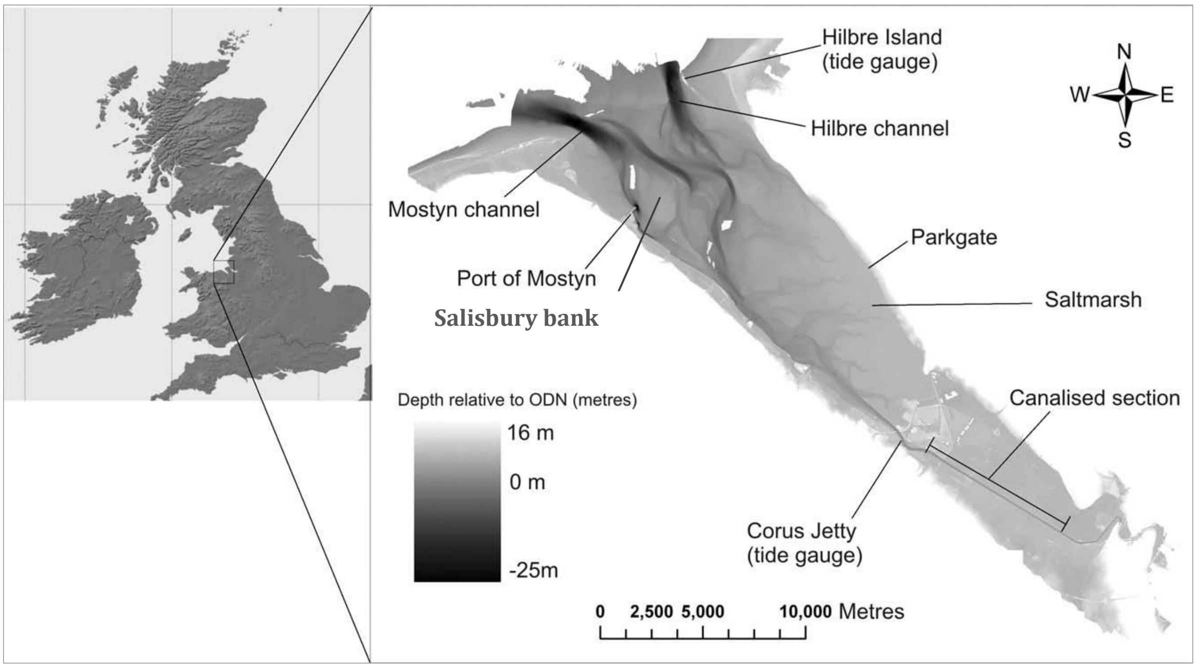

Figure 2.1 The location and setting of the Dee estuary (Moore et al, 2009)

2.2 Brief History

The Dee is a coastal plain estuary formed during the transgression and drowning of valley cut by the Dee River during the sea-level lowstand (some 20,000 years ago). Silting of the Dee Estuary and the associated growth of salt marsh has been taken place progressively during the historical time due to the post-glacial rise of sea-level (Marker, 1967). The natural estuary extended as far inland as Roman city of Chester (2000 BP) giving a length of 35-40 km. Canalization of the river at the head of the estuary during the 18th century and associated land reclamation drastically altered the hydrodynamic regime and reduced the estuary length. Canalization forced the channel to shift towards the western shore which caused heavy siltation and accretion on the eastern shore due to the low current conditions (Moore et al., 2009). The high level of siltation led the estuary becoming shallower and mudbanks and sand banks increased in elevation, huge area became colonized by saltmarshes. This saltmarsh-induced land reclamation further led to a reduction of the effective estuary length.

2.3 Hydrodynamics

The Dee estuary is situated in a macrotidal environment which makes the system very high energy and dynamic system. This estuary is characterized by the presence of waves at its outer margins and strong tidal flows in its channels. The average tidal prism in the Dee is 4×10^8 m^3, representing a volumetric increase of over 80% between mean low water and mean high water, where the annual mean river discharge is only 31 m^3/s making the Dee a strongly tidal dominated estuary (Bolanos and Souza, 2010). This tidal regime results in sediments transported into the estuary on the flood tide only being partially removed on the ebb, thus there is a net accretion of sediment within the estuary.

Tidal flows are responsible for the majority of morphological changes to the sea-bed within the estuary. The tidal limit of the river is at Cheater, 35 km inland from the estuary mouth. The mean spring tidal range at Hilbre Island near the mouth of the estuary is 7.7 m and the neap tide range is 4.1 m. The spring tide diminishes to 4 m at Flint and 2.5 m at Chester (Olds and Davison, 2009).

2.4 Morphology

The Dee Estuary consists of highly diverse and complex morphological features. The main channel bifurcates 12 km seaward from the canalised river at the head of the estuary, resulting in two deep channels extending into Liverpool Bay as illustrated in Figure 2.1. The bed of the estuary comprises of mixture of sediments containing range of non-cohesive and cohesive sediments (Bolanos and Souza, 2010). The underlying solid geology is generally overlain by 20-30 m of subsequently deposited sediments (Olds and Davison, 2009). Rocky outcrops are only found in the estuary around Hilbre Island.

Morphological changes of the Dee Estuary have been studied by HR Wallingford (2007) and Moore et al. (2009) in detail, particularly between 2003 and 2006 following the LiDAR surveying carried out during that period. Following detail sediment volumetric changes of the estuary between 2003 and 2006 by HR Wallingford (2007), bathymetric changes have been identified over much of the estuary. Further, this study has highlighted that the largest sediment fluxes are observed to the area of east Salisbury bank indicating this area was being particularly energetic between the period of 2003 and 2006.

Morphological evolution of the Dee Estuary between 2003 and 2006 has been also studied by Moore et al. (2009) and identified that there is a net sediment import into the estuary. However, it has been suggested that the Dee may be approaching morphological equilibrium and the rate of accretion may therefore decrease in the future.

2.5 Ecology

The Dee Estuary contains extensive area of intertidal sand and mudflats and saltmarshes which are nationally and internationally important area for an abundant population of wildlife. Saltmarshes account for approximately 2,480 hectare of habitat in the Dee Estuary, which is 7% of the UK total for this habitat. The distribution of saltmarshes is increasing as the estuary accretes and new areas of mud and sand flats develop and are colonised. Because of its ecological and nature conservation interest, the Dee Estuary has been designated as a Ramsar Site, Special Protection Area (SPA) and Site of Community Importance (SCI). It is also a Site of Special Scientific Interest (SSSI) under national legislation (Olds and Davison, 2009).

3. LITERATURE REVIEW

3.1 Introduction

The evolution of an estuary is a result of continuous non-linear interaction between water flow and sediment transport and underlying geology (Hibma, 2004). Because of its complex nature and it involves a wide range of time and space scales, prediction of morphodynamic evolution is challenging and still limited. Therefore, it is essential to have an in-depth knowledge of estuarine processes in order to understand and predict its long-term morphological behaviour. Hence, this chapter reviews key estuarine processes, approaches that have been studied in literature for the prediction of long-term morphological evolution, particularly numerical models and also presents methods of validating such models.

3.2 Definition and Classification of Estuaries

Estuary is a term which was derived from the Latin ‘aestus’ meaning tide, refers to a tongue of the sea reaching inland (Woodroffe, 2002). There are several definitions of estuary in literature. However, a definition set by Cameron and Pritchard (1963) is broadly accepted and used to describe an estuary as ‘a semi-enclosed coastal body of water having a free connection with open sea and within which the saline water is measurably diluted with the fresh water derived from land drainage’. An estuary typically has three main sections as illustrated in (Figure 3.1): a lower (or marine) estuary, in free connection with the open sea; a middle estuary, where the mixing of saline and fresh water occur; and upper (or fluvial) estuary, usually dominated by freshwater influences. However, the upper estuary is subjected to daily tidal rise and fall, like the rest of estuary (Brown et. al., 1999). Estuaries with wider mouth and narrow heads have a large tidal range which eventually leads for higher tidal amplitudes in the upstream parts (d’Angremond and Pluim-Van der Velden, 2001).

Estuaries are classified based on different schemes by many scientists. However, here the most common three classification schemes based on geomorphology, vertical structure of salinity and tidal range are described and a recent classification provided by Fairbridge (1980) is presented.

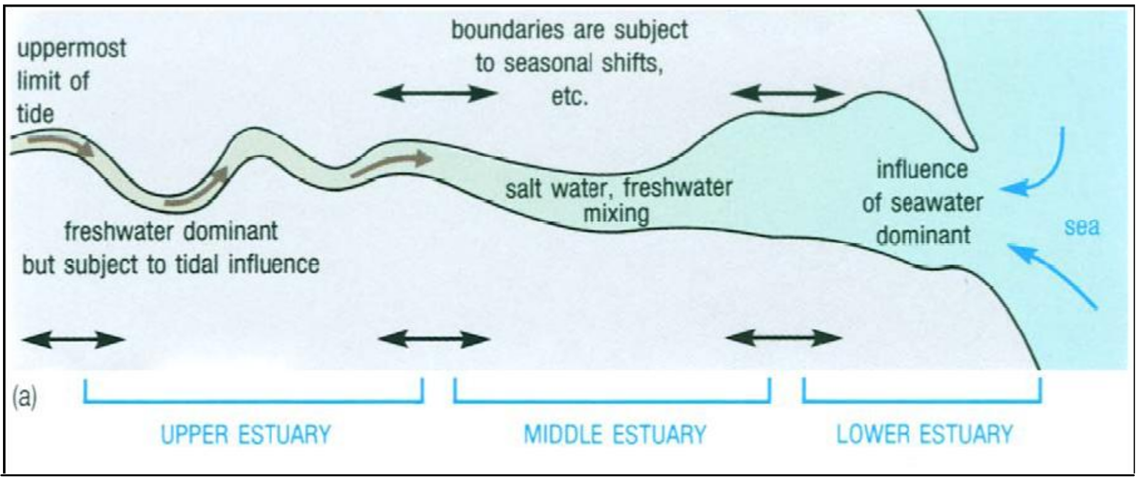

Figure 3.1 A schematic map of a typical estuary (Brown et. al., 1999)

Pritchard (1960) classified the estuaries into four categories (Figure 3.2) from the geomorphologic point of view are briefly elaborated below with examples (Perillo, 1995).

a) **Drowned river valleys:** They were formed by the flooding of river valleys following a rise in sea level over geological time. Generally they have a funnel shape with an exponential increase of the cross-section towards the mouth. These estuaries are shallow and wider, with depths about 10 m and reaching about 20-30m towards the mouth. Most of the world's estuaries correspond to this category; well known examples are Chesapeake Bay and Delaware Bay.

b) **Fjords:** In contrast to drowned river valleys, they are often associated with high latitudes where the glacial activity is intense. They are often located in rocky shores where the sediment supply is relatively low and seasonally variable. Fjords are characterized by an elongated deep channel (several hundreds of meters) with narrow and relatively uniform cross-section. Good examples of fjords can be seen along the Norwegian coast.

c) **Bar-built estuaries:** These estuaries are also referred as coastal lagoons and they occur on river valleys where sedimentation rate high. Because of that they are mostly very shallow with small tidal ranges and river discharges. Littoral processes are dominant in the local environment which accumulates the sediments near the mouth of the estuary and forms bar. Bar-built estuaries are common wherever the coastal zone is characterized by deposition of sediment. Examples of this type of estuaries can be found on sub-tropical region of America.

d) **Tectonic estuaries:** These estuaries are not clearly fall into any of the above three categories. They are formed by earthquake or by fractures of earth's crust and creases that generated faults in regions adjacent to the ocean. A very good example of this type of estuary is San Francisco Bay in the US.

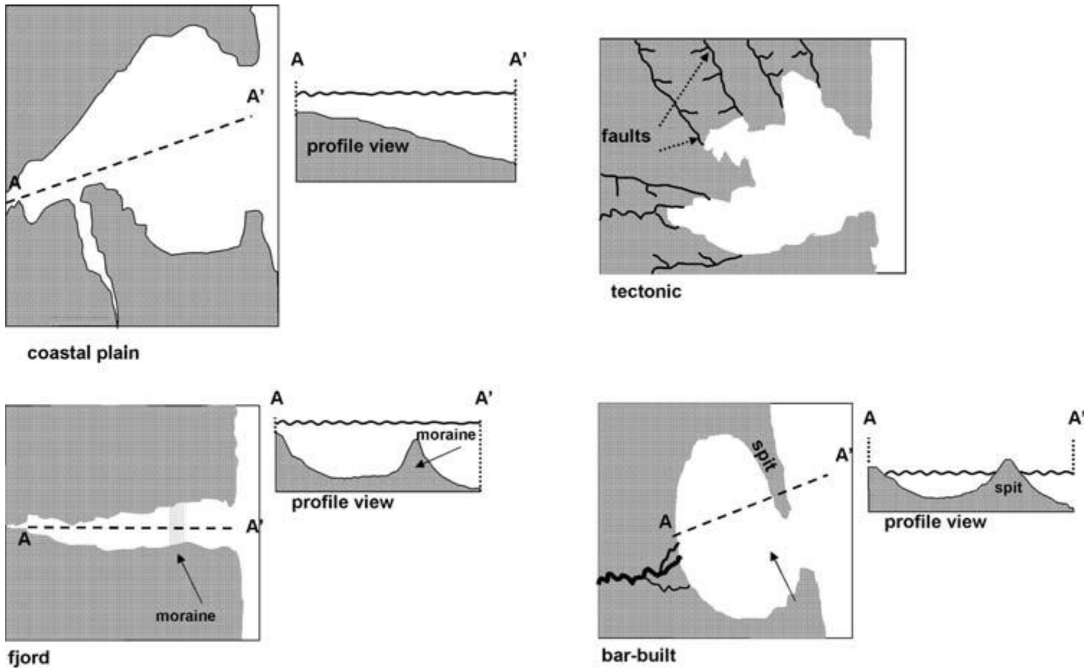

Figure 3.2 Classification of estuaries based on the geomorphology (Valle-Levinson, 2010)

Estuaries also been classified based on vertical structure of salinity as salt wedge, strongly stratifies, weakly stratified or vertically mixed (Figure 3.3) (Cameron and Pritchard, 1963). The mechanism of estuarine circulation is discussed in section 3.3.2.

- Salt wedge estuaries typically occur where the tidal prism is small to mix with the high river discharge; typical example is the Mississippi (USA). These estuaries are strongly stratified during the flood tides, when the saline water intrudes in a wedge shape. During the dry period some of this system loses their salt wedge nature (Valle-Levinson, 2010).
- Strongly stratified conditions occur in estuaries when the river discharge is moderate to large and tidal prism is weak to moderate. These estuaries shows similar stratification with the salt wedge estuaries, however the stratification is strong throughout the tidal cycle.

- Estuaries with larger tidal ranges, where the tidal prism is greater than the river discharge, are classified as vertically mixed. Water in the estuary is moved up and down the estuary by the tidal rise and fall into the estuary (Woodroffe, 2002).
- Weakly stratified or partially mixed estuaries lie between those two extreme cases, where the river discharge is weak to moderate and the tidal prism is moderate to strong. Many of the mesotidal estuaries exhibit this behaviour such as Chesapeake Bay, Delware bay and James River (Valle-Levinson, 2010).

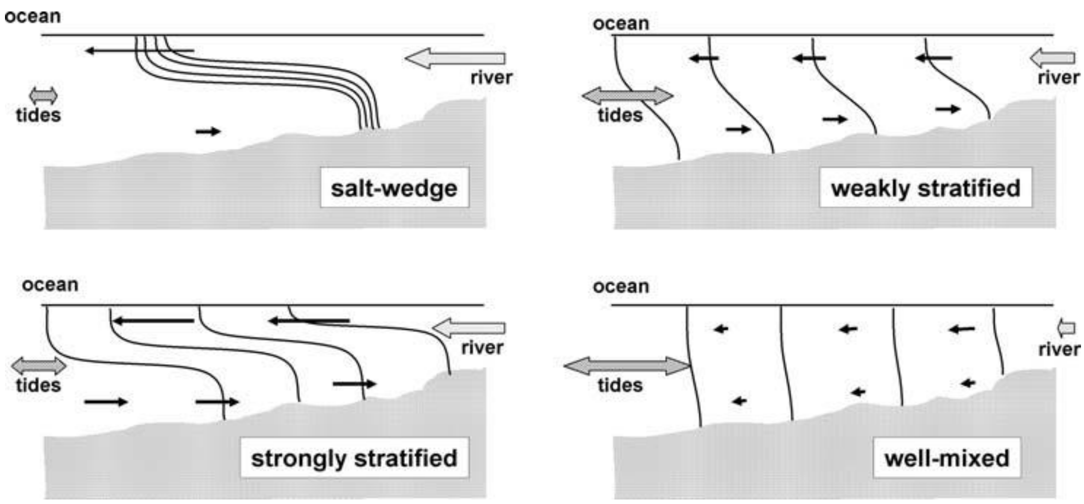

Figure 3.3 Classification of estuaries on the basis of vertical structure of salinity (Valle-Levinson, 2010)

Hayes (1975) classified the estuaries, having coarse-grained sediment, into three main categories based on the relative impact of the tidal range and wave action (Van der Wegan, 2005).

a) **Micro-tidal estuaries:** (tidal range of 2-4 m) are mostly dominated by wave action and storm depositions. The principle forms of deposition are flood deltas, spits, bars, beaches etc. Chesapeake Bay is a best example for micro-tidal estuary.

b) **Meso-tidal estuaries:** (tidal range of 2-4 m) Many estuaries on the west coast of USA fall into this type, where the tidal currents are the dominant. The major forms are tidal deltas, tidal flats and saltmarshes.

c) **Macro-tidal estuaries:** (tidal range > 4 m) are often funnel shaped and with wider mouth having linear sand bodies. Examples are Bay of Fundy (Canada) and Tay (Scotland).

Most recently, Fairbridge (1980) provided the new and more comprehensive physiographic classification scheme for estuaries on the basis of physiographic and hydrographic factors.

i. Fjords (deep U –Shaped valleys in areas which have had ice cover)
ii. Rias (V – shaped river valleys drowned by sea-level rise, and generally with bedrock margins)
iii. Coastal plain estuaries and sedimentary coasts
iv. Delta-front estuaries (delta distributaries)
v. Bar-built estuaries
vi. Blind estuaries (blocked or periodically closed coastal lagoons)
vii. Structural or tectonic estuaries (which includes inlets that owe their origin to a range of tectonic factors)

3.3 Estuarine Processes

Estuarine processes are highly complex and often exhibit non-linear behaviour, which are hard to understand and predict accurately. This section reviews the basics of the key estuarine processes which are mostly relevant to tidal dominated estuaries; thus wave processes are not included in this discussion.

3.3.1 Tidal processes

The main trigger for the hydrodynamic processes in estuaries is the water movement in and out of the estuaries. The water movement is mainly caused by tide, waves, wind and the density gradient between saline and fresh water. Among these hydrodynamic factors, the tidal process is the predominant one in well-mixed, macro-tidal estuaries, which is focussed on this particular study.

The tide generated by the interaction between Sun and Earth is denominated diurnal, and has a period of 24 hrs 50 min. The tide generated by the Moon interacting with the Earth is called semi-diurnal tide and has a period of 12 hrs 25 min. When the tide generating forces from the Sun and Moon are acting in the same direction, in phase, spring tides occur, which gives relatively larger tidal ranges. When the Sun and Moon are out of phase, their interaction with the water mass on Earth does not coincide, generating the neap tides, with small tidal range.

In constricted basins such as estuaries, tidal inlets and coastal lagoons, when the tide floods, water from the ocean penetrates the basin and when it ebbs, water leaves the basin. The volume of water exchanged in this process is called tidal prism and can be estimated, in a simplified way, measuring the area of the basin to the upper limit of the influence of the tide and multiply it by the tidal variation (Carter, 1998).

The astronomical tide is composed of large number of constituents varying from quarter-diurnal, semi-diurnal and fortnightly diurnal whose non-linear interaction results in a complex physical problem (Aubrey and Speer, 1985). Along most of the coastlines, the dominant astronomical constituent is the semi-diurnal lunar tide, M_2. In an estuary with little fresh water input and larger tidal amplitude compared to the channel depth, significant overtides and compound tides develop from the dominant offshore equilibrium constituents.

Tides in estuary can be either reflective or progressive (Woodroffe, 2002). In shorter estuaries (where the length of the estuary << tidal wave length), tides tend to be reflective; whereas they are progressive for the opposite case. According to Friedrich and Aubrey (1988), in frictionless estuary where the tidal amplitude is significantly larger than the water depth, the tide moves as a shallow-water wave. The crest moves faster than the trough, resulting in a shorter flood and longer ebb, and highest velocity currents during the flood. However, tidal propagation in shorter estuaries is complicated further by co-oscillation due to tidal wave reflection from the head.

Astronomical tides which entering an estuary are strongly distorted by nonlinear effects that are induced by bottom friction and other physical processes, causing in asymmetric shallow water tides (Kang and Jun, 2003). The tidal distortion occurs along many of the estuaries, in terms of amplitude, symmetry, and duration of flood and ebb tides (Woodroffe, 2002) due to the varying geometry of the continental shelf. Figure 3.4 shows how the tidal amplitude varies as a result of changes in width of the estuary. An estuary is referred as ‘flood-dominant’ or ‘flood-asymmetric’ when the duration of the falling tide exceeds that of rising tide resulting in a larger peak flood current; whereas the system is referred as ‘ebb-dominant’ or ‘ebb-asymmetric’ when the duration of the falling tide is shorter than that of the rising tide leading to a strong peak ebb current (Walton, 2002). In other words, an estuary can be classified as 'flood-dominant' if the asymmetry in the tide causes a net sediment accumulation, whereas the opposite case is referred as 'ebb dominant' (Robins and Davies, 2010).

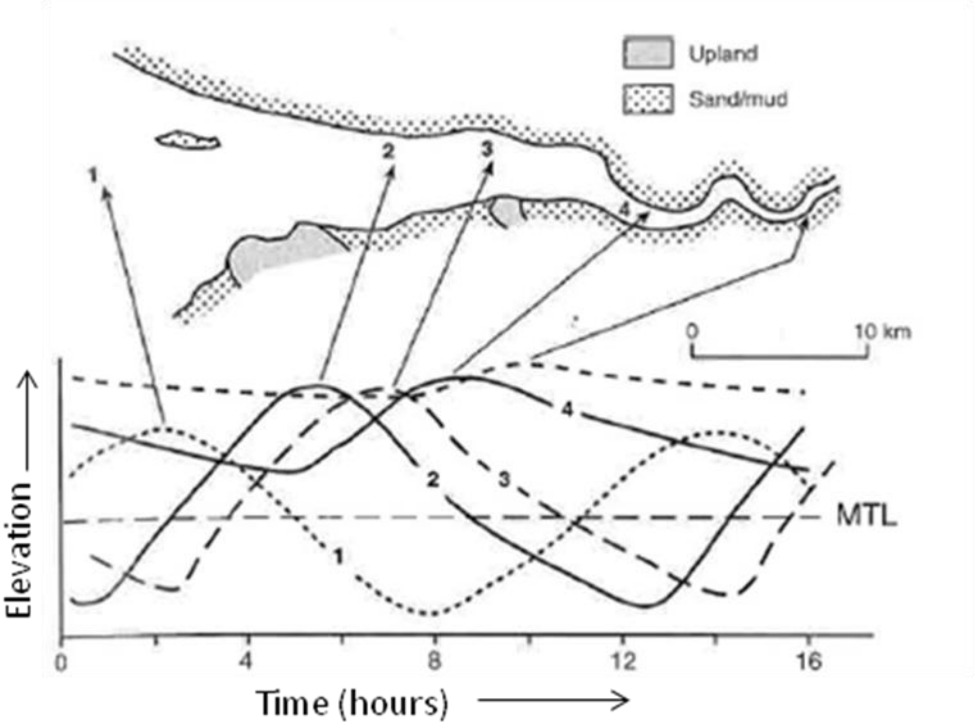

Figure 3.4 Distortion of tidal wave propagating up a schematic estuary (Woodroffe, 2002)

In shorter estuaries, the flood currents are more intense than the ebb currents which lead to lower the ability to flush out the entering sediments effectively. In contrast, an estuary with stronger ebb than flood currents may represent a more stable condition. The magnitude of the velocity asymmetry depends on the non-linearity of the tide (Aubrey and Speer, 1985).

In shallow estuaries, the non-linearity of the frictional influences a greater frictional resistance at low water than at high water, yielding relatively larger flood velocities than ebb velocities (Dronkers J. 1986). Consequently, the time delay between low water at the mouth and at the head of an estuary is greater than the corresponding time delay at high water. This effect ultimately results in a longer ebb tide and shorter flood tide, and highest velocity currents during flood, hence flood dominant (Friedrichs and Aubrey, 1988).

According to Lanzoni and Seminara (1998), weakly dissipative (deep) estuaries tend to be ebb-dominant while strongly dissipative (shallow) estuaries turn out to be flood-dominant. Further, based on Friedrich and Aubrey (1988)'s studies;

- Ebb asymmetry occurs when $a/H < 0.2$
- Flood asymmetry occurs when $a/h > 0.3$

Where, a - off-shore M_2 tidal amplitude, H - average depth of estuary below means sea-level.
However, in reality, some parts of an estuary may experience flood-asymmetry while other parts of the estuary might tend to show ebb-asymmetry (Robins and Davies, 2010).

3.3.2 Estuarine hydrodynamic processes

Estuarine hydrodynamics is generally associated with the interaction of marine processes, particularly tides, with fluvial discharges and water already present at the system. Many of the principles of river hydrology apply to estuaries, although a major difference is that tidal flows in estuaries are bi-directional (Woodroffe, 2002) whereas the river flow is often unidirectional.

The velocity of the tidal current strongly depends on the tidal magnitude and the topography of the bottom. According to Woodroffe (2002), there are two types of flow in estuaries; tidal currents induced by the tidal flow, which mainly contribute to the physical and advective processes, and residual currents which mainly results from density differences resulting from mixing of saline and fresh water. The tidal propagation is described in the section 3.3.2, hence residual currents that results from the density variation is described here.

Seawater has salinity about 3.5% whereas the fresh water has essentially zero salinity. This difference in salinity levels leads to density differences between saline and fresh water. This density different plays a major role in the flow pattern in an estuary. When the tide floods, the heavier seawater enter the estuary near the bottom, and that the lighter river water tends to flow towards the sea near the surface (Figure 3.5). Thus, with the flood and ebb tide, a salt wedge tends to move in and out of the system. This implies that the angle of interface between the fresh water and the salt water also varies with the tide. The estuary is termed as stratified if the angle of interface is almost horizontal, whereas it is referred as well mixed if the angle of interface is approaching vertical (d’Angremond and Pluim-Van der Velden, 2001).

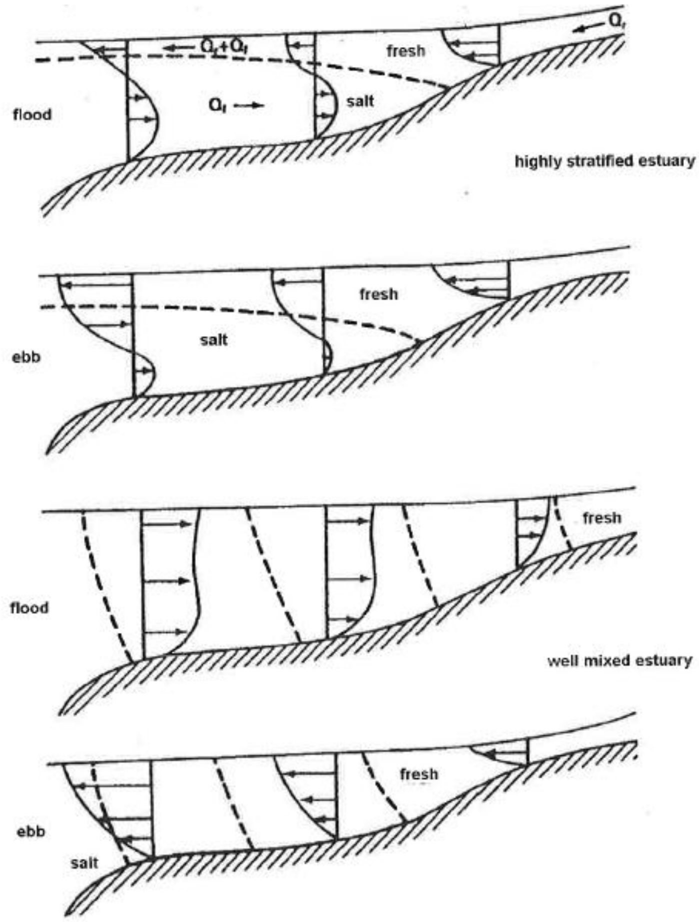

Figure 3.5 Stratification in an estuary: density variations and velocity profiles (d’Angremond and Pluim-Van der Velden, 2001)

The mixing of fresh and saline water in estuaries is a fundamentally important process, since it controls the nature of the longitudinal and vertical density gradients which, in turn, generate the estuarine density circulation (Allen et al., 1980). The key factor which causes mixing between the inflowing fresh water and sea water is turbulence, which intensifies diffusion. This turbulence is generated by currents arising from river flow, tides, or both. Therefore, any marked change in either will alter the mixing regime, in proportion to the difference in turbulence.

3.3.3 Sediment transport processes

The sediment transport processes in estuaries is generally complex and is a function of hydrodynamic circulation and sediment characteristics of the bed. Estuarine sediments can be derived from river discharge, catchment, and continental shelf or from eroded shoreline (Woodroffe, 2002). Thus many of the estuaries are often comprised of mixture of sediments having range of varying grain sizes which increase the complexity of the sediment transport processes further.

Flood/ebb tidal asymmetry plays a significant role in estuarine sediment transport processes and morphodynamics (Brown and Davies, 2010). ‘Flood dominant’ estuaries tend to infill their channels with coarser sediments while ‘ebb-dominant’ systems are likely to flush bed-load sediment seaward more effectively and represent more stable geometry (Speer and Aubrey, 1985).

Movement of sediment from the bed begins when the shear stress between the sediment and the bed becomes sufficiently great to overcome the gravitational force and frictional forces that holds the sediments on the bed (Brown et al., 1989). There will be a critical shear velocity corresponding to the critical shear stress and the grain size which determines the sediment movement. However, the relationship between the grain size and the critical shear stress is not a linear one.

The water depth is greater during the high water (HW) compare to low water (LW) which in turn reduces the duration between LW and the following HW and increases it between HW and the subsequent LW. This results in a shorter flood tidal phase and longer ebb tidal phase. From the concept of mass conservation, the peak flood velocity exceeds the corresponding peak ebb velocity. Although ebb duration is longer the velocity may barely exceed the threshold velocity for a short period. In contrast, during flood phase the velocity is predominantly above the critical velocity (Figure 3.6). This results in a net sediment transport during the flood tide. Consequently the estuary will behave as a sediment sink building up of inter-tidal banks.

Tidal movement and waves stir up sediment from the bed during the high tides and deposits the material again in more sheltered areas at times during the low water. The continuous interaction of this tide, waves and sediments alter the bed and results in an estuarine morphology.

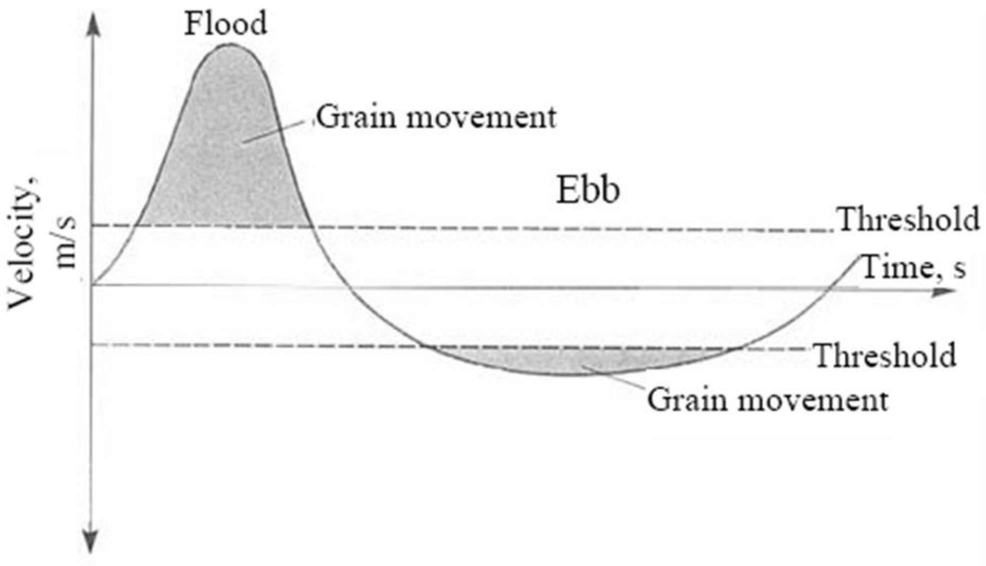

Figure 3.6 Typical shallow water tidal asymmetry (Brown and Davies, 2010)

3.3.4 Morphological evolution

Estuaries were created during the postglacial sea-level rise (~15,000-8,000 years BP) when rapid sea-level rise drowned river valleys. Throughout the historical time period, sediment deposition has created the present-day estuaries consisting of channels, sandflats and saltmarshes with an underlying hard geology. The present morphology of the estuary depends on how the hydrodynamic processes redistribute the soft sediment over the estuary (Brown and Davies, 2010).

Estuarine morphology is governed by a combination of various factors such as hydrodynamic conditions, the sedimentary environment and sediment supply, underlying geology (Moore et al., 2009) and human interventions (Figure 3.7). The morphological evolution of an estuary is a result of continuous non-linear interaction between non-linear tidal propagation and related sediment motion and the bed topography (Hibma, 2004). These non-linear interactions can results in residual currents leading to net sediment erosion or accretion. As these processes continue over the long time period, gradually evolution of the estuarine morphology takes place. Morhphologcial changes have important implications for the coastal environments, particularly in estuaries which are used to be areas of high commercial, recreational and ecological interest (Moore et al., 2009).

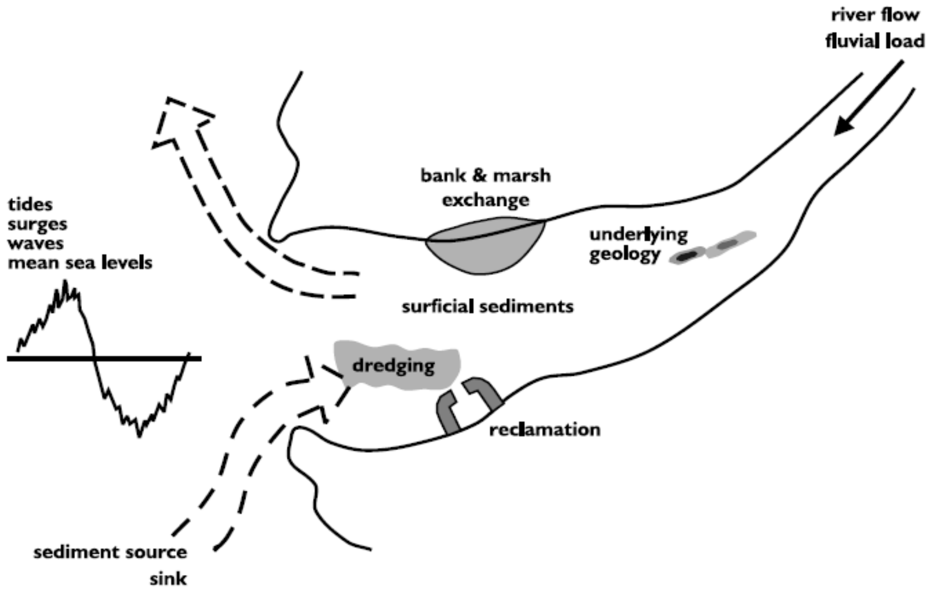

Figure 3.7 Schematic of major factors influencing the estuarine morphology (Prandle, 2009)

The morphological changes in an estuary take place at different time and spatial scales through complex interactions. Time scales of estuarine morphological evolution may vary from few hours to days, months to few years and decades to millennia (Karunarathna et al., 2008). A clear distinction between the morhphological features at different time and spatial scales was introduced by De Vriend (1996). According to that, the smallest morhphological bedforms such as ripples, dunes and sandwaves are categorised as micro-scale features, which take place at essentially smaller time scale than the corresponding morphodynamic behaviour. Meso-scale phenomena are identified as the primary morphodynamic behaviour, due to the interaction of tidal processes and the bed topography. Features such as alternating and interacting flood and ebb channels, tidal flats and shoals are classified as meso-scale elements. Macro-scale phenomena concern slow trends at scales much larger than the corresponding primary morphodynamic behaviour. Well-known macor-scale features are inlet gorge and the ebb tidal delta. The entire estuary and the adjacent coastal area belong to mega scale.

Estuaries in different physical settings (as explained in 3.2) display different types of morphological behaviour. However, estuaries that occur in macrotidal environment are particularly being interest of many scientists and in this study as well.

Estuaries that occur in macortidal settings are highly dominated by the tidal currents and they are typically funnel shaped with wide entrances tapering upstream (Chappell and Woodroffe, 1994). There are three primary zones with distinct channel morphology can be identified (Figure 3.8) in most of the macro tidal estuaries; upstream of river dominated zone, central tide dominated zone and seaward of the marine dominated zone (d'Angremond and Pluim-Van der Velden, 2001). The upstream of the estuary is relatively straight with the net seaward movement carried by the fluvial processes. The central zone often governed by both river and marine processes, which has a highly sinuous channel. The seaward of the zone is funnel shaped, and the net sediment moves landward direction.

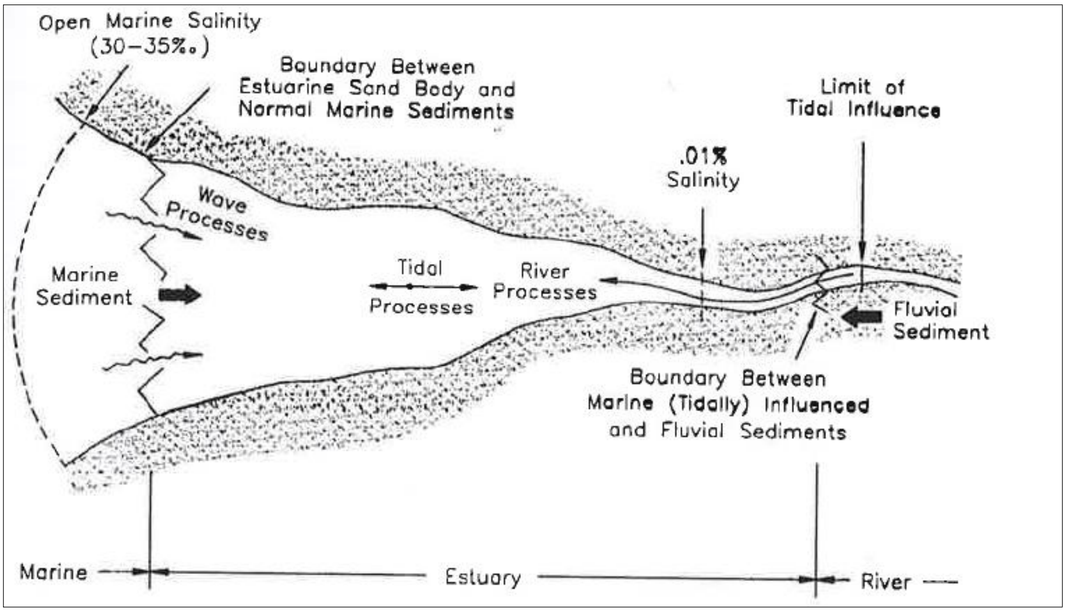

Figure 3.8 Physical processes in estuaries (d'Angremond and Pluim-Van der Velden, 2001)

Morphodynamic and hydrodynamic processes are strongly coupled in long-term estuarine evolutionary processes (Lanzoni and Seminara, 2002). The feedback mechanism that comes from the morphological changes affects the hydrodynamic conditions and sediment movement in the estuaries (Moore et al, 2009). Particularly, changes in the mean water depth and changes in the elevation of the intertidal areas may alter the tidal regime of the estuaries. This feedback mechanism combination with the non-linear interactions have made the estuarine morphological evolution a further complex phenomenon to predict.

3.4 Approaches for prediction of estuarine morphological behaviour

Ability of understanding and prediction of estuarine and coastal morphological behaviour is crucial to coastal engineers and coastal managers. Mathematical models are particularly attractive due to their flexibility and also complexity of the estuarine system makes physical scale modelling very difficult (De Vriend, 1996). Mathematical models are indispensible tools for coastal engineers in studying and analysing various coastal problems. Much of the effort has been taken during the last century by several researchers in formulating the natural processes into mathematical models. There have been different types of approaches developed and applied to investigate the coastal morphological evolution on meso and macro-scales. Each of the models has its own applicability due to the model formulations and various applied assumptions (Hibma, 2004). Literally, there are two well known approaches exist for the prediction of estuarine morphological behaviour;

- Process based models
- Behaviour oriented models

The philosophy behind coastal morphodynamic modelling and the state-of-the-art were given by De Vriend (1996).

3.4.1 Process-based models

Process-based numerical models are widely recognised as valuable tool for understanding and predicting coastal area morphological developments. Present-day computer technology and the development of powerful software systems for numerical modelling of waves, current, and sediment transport have brought process-based models of morphological evolutions within the reach of estuarine research.

This approach is based on a detailed formulation of underlying physical processes (Van der Wegen, 2010) such as waves, tides and currents, sediment transport, and bed-level changes into mathematical terms based on first physical principles (conservation of mass, momentum, energy, etc) (De Vriend, 1996). Process based models were developed based on physical understanding of small scale coastal behaviour over timescales which are basically hydrodynamics (i.e order of magnitude smaller than the scale of morphodynamics) (De Vriend et al., 1993). This approach is the use of two- or three dimensional hydrodynamic models combined with sediment transport and morphodynamic models and known as ‘bottom-up models’ (Karunarathna, 2008).

Process-based morphodynamic models generally consist of a number of modules which describe waves, currents, and sediment transport, respectively (De Vriend, 1996). The dynamic interaction between these processes is used sequentially or in a time loop as shown in below Figure 3.9. According to De Vriend (1996), models which take the interaction with the topographic changes into account are called ‘Medium-Term Morphodynamic Models’ (MTM models). These models are particularly able to describe the mesoscale dynamic behaviour of a morphological system such as formation and migration of morphological features. Models which do not consider this interaction and only describe the micro scale phenomena (accretion/erosion rate) on a given system are called ‘Initial Sedimentation/Erosion Models’ (ISE). Here the term ‘initial’ is relative to the morphodynamic scale of the phenomena of interest.

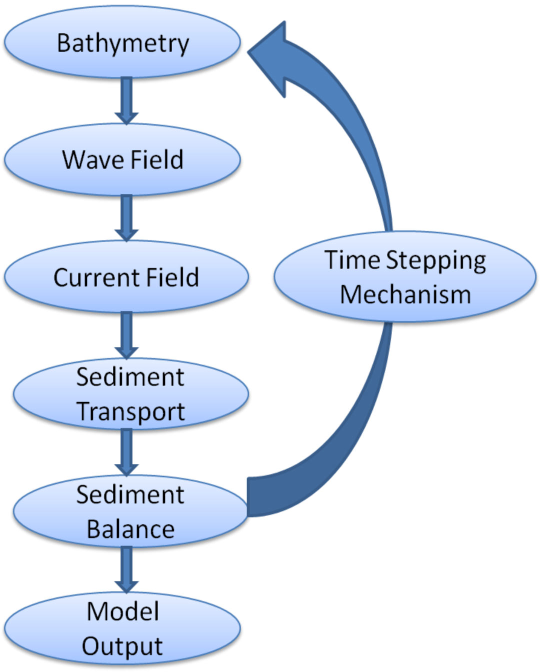

Figure 3.9 Structure of Typical Medium-term Morphodynamic Model (De Vriend, 1996)

Coastal area models were developed by several research institutes and universities such as Danish Hydraulic Institute (DHI), Delft Hydraulics (DH), HR Wallingford (HR), Service Technique Central Ports Maritime Central Navigables (STC) and the Civil and Engineering Department of the University of Liverpool (UL). All five models has the same basic structure as they consist of wave, current, sediment transport and bed level change modules. However, they had different degrees of interaction between different processes and different type of formulas. Detail description and inter-comparison of these five coastal area morphodynamic models are given by Nicholson et al. (1997). Intercomparison was achieved by setting-up each model to run the same hypothetical offshore breakwater layout and sensitivity of the model results were examined for different forcing conditions. This research revealed that the choice of sediment transport formula had influence on the resulting morphology.

Over the last couple of decades, coastal morphological modelling has made a significant progress (Sutherland, 2004) with the recent innovation and rapid developments in computer technology. Such models consider the initial shape of the bed and update it at regular intervals, along with re-computing the wave, current and sediment transport patterns (Soulsby, 1997). Presently, the state-of-the-art process based models are capable of predicting estuarine morphology, although not yet on large time scales (decades and centuries) (Brown, 2009). A major drawback of process-based modelling is that detailed description of small scale hydrodynamic processes is required to simulate the large scale morphological evolution (Van der Wegen) of given system. Especially in long-term modelling, this leads to very long computation time and requires huge storage space on computers. It is therefore various techniques have been proposed in literature and applied in long-term morphological simulations in order to reduce the computation time. The most common approaches were proposed by Latteux (1995), Lesser (2004) and Roelvink (2006) are described in section 3.5.

3.4.2 Behaviour-Oriented Models

Despite of the latest computer technology available today, the process-based models are still unable to cover the time spans which are much larger than the principal inherent morphological time scales (De Vriend, 1996). In addition, running these models over a long period of time does not necessarily accurately predict long-term coastal morphological behaviour, because process-based models do not describe small residul sediment fluxes and non-linear behaviour that becomes important in the long run (De Vriend et al.,1993). This has boosted the formulation of behaviour-oriented models which are based on the elementary physics.

This approach is also literally known as aggregated or hierarchical models (Hibma, 2004) and top-down models, are generally derived empirically from analysing the observed long-term morphological evolution or from the whole estuary regime concept such as volume, energetic, entropy etc (Huthnance, 2007)**.** This approach uses geological and geomorphological evolution models which are designed to simulate morphological behaviour over very long period (Karunarathna, 2008). These models are designed to predict the long-term physical response of an estuary with respect to natural changes (e.g sea-level rise) and changes followed by human interference. Thus, behaviour-oriented models aim to represent the observed morphological behaviour of a coastal system with a simple mathematical model that not necessarily related to the underlying physical processes.

Many top-down models make use of equilibrium concepts, based on the idea that feedback between different processes in a system will tend to yield equilibrium morphology, where if forcing conditions remain constant, no net change in morphology will occur (Rossington, 2008). Very good examples of this type of models are the box model of Di Silvio (1989) and the ASMITA (Aggregated Scale Morphological Interaction between a Tidal basin and the Adjacent coast) (Stive et al., 1998). ASMITA model basically describes the morphological interaction between a tidal lagoon or basin and its adjacent coastal environment. In this model, tidal inlet is schematised into a set of morphological elements (ebb-tidal delta, channel, tidal flats and tidal channels) as shown in Figure 3.10. ASMITA model characterises the tidal inlet by sediment volume of each model element in the system defined. The element volumes in a standard schematisation are defined as below (Rossington, 2008);

- Tidal flats – The sediment volume above the mean low water
- Channel – The water volume below the mean low water
- Ebb-tidal Delta – The excess sediment volume above a hypothetical non-inlet shore-face, seaward of the estuary mouth

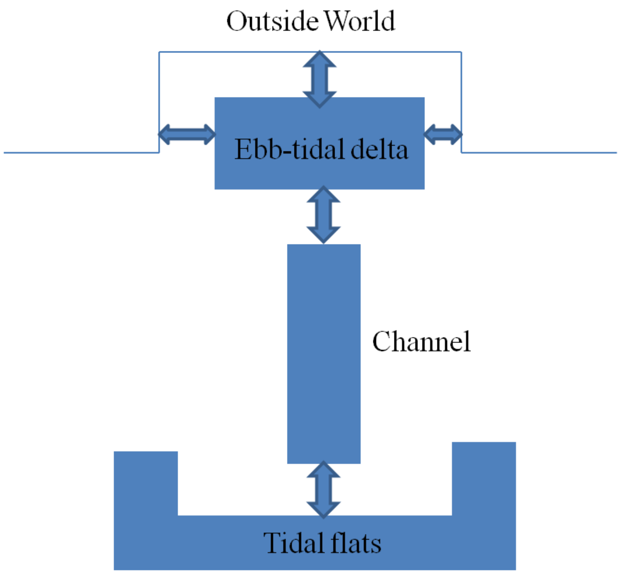

Figure 3.10 Elements used in the ASMITA concept (van Goor et al., 2003)

These three elements interact through sediment exchanging between elements. This interaction plays an important role in the morphological evolution of the whole system. Sediment exchange volume is driven by the difference between the elements' equilibrium volume and the actual volume. When all these elements are in equilibrium, no sediment exchange will take place. Fundamental of this model schematisation can be found in van Goor et al., (2003). Rossington (2008) has applied ASMITA for six UK estuaries (Portsmouth Harbour, Langstone Harbour, Chichester Harbour, Humber, Ribble and Southampton Water) with different morphologies and management histories.

The major advantage of this approach is that the model combines empirical relationships with process based sediment transport equations which leads to a time efficient modelling approach compared to the approach of process-based modelling. One of the drawbacks of top-down method is that detailed morphological information and dynamics are lost and the results are strongly depend on the equilibrium assumptions (van der Wegen, 2010).

3.5 Techniques in Long-term morphological simulations

Long-term morphological simulations using process based models, which are designed to reproduce short-term processes, and running on the long-term leads to excessive time consuming computation as described in section 2.4.1. One of the key concerns in carrying out long-term morphological simulations is therefore the techniques applied to bridge the gap between the short-term hydrodynamic and transport processes, varying over hours to days, and morphological changes, often taking place over much longer time scales (Roelvink, 2006). The most important strategies for the long-term morphological modelling were proposed by Lattuex (1995) and Roelvink (2006), are described in the following sections.

3.5.1 Representative tide

A very pragmatic technique aiming at the reduction of computational time that is essential for the long-term morphological simulations under the tidal action is given by Latteux (1995). It is an input reduction technique which is based on the idea that the residual (long-term) effects of smaller-scale processes can be obtained by applying models of those smaller-scale process forced with reduced ‘’representative’’ inputs. In the case of tidal forcing, computation of flow pattern over each tide cab be rather costly. Using 2D process-based model Lattuex (1995) has investigated the possibility to represent the whole tidal cycle over the relevant period by only a small number of tides and thus reducing the input considerably. It is also termed as ‘morphological tide’.

As discussed by Latteux (1995), morphological tide can be estimated by simulating a lengthy period of the complete tidal record (full spring-neap cycle) and then selecting the individual tidal cycle from this simulation which has a mean sediment transport pattern closest to the mean sediment transport pattern of the full simulation. The best representative tide was somewhat larger than (7 to 20%) the mean tide. Additionally Latteux also investigated another way of simulating the yearly tidal cycle with any single tide by multiplying the results of different tides by a factor in such a way that yearly evolution was reproduced properly. Based on the results it was concluded that, due to strong non-linear relationship between flow velocity and sediment transport, bed changes are mainly resulting from spring tides.

Morphological changes take place on far longer time-scales than changes in the hydrodynamics. Thus, number of morphological time step would be huge if morphology has to be simulated over the each hydrodynamic time step. Therefore, Lattuex (1995) also distinguishes 4 methods to reduce the number of morphological time step;

- **Straightforward extrapolation:** Assuming no flow modification take place as long as the bed changes do not exceed a certain threshold. The results of computed bed changes on first tide, with a fixed bed are extrapolated for number of N tides (N is called filtering coefficient). Although this method leads rapid instabilities.
- **Time-cantered extrapolation:** Similar to the first method, however this tide is no longer the first one, but using a predictor-corrector approach bed change of N tide is predicted first. Based on that sediment transport and bed-level changes are calculated for tide N+1 using continuity correction for hydrodynamics. Finally, the average sediment transport and bed level changes are calculated resulting in a corrected bed level at N+1.
- **Elongated tide:** Simulating N number of tides by a single one, extended N times, so that a longer time step can be used on morphological simulations. This method allows bed forms to propagate, but the effect of subsequent tides is not ensured. At each time step the bed level changes are no longer negligible, and the flow conditions are adjusted via the 'continuity correction'.
- **Expansion of sediment transport as a function of bed evolution:** This method assumes that neither flow, nor free surface are disturbed by bed changes, as long as these changes are small compared to the water depth. Thus, the sediment transport is calculated for different bed level changes without solving the full hydrodynamic equations.

3.5.2 Rapid Assessment Method (RAM) and Online Method

Morphological updating is an important component of integrated coastal area modelling. Roelvink (2006) has distinguished two main approaches namely the Rapid Assessment Methodology (RAM) and the online method. RAM method is an extension of the 'continuity correction' method. The 'continuity correction' is a frequently applied method to adjust the flow filed after small changes in the bathymetry. The flow pattern is assumed not vary for small bed level changes.

RAM uses the tidal averaged sediment transports, in combination with the continuity correction. This method assumes that the tide-averaged transport rates are function of flow and wave patterns which do not vary on morphological time scale, while the local depth vary on this time scale. Thus, transport at a given location is simplified as only a function of the water depth. When the bottom changes become too large, a full simulation of the hydrodynamics and sediment transport is carried out for number of input conditions. Finally a weighted averaged sediment transport is then determined, which is the basis for the next RAM computation. The updated bathymetry is fed back to into the detailed hydrodynamic and sediment transport model; here the computations to update the wave, flow and sediment transport field can be done in parallel using different processors. This would significantly reduce the simulation time in long-term morphological modelling.

Another method to accelerate the morphological updating scheme is the use of 'morphological factor' (MF) given by Lesser et al. (2004). Morphological factor is a device used to deal with the time scale difference between hydrodynamic and morphological developments. It works by simply multiplying the bed level change rates by a constant factor (equation 4.1), thus morphological time step can be effectively increased.

$$\Delta \mathrm{t_{mor}} = (\mathrm{MF}) * \Delta \mathrm{t_{hyd}} \tag{4.1}$$

Where, Δt_{mor} – Morphological time step; Δt_{hyd} – Hydrodynamic time step; and MF – Morphological Factor.

The assumption is that nothing irreversible happens within an ebb or flood phase, even when all changes are multiplied by a factor n. However, application of morphological factors has limitations depending on the characteristics of the location under consideration. Therefore selection of a suitable morphological acceleration factor has to be made by judgement and carrying out sensitivity tests by the modeller.

Roelvink (2006) has investigated the 'Online' method with morphological factor. It gives a new insight into the long-term morphological modelling. Online method updates the flow and sediment transport and bottom with a morphological factor at every hydrodynamic time step (order of 1 minute). An advantage of the online method is, that short-term processes are coupled at flow time step which makes easy to include various interaction between flow, sediment and morphology. Another benefit over the 'elongated tide' approach proposed by Lattuex (1995) is that no continuity correction is required.

According to Roelvink (2006), although Online method is an improvement over the other approaches, its exaggeration of the short-term changes due to tide and varying forcing conditions still puts a limitation on the application of the morphological factor. Therefore a Parallel Online method allows for different parallel processes to be carried out at the same time and merging the processes for weighted morphodynamic update will increase the numerical stability. Roelvink (2006) has tested these approaches for a tidal inlet case with the application of Delft3D and it was concluded that the 'parallel online' method gives a best way to bridge the gap between short-term hydrodynamic changes and long-term morphological evolution, without violating the basic physics.

3.6 Assessment of Morphological models

Assessing the performance of mathematical models of coastal morphology is an essential part of establishing their credibility (Sutherland, 2004). Evaluation process of these coastal area models are often done by comparing the model output with the observed dataset. In the past this has usually been done by comparing model prediction with the observed behaviour and the modeller used to make subjective judgement of the goodness of fit. However, quantitative assessment of model performance becomes important for the model that needs to be used as an engineering tool. Sutherland et al. (2004) suggest Brier Skill Score is one of the most appropriate methods of evaluating the performance of a morphological model.

3.6.1 Brier Skill Score approach

Brier Skill Score (BSS) is commonly used methodology in meteorology and has already been applied to the coastal morphodynamic modelling by Brady and Sutherland (2001) and Sutherland et al. (2004). According to Sutherland et al. (2004), performance of a coastal morphological model relative to baseline prediction can be quantitatively assessed by using Brier Skill Score. Skill is a non-dimensional measure of a prediction relative to the accuracy of a baseline prediction. The Brier Skill Score (BSS) is derived from the mean square error ($MSE_{(Y,X)}$) between the model prediction and observation, and mean square error ($MSE_{(B,X)}$) between the baseline and final observation. Thus BSS is given by;

$$BSS = 1 - \frac{\mathrm{MSE(Y,X)}}{\mathrm{MSE(B,X)}} = 1 - \frac{(Y-X)^2}{(B-X)^2} \tag{4.2}$$

here $MSE_{(Y,X)}$ and $MSE_{(B,X)}$ are given by;

$$\mathrm{MSE(Y,X)} = \frac{1}{J}\sum_{j=1}^{J}(y_j - \mathrm{x_j})^2 = (Y - X)^2 \qquad (4.3)$$

$$\mathrm{MSE(B,X)} = \frac{1}{J}\sum_{j=1}^{J}(b_j - \mathrm{x_j})^2 = (Y - X)^2 \qquad (4.4)$$

where, Y - a set of J observations (y_1, y_2, ... y_J); X – a set of J model predictions (x_1, x_2, ...x_J); and B – a set of J baseline/initial observations (b_1, b_2, ...b_J)

BSS = 1 ; Perfect prediction

BSS = 0 ; No change / modelling the baseline conditions

BSS < 0 ; Model predictions are further away from the measured conditions than the baseline conditions

Above equation 4.2 shows that the denominator depends on the accuracy of the initial and final measurements taken. Generally, the error of a perfect prediction is taken to be zero. However, the above method simply ignores the presence of measurement errors. In reality bathymetric surveys always contain some errors in the measurement. There are two methods have been proposed to account for measurement errors. The first one gives adjusted BSS (Equation 4.5), is a refinement of the Equation 4.2 proposed by Sutherland et al. (2001). Here it is assumed that the surveys of baseline and final are made in the same way.

$$BSS_p = 1 - \frac{\mathrm{MSE(B,X) - MSE(Y,X)}}{\mathrm{MSE(B,X)} - 2\delta^2} \qquad (4.5)$$

where δ - measurement error.

The assumptions above imply that $\mathrm{MSE(B,X)} = (\mathrm{B_A} - \mathrm{X_A})^2 + 2\delta^2 \geq 2\delta^2$ so the denominator of Equation 4.5 will be positive or zero. Therefore, this gives higher magnitude of skill scores than the standard BSS (Equation 4.2).

There is another method proposed by Van Rijn et al. (2003) which gives alternative method for adjusting the BSS for measurement error, is given by;

$$BSS_{VR} = 1 - \frac{(|\mathrm{Y - X}| - \delta)^2}{(\mathrm{B - X})^2} \qquad (4.6)$$

with $(|\mathrm{Y - X}| - \delta)$ set to zero if $|\mathrm{Y - X}| < \delta$

Van Rijn et al. (2003) proposed a classification scheme for the Brier Skill Scores, particularly for the morphological models, shown in first two columns of Table 3.1, based on the judgement Sutherland et al. (2004) has provided the classification for the modified version, BSS_p.

Table 3.1 Classification table for Brier skill Score (Sutherland et al., 2004)

	BSS_{vr}	**BSS**	**BSS_p**
Excellent	1.0-0.8	1.0-0.5	1.0-0.8
Good	0.8-0.6	0.5-0.2	0.8-0.3
Reasonable/fair	0.6-0.3	0.2-0.1	0.3-0.15
Poor	0.3-0.0	0.1-0.0	0.15-0.0
Bad	< 0.0	< 0.0	< 0.0

4. MODEL DESCRIPTION

4.1 Introduction

The modelling simulations in this study were carried out with the HR Wallingford modelling framework, PISCES (Chesher et al., 1993). PISCES is a state-of-the-art, fully interactive coastal area modelling framework, capable of simulating various processes of wave propagation, current distribution, and the resulting sediment transport in complex coastal areas. For this study PISCES comprised the flow model (TELEMAC-2D) and sediment transport model (SANDFLOW). Hence this chapter provides description of each models including theoretical background on what they are based on.

4.2 Flow Model (TELEMAC 2D)

TELEMAC-2D is a two dimensional depth averaged finite element flow model, developed by National Hydraulics and Environmental Laboratory (LNHE) in Paris. TELEMAC-2D uses the finite element technique to solve the shallow water equations, continuity and momentum equations, for every node within the domain. The advantage of using finite elements is the possibility of using a very flexible grid. The various variables (bed elevation, water depth, free surface level, u and v velocity components) are defined at the nodes (vertices of triangles) and linear variation of the water and bed elevation and of the velocity within the triangles is assumed.

There is no particular limit on the time step for a stable computation but it is best to ensure that the Courant number based on propagation speed is less than about 10. It is found that if the solution is nearly steady then few computational iteration are required at each step to achieve the required level of accuracy, which in TELEMAC is computed according to the actual divergence from the accurate solution. The computation at each time step is split into two stages, an advective step and a propagation-diffusion step.

The finite element method used is based on a Galerkin variational formulation. The resulting equations for the nodal values at each time step are solved using an iterative method based on pre-conditioned conjugate gradient methods so that large problems are solved efficiently.

TELEMAC requires as input finite element mesh of triangle grid elements, having bathymetric data at each node covering the area to be modelled. A file contains keyword values are used to steer the computation, this steering file act as the control panel for the modelling process. The main results at each node of the computation mesh are the depth of water and the depth-averaged velocity components. The user can select range of output parameters including velocity, discharge, water level, bed-level, water depth etc. The model results are processed using the interactive graphic system MERMAID.

4.3 Sediment Transport Model (SANDFLOW)

SANDFLOW-2D is the sediment transport modelling module of the PISCES, developed by HR Wallingford. SANDFLOW-2D uses the flows calculated by TELEMAC-2D to execute the non-cohesive sediment transport in the domain and thereby identify the areas of potential siltation and erosion.

The sediments under consideration here are very fine and fine sands (d_{50}~ 0.06 to 0.25 mm) which mainly move in suspension. However, the model can also be used to identify the trends in the case of medium sand (d_{50}~ 0.25 to 0.5 mm). The main factors controlling sand transport in this model are;

- Advection by currents
- Settlement under gravity
- Turbulent diffusion in all directions (but only the vertical component is of significance under most circumstances)
- Exchange of sediment between the flow and the bed

Although sand transport in estuaries is really an unsteady, 3D problem, it has been shown by HR Wallingford that it can be dealt with using a 2D, depth-averaged model provided special provision is made to account for the vertical profile effects of the sediment concentration. Under these circumstances the depth-averaged, suspended solids concentration $c_{(x,y,t)}$ satisfies the conservation of mass equation.

$$\frac{\partial}{\partial t}(dc) + \alpha\left[\frac{\partial}{\partial x}(duc) + \frac{\partial}{\partial y}(dvc)\right] = \frac{\partial}{\partial s}\left(dD_s\frac{\partial c}{\partial s}\right) + \frac{\partial}{\partial n}\left(dD_n\frac{\partial c}{\partial n}\right) + S \qquad (4.1)$$

where, (u,v) - depth-averaged components of velocity (m/s); D_s - longitudinal (shear flow) dispersion coefficient (m^2/s); D_n - lateral (turbulent) diffusivity (m^2/s); (x,y) -

Cartesian co-ordinates in horizontal plane (m); (s,n) - natural co-ordinates (parallel with and normal to mean flow) (m); t - time (sec); d - water depth (m); S - erosion from or deposition on the bed (kg/m^2/s); α - advection factor to recover the true sediment flux from the product of depth-averaged quantities

Advection factor is introduced to compensate for the omission of the vertical profile in the sediment flux terms.

Bed exchange relation is simply formulated as;

$$S = \beta_s \omega_s (c_s - c) \qquad (4.2)$$

Where, c_s - depth-averaged concentration when the flow is saturated with sediment (kg/m3); ω_s is the representative settling velocity (m/s); $ß_s$ is a profile factor to compensate for integrating out the vertical profile of suspended sediment (it is to correct for higher sediment concentrations near the bed).

Deposition or erosion takes place depending on whether the instantaneous sediment load (c) exceeds or is less than the saturated value (c_s). Pick up of sediment from the bed is prevented if there is no sediment available on the bed. A shortage of material on the bed is reflected in a low concentration of suspended solids being advected away by the flow.

The evaluation of bed changes requires depth-averaged sediment concentration c_s. This is obtained from the sediment transport relation specified in the package (eg. Ackers-White, van Rijn and Simple power law) or any other relationship defined by the user.

4.4 Morphological Model (PISCES)

PISCES is a coastal area modelling framework, developed by HR Wallingford (1995), that performs the pre-processing for the morphological predictions by coupling the flow, wave and sediment transport models dynamically. PISCES is a FORTRAN 95 routine that performs the pre-processing for the morphological predictions as well as the iterated calls to TELEMAC and SANDFLOW to calculate flow and sediment transport. It also updates the bottom based on the SANDFLOW deposit fields to achieve a closed morphological loop.

The model performs morphodynamic simulations are completely automatic, with the user simply specifying the duration of the simulation and time step. Automatic updating of the hydrodynamics is performed according to the internal morphodynamic time step. This time step has to be given consistent with marinating a stable seabed. The morphological acceleration factor in this model is to assist in dealing with the difference in time-scales between hydrodynamic and morphological developments. Application of this factor reduces the computation time efficiently. However, sensitivity tests required in order to select an appropriate factor that allow

Figure 4.1 illustrates the PISCES model structure used in this study, which comprises the flow and sediment transport model. Starting from a given initial bathymetry, the flow model solves the shallow water equation for the currents over a given period (morphodynamic time step), using an iterative method. The resulting flow fields are then fed into the sediment transport model, which computes the sediment transport field over the same period. Bed level changes are subsequently calculated using the Equation 4.3 based on the sediment transport rates calculated by the sediment transport model. When there is a morphological factor applied, morphological changes calculated from the sediment transport field then multiplied by this factor. Consequently, the bed is updated based on the bed level changes to achieve a closed morphological loop. The updated bathymetry is looped back to the flow model in order to do the continuity correction, which means adjusting the flow field for the new bathymetry.

The main limitation to the continuity correction is that the bed level is assumed to remain constant during the hydrodynamic computation while the flow and sediment transport are considered invariant during the bathymetry update, whereas in reality the bed changes continuously over time. Hence, a concept limiting the morphodynamic time step was identified during the previous study (Chesher, 1993), stability analysis yields the requirement is given in Equation 4.4.

$$(1-P)\frac{\partial h}{\partial t} - \frac{\partial q_x}{\partial X} - \frac{\partial q_y}{\partial Y} = 0 \qquad (4.3)$$

where, h – bed-level relative to a fixed datum; t - time; q_x - sediment transport rate in the x-direction (m3/m/s); q_y - sediment transport rate in the y-direction (m3/m/s); and P - Porosity of the bed.

$$\Delta T_m \leq \frac{\Delta X}{\sqrt{2(C_x^2 + C_y^2)}} \tag{4.4}$$

$$C_x = \frac{\frac{1}{(1-P)}\frac{\partial q_x}{\partial x}}{\frac{\partial h}{\partial X}} = \frac{1}{(1-P)}\frac{\partial q_x}{\partial h} \tag{4.5}$$

$$C_x = \frac{\frac{1}{(1-P)}\frac{\partial q_y}{\partial y}}{\frac{\partial h}{\partial Y}} = \frac{1}{(1-P)}\frac{\partial q_y}{\partial h} \tag{4.6}$$

where, ΔT_m is the morphodynamic time step; C_x and C_y are the bed celerity in x and y directions respectively.

This technique involves a calculation of the celerity of the bed over the entire model domain and selecting the optimum time step that satisfy the stability criteria.

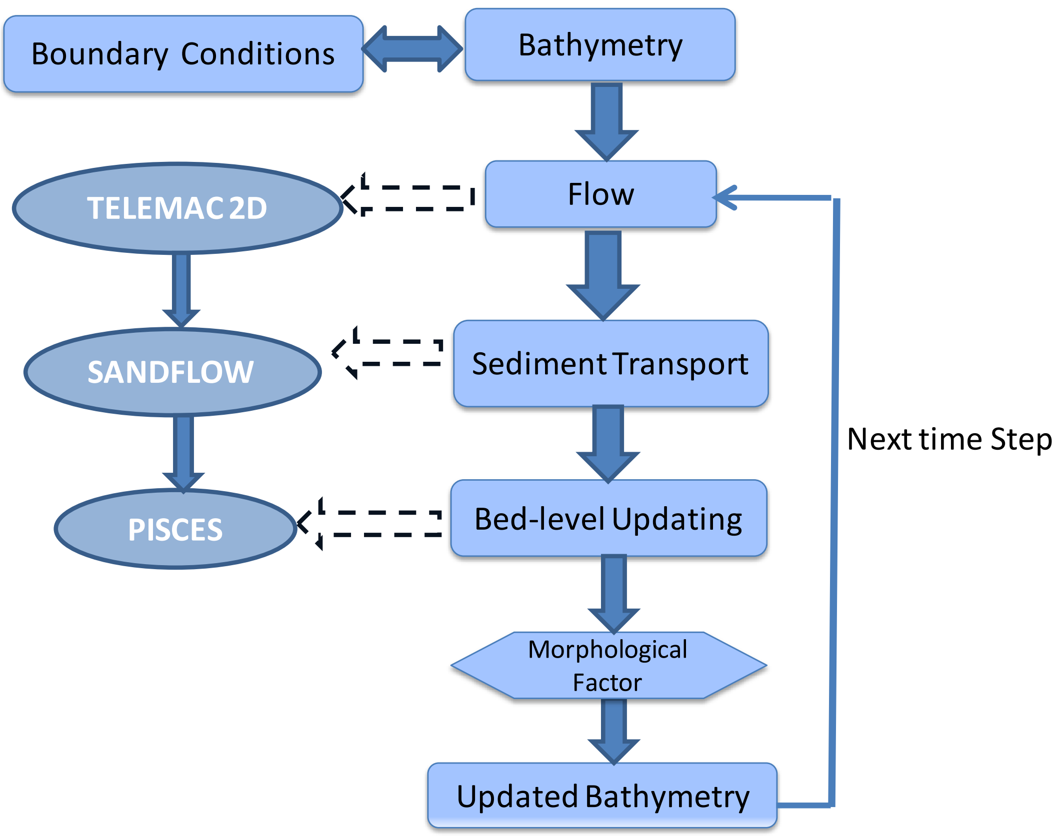

Figure 4.1 Model Flow Chart

5. METHODOLOGY

5.1 Introduction

Setting up an appropriate methodology that fits with the predefined objectives is an essential part of long-term morphological modelling. Thus, this chapter describes detailed methodology that has been adopted during this study, including data review, model bathymetry setup, and derivation of the boundary conditions, morphological model setup and morphological simulations. The model results and analysis are presented and discussed in the chapter 5.

5.2 Data Review

Data play an important role in various phase of long-term morphological modelling. The main data in this study includes bathymetry, tides and sediment grain sizes and are described in detail below. All these data were gathered from the previous studies carried out by HR Wallingford on the Dee Estuary in 2005 and 2007 period (HR Wallingford Reports, EX 5081 and EX 5514).

5.2.1 Bathymetry

The main source of the bathymetry data comes from Airborne LiDAR (Light Detection and Ranging) surveys of the Dee Estuary which were carried out by the Environmental Agency in 2003 and 2006. Other data consist of swathe bathymetry data, monthly estuary transects and Ports of Mostyn survey. (Table 5.1) shows the various data collected during the year 2003 and 2006 (data coverage is given in Appendix A1).

LiDAR is a technique for measuring depths of relatively shallow coastal water from the air using light detection techniques (Guenther, 2000). However, the data that results from LiDAR must be handled carefully, especially when surveying the bottom deeper than a threshold level. For instance, when surveying the channels, LiDAR tends to reflect on the water surface rather than reflecting on the bottom surface of the area. This is due to non-water penetrating nature of LiDAR compared to classical eco sounding method. Thus, the airborne surveys at the Dee Estuary were performed at low water, during the spring tides to maximize the exposed area. The deeper channels were surveyed separately using boat-based swath bathymetry.

Accuracy of LiDAR survey depends on the flying height. LiDAR mapping technology is capable of collecting elevation data with an accuracy of 15cm and horizontal accuracies of 1/1000th of the flight height (Engineering Manual). The 2003 and 2006 LiDAR surveys on the Dee Estuary have horizontal resolution of 1m and vertical accuracy of ~20-30cm.

Table 5.1 Bathymetry data collected in 2003 and 2006 (HR Wallingford, 2007)

2003	2006
LiDAR survey – EA (April)	LiDAR survey – EA (September)
Bathymetry survey – EA (June/July)	Swathe bathymetry (Pelorus surveys) (May \December)
Port of Mostyn survey (January)	Estuary Transects (Port of Mostyn) (September-October)

5.2.2 Tides

Table 5.2 summarises the tidal conditions around the study area taken from UK Hydrographic Office Tide Tables. However, morphological modelling simulation requires tidal water levels that vary spatially and temporally at the model boundary (see also section 5.7). This has been obtained from the previous study (HR Wallingford, 2005), which was driven from the Irish Sea Model. This gives time varying water levels at the Liverpool bay model (at 11 locations of the model boundary) over a full spring-neap cycle (Irish Sea model and driven tides are explained in appendix A2). The largest spring tide obtained has a range of around 9.5m, which is close to the range from highest astronomical tide to the lowest astronomical tide as shown in Table 5.2. Based on this spring-neap tides, tidal boundary conditions for the present model have been driven and are described in section 5.7.

Table 5.2 Tidal Conditions at the Dee Estuary area (HR Wallingford,2004)

Level or Range	Mostyn	Liverpool
CD to OD	4.5	4.93
MHWS (mCD)	8.5	9.3
MLWS (mCD)	0.5*	0.9
MHWN (mCD)	6.7	7.4
MLWN (mCD)	2.6*	2.9
Mean Spring tidal range (m)	8.0	8.2
Mean Neap tidal range (m)	4.1	4.5
Highest Astronomical Tide (mCD)	9.7*	10.5
Lowest Astronomical Tide (mCD)	0.0*	-0.2
Range from HAT to LAT (m)	9.7	10.7

*estimated from Liverpool data

(Chart datum (CD) is explained in Appendix A3)

Morphological tide;

Although the astronomical tide is deterministic and can be predicted accurately over a long time period, which makes the real-time representation of the tidal motion in a long-term modelling, prohibitively expensive (De Vriend, 1993). Computations at the scale of several years or decades cannot take into account the real alternation of fortnightly tidal cycles. Therefore, it was decided to use concept of 'morphological tide' that represents the tidal motion for the present morphological modelling study.

Morphological tide is defined as the tide in which the sediment transport rate, when scaled by an appropriate number of tides, yields the same transport as that over a full spring-neap cycle.

The 'morphological tide' was established by HR Wallingford during the previous study (Dee Estuary Modelling-Phase 2) for the Liverpool Bay Model. The study had concluded that the total transport could be accurately represented by means of a morphological tide. The resulting morphological tide has the tidal range of approximately 6.8m (HR Wallingford, 2005) (morphological tide obtained at 11 points of the Liverpool Bay model is shown in Appendix. A2)

5.2.3 Sediment grain size

Sediment grain size information for the Dee Estuary has been obtained from the HR Wallingford's previous study. Grab samples were taken at different locations of the Dee Estuary by Hydrosurvey (May and September 2003) and the sieve analysis was performed (HR Wallingford, 2004). Table 5.3 illustrates the grain sizes found to be at different regions (refer to the Figure 5.1) of the estuary.

Table 5.3 Sediment Grain-size Information at the Dee Estuary (HR Wallingford, 2004)

Region of the Estuary	Grain Sizes (mm)	Remarks
Port of Mostyn	0.15-0.45	Predominantly medium sand
Mostyn Deep	0.20-0.50	Medium sand with some fine sand on the north and south side of Mostyn Deep
Welsh Channel	0.06-0.20	Predominantly fine sand
Salisbury Channel	0.20-0.50	Medium sand with some fine sand

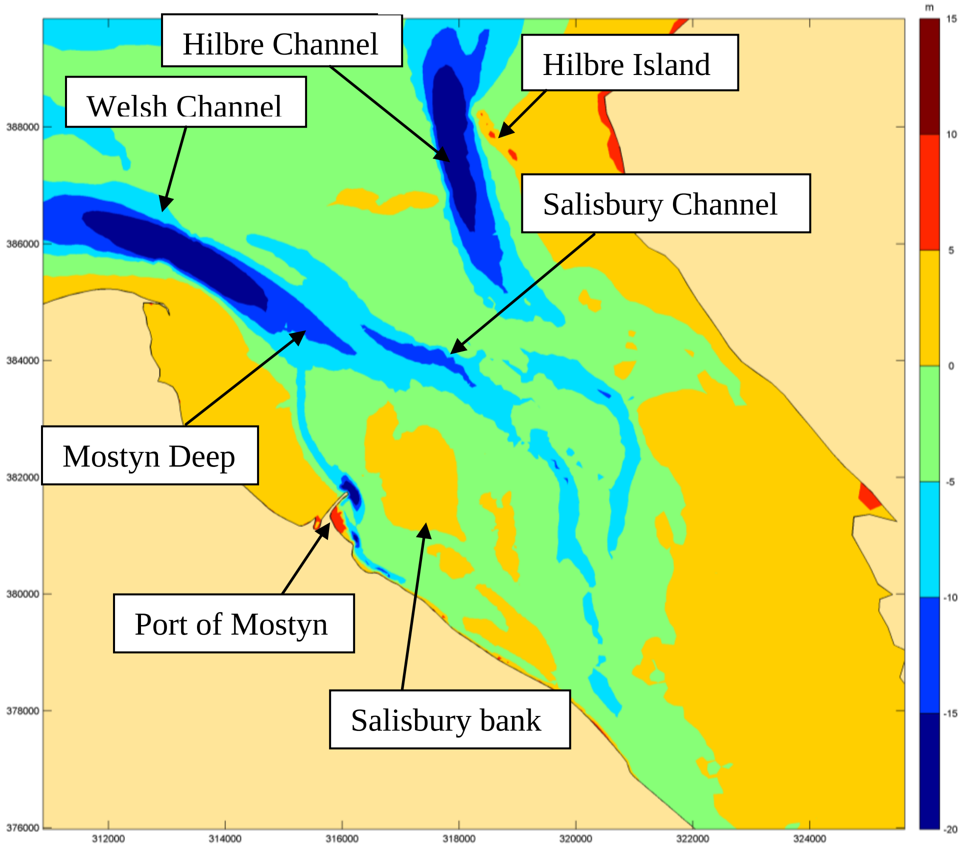

Figure 5.1 Different Regions of the Estuary

Further, based on the particle size distributions from the grab samples taken within the estuary were characterised by d_{10} = 0.09 mm, d_{50} = 0.20 mm and d_{90} = 0.35 mm.

Based on the above information, and since the present study focuses on the morphologically active regions where the channels tend to be predominantly sandy, it was decided carryout the morphological modelling with the median grain size of 0.20 mm. However, sensitivity tests have been performed using 0.10 mm and 0.30 mm grain sizes.

5.3 Model Bathymetries (2003 and 2006)

Creation of the bathymetry mesh is the first step to be taken during the modelling process in order to define the nodes where the computation of the model variables takes place. 'JANET', mesh processing software that allows generation of triangulated irregular mesh, on which dimensions are defined by the user in TELEMAC system, has been used to create the bathymetry meshes for this study.

Model bathymetries (for 2003 and 2006) for the present study are driven from the regional model bathymetries (Liverpool Bay Model) that was used in the earlier HR Wallingford's modelling study. The regional bathymetries which cover the entire Dee Estuary and adjacent Liverpool Bay have been obtained from the past study (HR Wallingford, 2007). The major steps involved in the bathymetry preparation are given below.

- The LiDAR data explained in section 5.2.1 were analysed carefully in order to filter out the areas with data representing the water surface than the seabed. Thus LiDAR data only used for bed levels above 1 m chart datum; below this level it represents the water level at the time of the flight rather than the bed level.
- The datasets described in the Table 5.1 were interpolated onto the triangular model mesh (Figure 5.2) that had been used in the earlier model study (HR Wallingford, 2005).
- Gaps in the resulting LiDAR dataset were filled with the swathe bathymetry data where possible
- In the case of 2006 bathymetry, absence of LiDAR or swathe data, remaining gaps were filled with data from the earlier model bathymetry (2003)

As described in section 4.1, TELEMAC uses finite element techniques so that the advantage is very flexible and irregular grid can be used. Therefore, the key area can be represented in more detail and the area near the model boundaries can be kept with coarser grids. The mesh size (Figure 5.2) varies as large as 4000m on the outer boundary, reducing towards the study area 20m in the vicinity of the Port of Mostyn.

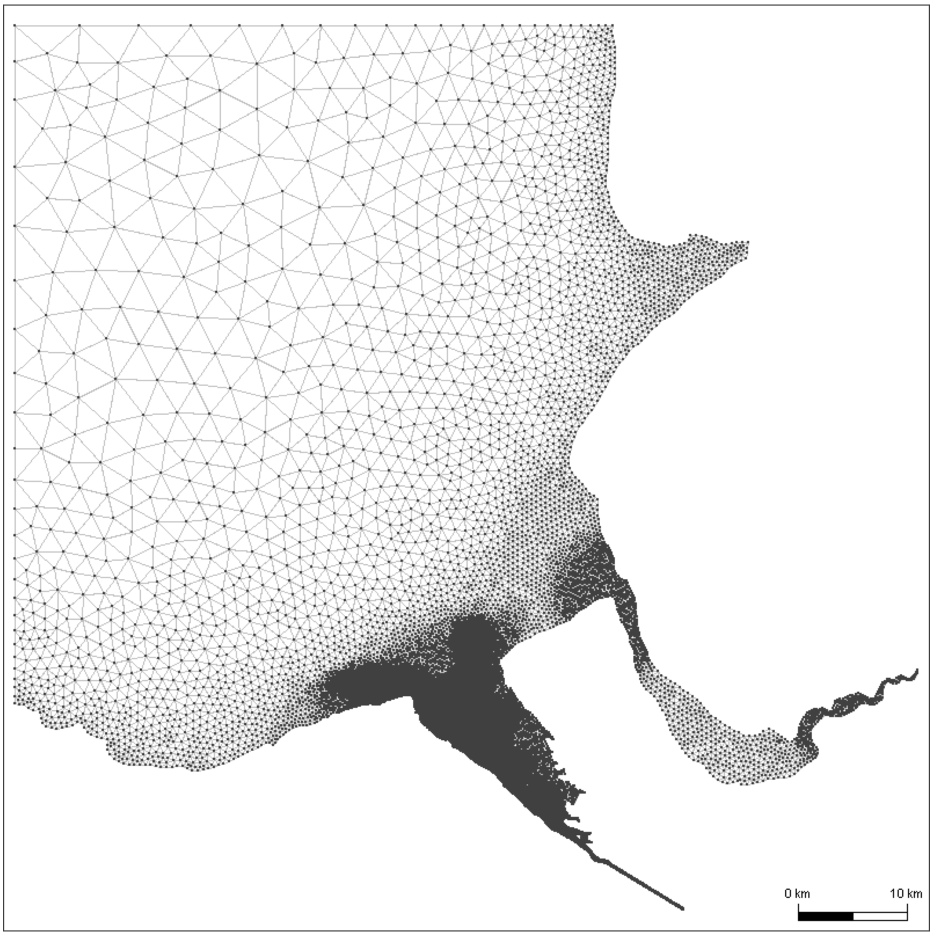

Figure 5.2 Liverpool Bay Model Mesh

The present study focuses mainly on the estuarine area and therefore the estuary area was cut down from the Liverpool Bay Model as shown in Figure 5.3. The resulting bathymetry mesh resolution had to be modified according to the modelling requirements. The bathymetry mesh with higher resolution would be much better in term of accurate representation of the area. However, this may lead in extensive simulation time, particularly in long-term morphological modelling. Hence resolution of the resulting bathymetry mesh was modified to be rather coarser in order to limit the number of elements and nodes that involve in the modelling processes. Main channels and morphologically active area of the estuary were still kept with reasonably higher resolution than the resolution at the model boundary. The resulting

Dee Estuary bathymetry is shown in Figure 5.4, which has been used throughout the present modelling studies. This model mesh has grid sizes varying from 50m in the key area, increasing towards the outer boundary of the study area to 700-800m.

Model meshes for the year 2003 and 2006 were created in the same procedure as explained above, but they interpolated with the corresponding bathymetry data from previous study. Thus both 2003 and 2006 model bathymetries have a common mesh, which makes easy to compare the model results with the 2006 datasets.

Detailed analysis of bathymetric changes between 2003 and 2006 was performed by HR Wallingford in 2007. However, in this study overall bathymetric changes of the Dee Estuary have been analysed quantitatively using Root Mean Square (RMS) values and the results are presented in section 6.2. This difference analysis is performed based on the above two model bathymetries of the Dee Estuary.

It can be noted in Figure 5.4, the model bathymetry have been defined in a way that the key area is sufficiently far from the open boundary. This ensures that any model boundary effects do not reach into the area of interest.

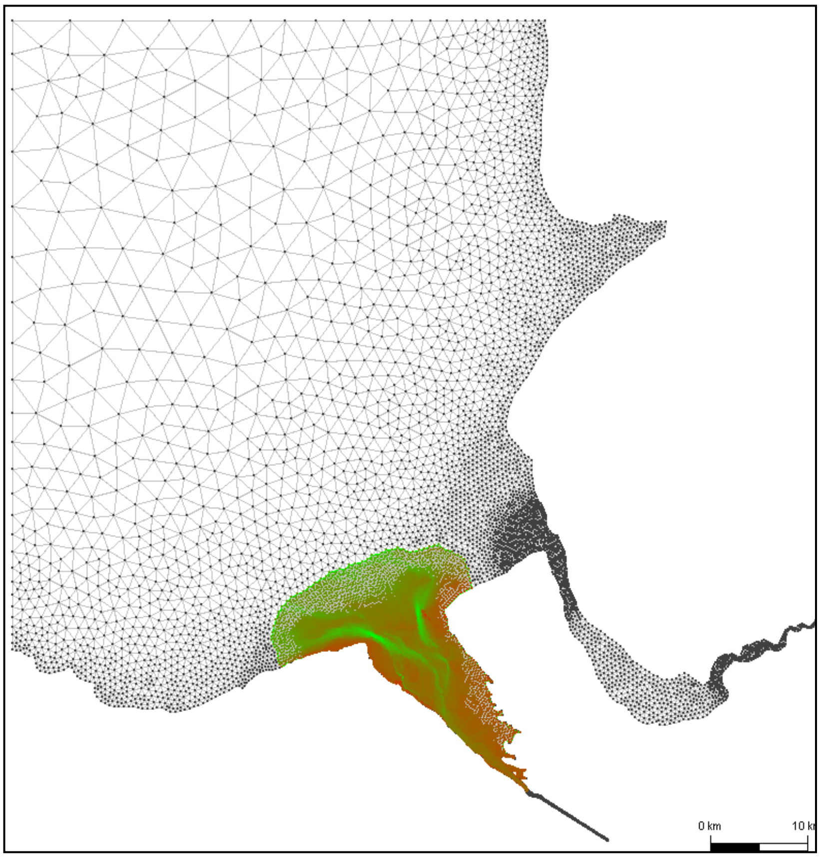

Figure 5.3 Extraction of Dee Estuary Model Bathymetry

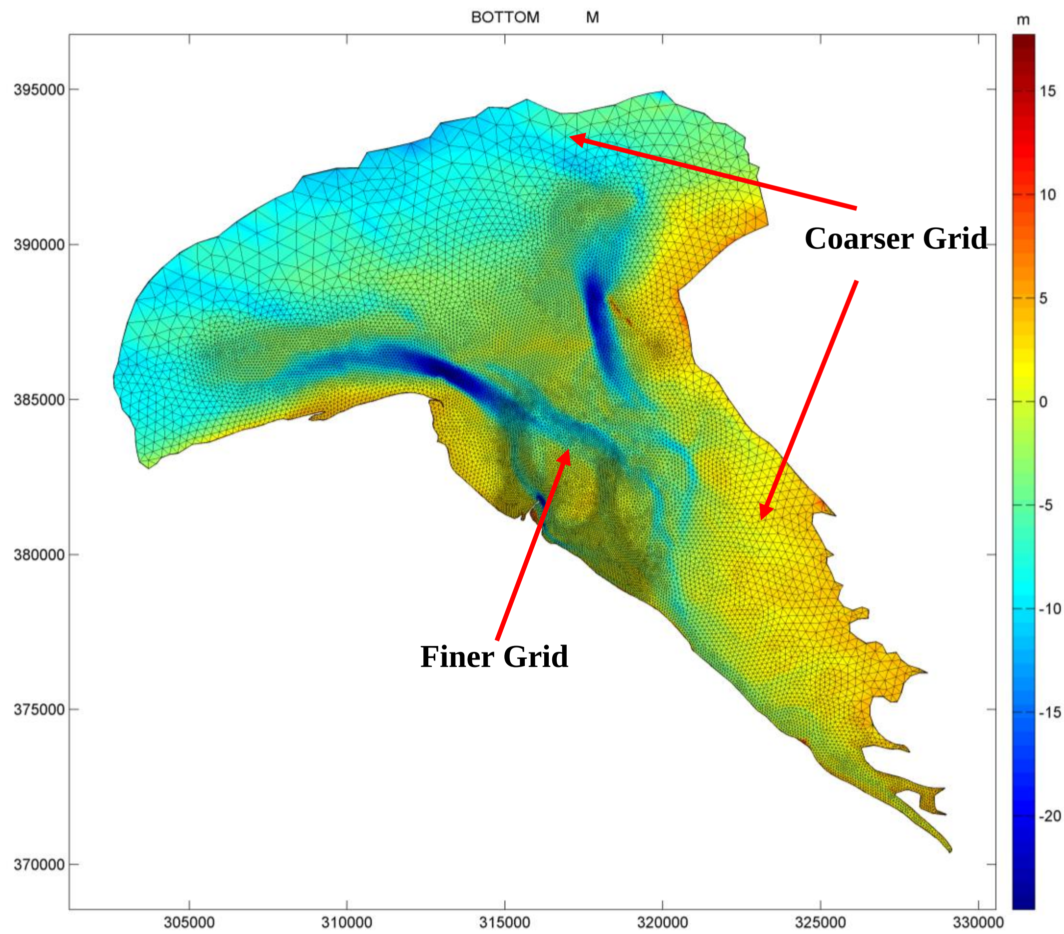

Figure 5.4 Model Bathymetry of the Dee Estuary

5.4 Boundary Conditions

Physically, boundary conditions of the model domain of calculations can be either liquid or solid. Generally, an impermeable condition exists for the solid boundaries, which does not allow any discharge across the boundary. Liquid boundary conditions can be either water level or discharge that varies over the time or constant. In this study, time varying water levels driven from the regional model (Liverpool Bay Model) have been used as the boundary conditions for the local model (Dee Estuary Model).

In order to extract the boundary conditions for the local model, the regional model was simulated for the period of a full spring-neap cycle (~ 14 days) using the tidal conditions explained in section 5.2.2. The time varying water levels were extracted at the Dee Estuary model boundaries the over a spring-neap cycle (the resulting tides are given in Appendix. A2).

The same procedure was done in order to extract the boundary conditions that correspond to the morphological tide. This was obtained by running the regional model with the morphological tide explained in section 5.2.2, and extracting the time series of water levels at the prescribed boundary points in the local model.

5.5 Morphological Model Setup

Once having the model bathymetry that represents the study area and necessary boundary conditions, next step is to setting up the model parameters that required for the morphological simulation. Morphological simulations were performed with the HR Wallingford modelling framework, PISCES (Chesher et al., 1993) which comprises of the flow model (TELEMAC-2D) and the sediment transport model (SANDFLOW). The regional model used in this study had been previously calibrated in the area of both Liverpool and Dee Estuary. Therefore, local model, which was driven from the regional model, has been used without any further calibrations.

All these models read physical and numerical inputs given by the user in the steering file, known as the control panel of the system. Hence morphological model setup includes setting up each of the steering files of above model. Setup of the each module is explained below (sample steering files are given in Appendix A4).

5.5.1 Flow model

Time step in the flow model has to be satisfied with the courant number criterion, thus it was kept as 2.5 seconds in order to keep the maximum courant number below 10. The number of time steps required for a complete morphological loop was calculated, which gives when dividing the morphological time step by the flow time step. The state of the model at the beginning of the simulation was defined with a constant free surface elevation of 2m over the entire model domain. Therefore, the water depth at each point is calculated as the difference between the bottom elevation and the free surface elevation in the domain (User manual, TELEMAC). Time varying water level boundary conditions (as explained in section 5.2) were imposed at the open boundary of the Dee Estuary Model (Figure 5.5). (The option for boundary conditions is explained in Appendix. A5)

The simulation period in this study was decided based on the time period between the first and second surveying of LiDAR. Accordingly, the morphological simulation has to be carried out for the period 3 years and 4 months. This needs the boundary condition to be extended to cover the full simulation period. This has been done by repeating the time series of spring-neap boundary conditions by appropriate number of times.

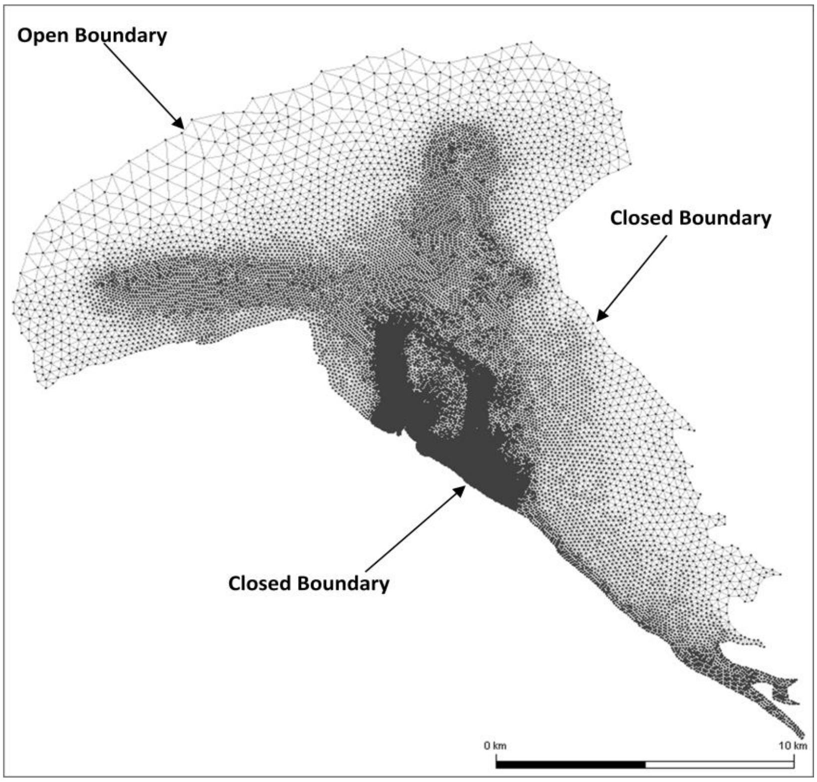

Figure 5.5 Boundary Definitions

A constant bed friction in space and time was applied for simplicity using law of Nikuradse's friction coefficient (0.01). The viscosity applied in the modelling is using Elder model which offers the possibility of specifying different viscosity values along and across the current, corresponding dispersion coefficients are 6 and 0.6 respectively. A coefficient that represents the overall viscosity has to be defined which characterises the extent and shape of recirculation. Smaller viscosity values tend to dissipate only small eddies, whereas higher ones will tend to dissipate large recirculation (TELEMAC user manual). Therefore this value has been defined as 1×10^{6} m^2/s considering the expected recirculation processes in all models (corresponding to the molecular viscosity of water, being the default value of 1×10^{4} m^2/s). The accuracy required during solution of the propagation step was kept as 10^{-4}.

5.5.2 Sediment transport model

SANDFLOW-2D uses as input the elevation and flow results from the TELEMAC run. Time step in this model kept to be 10 s which is 4 times larger than the one used in the flow model. An initial distribution of the sand over the entire domain is given in order to allow the model to pick up sediment from the bed. This value was chosen as a uniform distribution of 100,000 kg/m^2, considering the long simulation period.

Sediment transport relation applied in this model was based on Van Rijn's formula which gives the total sediment transport. Therefore, the current model does not distinguish between bed load and suspended load. As explained in section 5.3.2, a uniform median grain size of 0.20 mm was used in the sediment transport model. However, a sensitivity test performed with the grain size of 0.10 mm and 0.30 mm. The other physical parameters such as temperature and salinity in the model were kept as default.

5.5.3 Morphodynamic Model

Having setup flow and sediment transport model, it remained to couple them together using the PISCES interface, it reads the steering files of flow and sediment transport model. Model can be run either from the scratch or staring from the exiting initial conditions (flow and sediment transport results). The second option is not favourable for the long-term simulations as it requires the flow and sediment transport model have to be simulated individually for the required time period, which is computationally expensive. Therefore, all the models runs were carried out from the scratch in this study.

The starting time step was given as 12.5 hrs (approximately a tidal period), which removes the initialisation problems of the hydrodynamic calculations. Considering the long simulation period, the time step in this morphological model was kept as 12.5 hrs, which is the period of hydrodynamic forcing (tidal period). This means the bed updating takes place after each tide is simulated and the flow will be recalculated subsequently. The bed remains static over this time period, which is an assumption as stated in the model description 4.4. Flow overlap period was set to be 1 hr, which removes any initialisation problems during the hydrodynamic calculations that taken place over the each morphological time loop. (How the morphological time step and flow overlap work is elaborated in Appendix. A6)

Selecting a suitable morphological factor is purely based on the judgment and the stability requirements of the model. Therefore, several model runs were performed with different morphological factors, are explained in the following section.

5.6 Morphological Model Simulations

Morphological model simulation has to be carried out starting from the baseline conditions (2003) for the period of 3 years and 4 months, which allows subsequently comparing the model results with the observations in 2006. This requires simulation over ~80 spring-neap cycles (2400 tides) to cover the period between first and second bathymetry surveys. From the initial model runs, it was estimated that, simulation over a spring-neap cycle (14.8 days) requires ~5 days of running. This implies that the full simulation requires a period more than one, which is very long compare to the period available for this study. Therefore, it was decided to apply various input reduction techniques in order to have reasonable computation time that is achievable within this study period.

Morphological time step;

In order to reduce the computation time, it was decided to update the bathymetry on the time scale of hydrodynamic forcing (over each tide), which gives morphodynamic time step of 12.5 hrs. This assumes that the morphological changes within this time are not significant. Simulation with the morphological time step 12.5 hrs needs 3½ days. However, a simulation with 1 hr time step was also performed over a spring-neap cycle in order to compare the model performance with 12.5 hrs time step.

Morphological factor* (MF)*;

Unlike the flow computation, bed updating does consume much long time as it works at longer time steps (12.5 hrs) compared to the flow calculations (2.5 s). Thus, even though applying longer morphological time step, computation time does not reduce effectively. Therefore, in order to accelerate the simulation, it was decided to apply a morphological factor to reduce the computation time effectively. It was estimated that morphological factor of 10 would reduce the computation time drastically by 10 times. However, the model was not stable and failed after 5 days of simulation. It is mainly because of wetting and drying of the intertidal area over the tidal cycle. Problems encountered with the present morphological model are described in Appendix A7.

Having identified that the application of higher morphological factor in the present model has several uncertainties in prediction of the bed evolution, it was decided to run the simulation with the MF 1 and the morphological time step of 12.5 hrs.

Morphological tide;

Period of the morphological tide in this study is 24.5 hrs (~ 1 day), which represents the forcing conditions over a full spring-neap tidal cycle. However, the morphological changes have to be multiplied by a factor of 14 after simulation over each tide. This requires a morphological factor of 14 has to be applied in the model in order to scale the changes over a morphological tide. However, as the model has several uncertainties in working with morphological factors, it was decided to run the model for a number of morphological tides and compare results with those modelled over the spring-neap tides.

6. RESULTS AND ANALYSIS

6.1 Introduction

This Chapter starts with presenting the results and analysis of bathymetric changes between 2003 and 2006, which had formed the basis for the present modelling study. The model results are then presented and discussed. The analyses of the model results in this study are mainly described in three parts: typical flow and sediment transport patterns and analysis of the bed development over the simulation; comparison of the model predictions with the observations; comparisons of model results between different model runs. In addition to that, results of the sensitivity analysis for different grain sizes are also presented. Finally, the results are summarised and the overall the model performance is discussed briefly in term of predicting observed morphological changes in the system.

6.2 Bathymetric Change Analysis

Bathymetric changes between 2003 and 2006 shown in Figure 6.1 are based on the model bathymetries of the present study. From the Figure 6.1 (c) it can be seen that much of the changes have been occurred on the east Salisbury bank. Although Welsh channel shows deepened extensively, these apparent changes in bathymetry may be the results of interpolations took place to fill in the data gaps around that area.

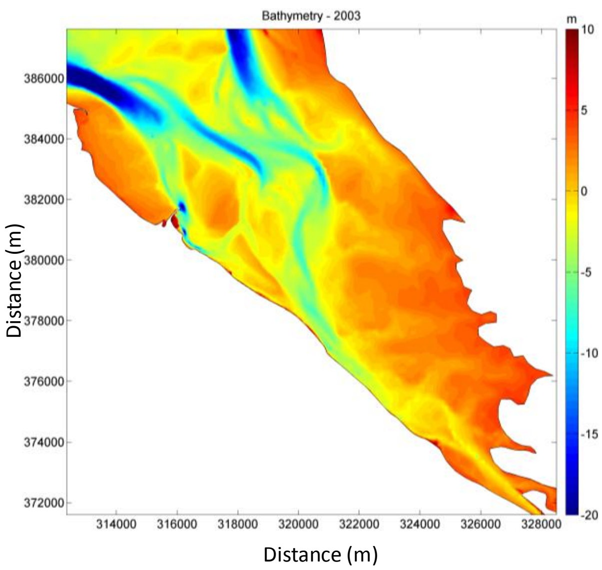

a.) Model Bathymetry – 2003

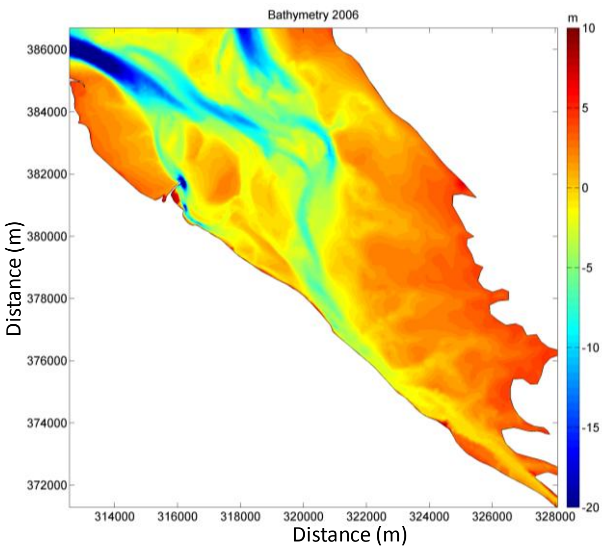

b.) Model Bathymetry – 2006

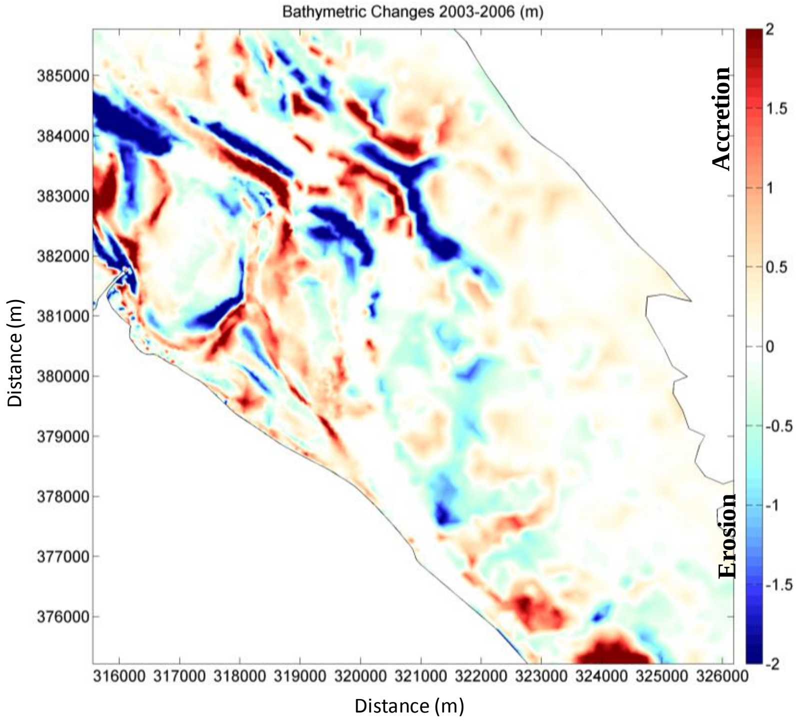

c.) Model Bathymetry difference 2003-2006

Figure 6.1 Bathymetric changes between 2003 and 2006

Since this study aims to assess the model performance objectively, quantifying the observed changes at different regions of the estuary becomes important. The bathymetric changes have been analysed in different regions of the estuary (Figure 6.2), which characterise various features such as channels, shallower areas, sand banks and mud flats. Root Mean Square (RMS) differences in bed levels at each regions of the estuary are shown in Table 6.1.

Table 6.1 RMS and Mean bed-level changes between 2003 and 2006

Bed-level (mCD)	Region of the estuary	RMS (m)	Mean (m)
< -10	A	1.98	-0.93
-10 - -5	B	1.95	-0.52
-5 - 0	C	0.65	0.45
	D	1.39	0.14
	E	1.60	0.04
	F	0.86	0.02
	G	1.33	0.14
	H	0.76	0.35
	I	0.73	-0.35
0 - 5	J	0.69	0.11
	K	0.89	0.52
	L	0.55	-0.02

* Negative and positive mean values indicates erosion and accretion respectively

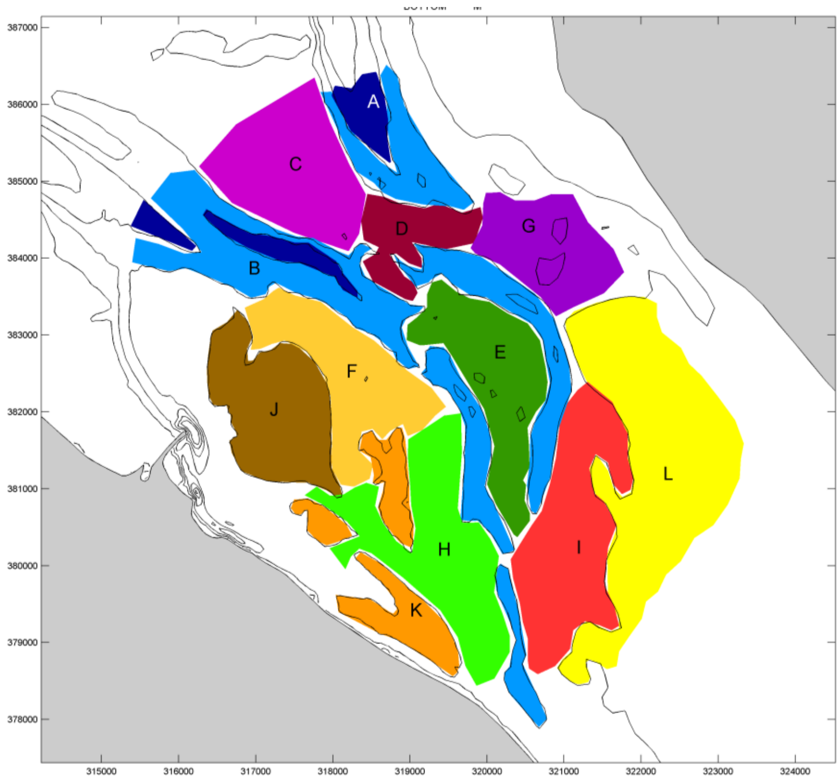

Figure 6.2 Selected regions of the estuary for analysis

Characterisation of the regions shown in Figure 6.2

- A – Deep Channels
- B – Shallow Channels
- C – Shallower banks between two deeper channels
- D – Shallower bank south of the Hilbre channel
- E – Shallower area between small channels
- F – East Salisbury bank
- G – Southeast of the Hibre channel
- H – South Salisbury bank
- I – South small channels
- J – Salisbury bank
- K – Sand banks south of the Salisbury bank
- L – Mud flats

Points of data extraction at each region for the analysis are given in Appendix. A8.

The same regions in Figure 6.2 have been used for various analyses in section 6.4 and 6.5 as well.

According to the Table 6.1, the highest bed level changes in the order to 2 m have been obtained in the channels, which are predominantly due to erosion. Region D, E and G, which are shallower areas between deeper channels, show changes around 1.5 m by accreting. Bed level changes in the areas of sand banks and mud flats are comparatively lower and are in the range of 0.5 – 1.0 m. On the whole, much of the shallower regions (above -5 mCD) have been accreted whereas, the channels are pronominally undergone erosion between 2003 and 2006. However, it should be borne in mind that these RMS and mean values are an estimate of the overall changes and direction (erosion/accretion) of changes in each region. The actual changes may therefore be higher/lower than these values, as bed-level changes are not uniform within the region.

6.3 Model Results

The main results obtained from the Morphological modelling include;

- Current pattern
- Sediment transport pattern
- Morphological development

This section presents the current and sediment transport patterns and bed-level changes obtained from the model simulation with the spring-neap boundary conditions where the morphological time step is 12.5 hrs. Bed-level changes of different model simulations are presented and discussed in sections 6.5 and 6.6.

6.3.1 Current patterns

Figure 6.3a and 6.3b shows the current vectors during a spring and neap tide respectively, the relevant tide is shown on the bottom right. A maximum current of 2 m/s has been obtained in Welsh Channel during the spring tide, whereas it declines in the order of 0.1 m/s during the neap. There is a notable difference in the area flooded during the spring and neap. Almost 95% of the estuary area being flooded during the spring tides whereas; at least two-third of the area with saltmarshes and sandbanks are exposed during the neap tides.

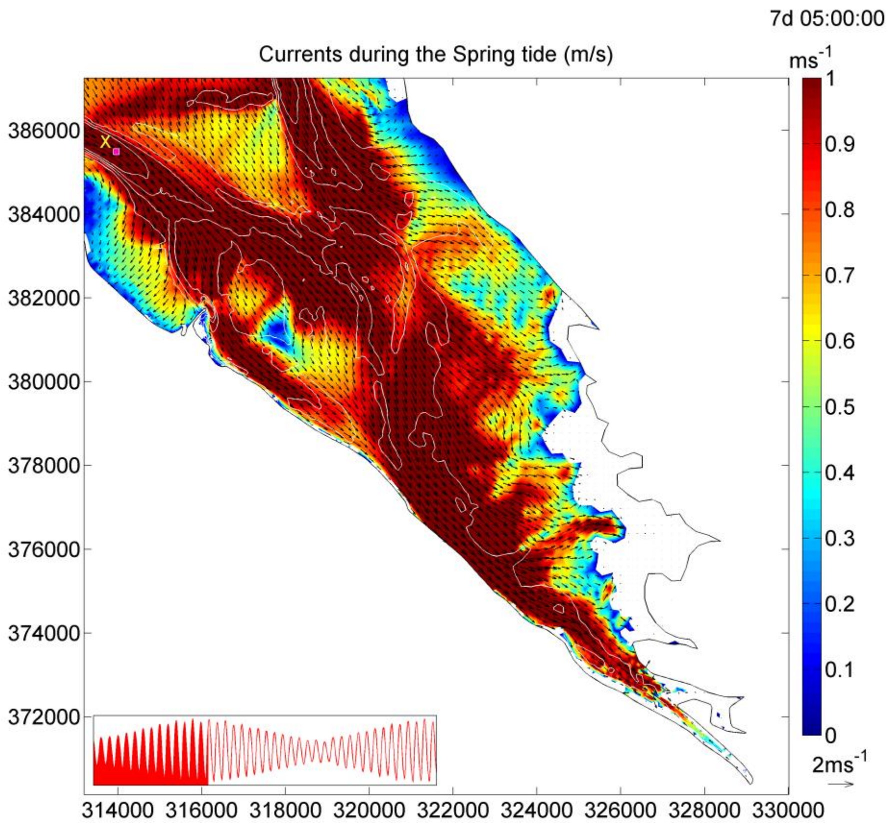

a) Current pattern during Spring tide

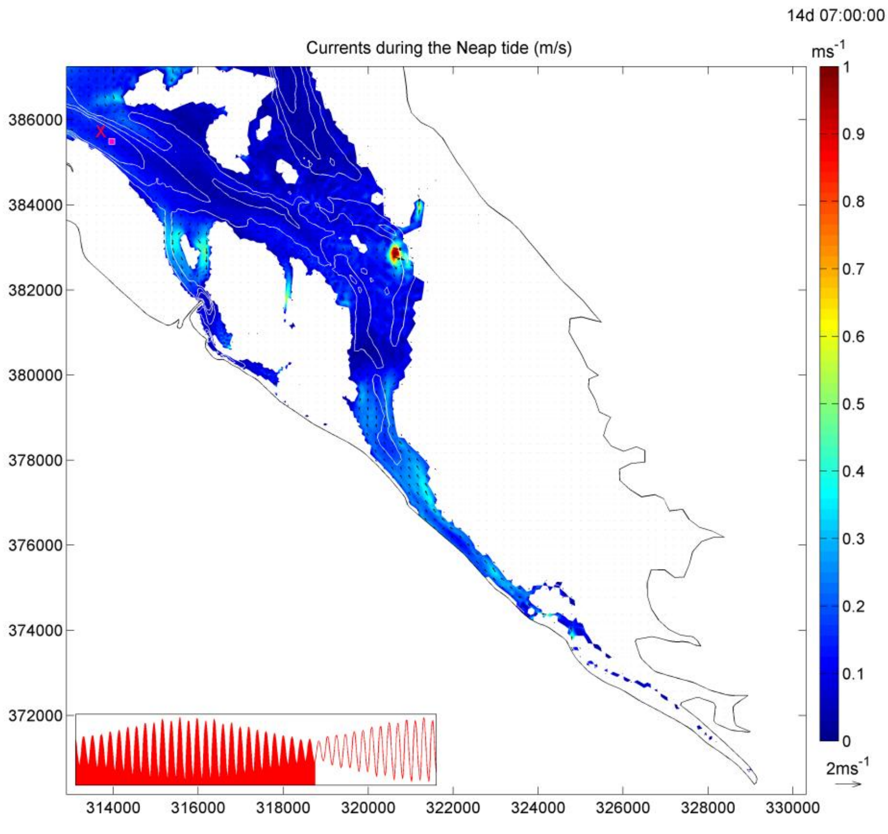

b) Current pattern during neap tide

Figure 6.3 Current Patterns during spring and neap tides

6.3.2 Sediment transport pattern

Figure 6.4 shows the net sediment flux during the spring tide. High rates of transport can be seen in the vicinity of the convergence of Welsh and Hilbre Channels, where the bed level changes also observed to be higher in this area. The sediment transport fluxes increases along the channel, south of the Salisbury Bank. Again, it was observed that the transport rate under neap tides is an order of magnitude lower than under spring tide. Over the entire estuary the net sediment transport is in the direction of the flood tide. During the neap tide of the cycle there was hardly any sediment movements observed in the model.

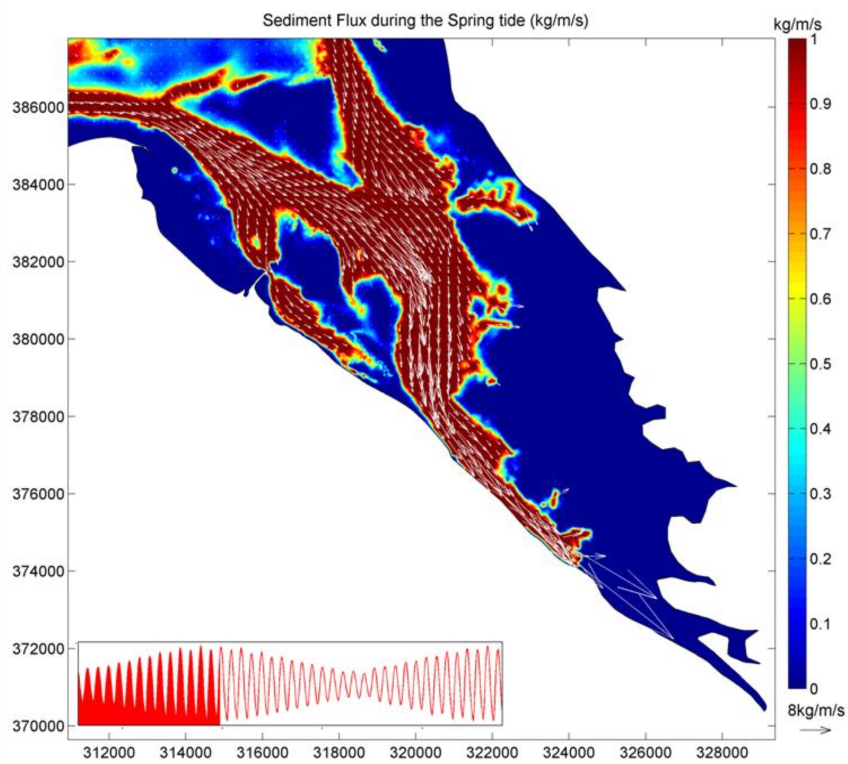

Figure 6.4 Sediment flux during the spring tide

6.3.3 Morphological Changes

The morphological changes obtained after simulation over a spring-neap tidal cycle is shown in figure 6.5. Contours shown in the model results are based on the bed-levels at the beginning of the simulation. Mostly, erosion and accretion have occurred at the areas, east side of the Salisbury Bank, where it was already identified as energetic from the observations. It can be clearly seen that much the shallower areas between the channels has been eroded and the material been deposited in the adjacent deepest part of the channels. This effect is clearly visible in the region of south Hilbre

Channel. Whereas, in real situations, possibly water flow can occur over or around a bump instead of eroding the raised areas.

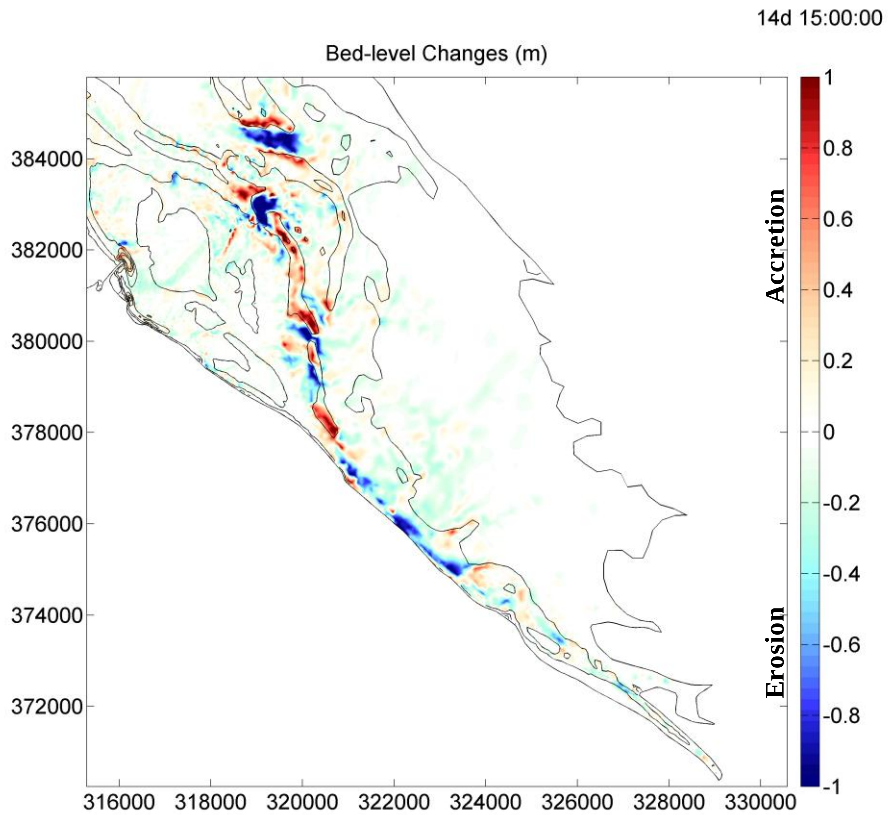

Figure 6.5 Morphological changes after a spring-neap cycle

In Figure 6.6, cumulative bed level changes at different stages of the simulation are illustrated. Much of the morphological changes have occurred during the first two spring-neap cycles (~28 days), are clearly visible (Figure 6.5). On the top right of the each Figure indicates the simulation time. After 4 spring-neap cycles, there is hardly any differences in cumulative bed-level changes. In order to quantify this effect, time series of bed-levels and cumulative bed-level changes were extracted at several locations from the model results.

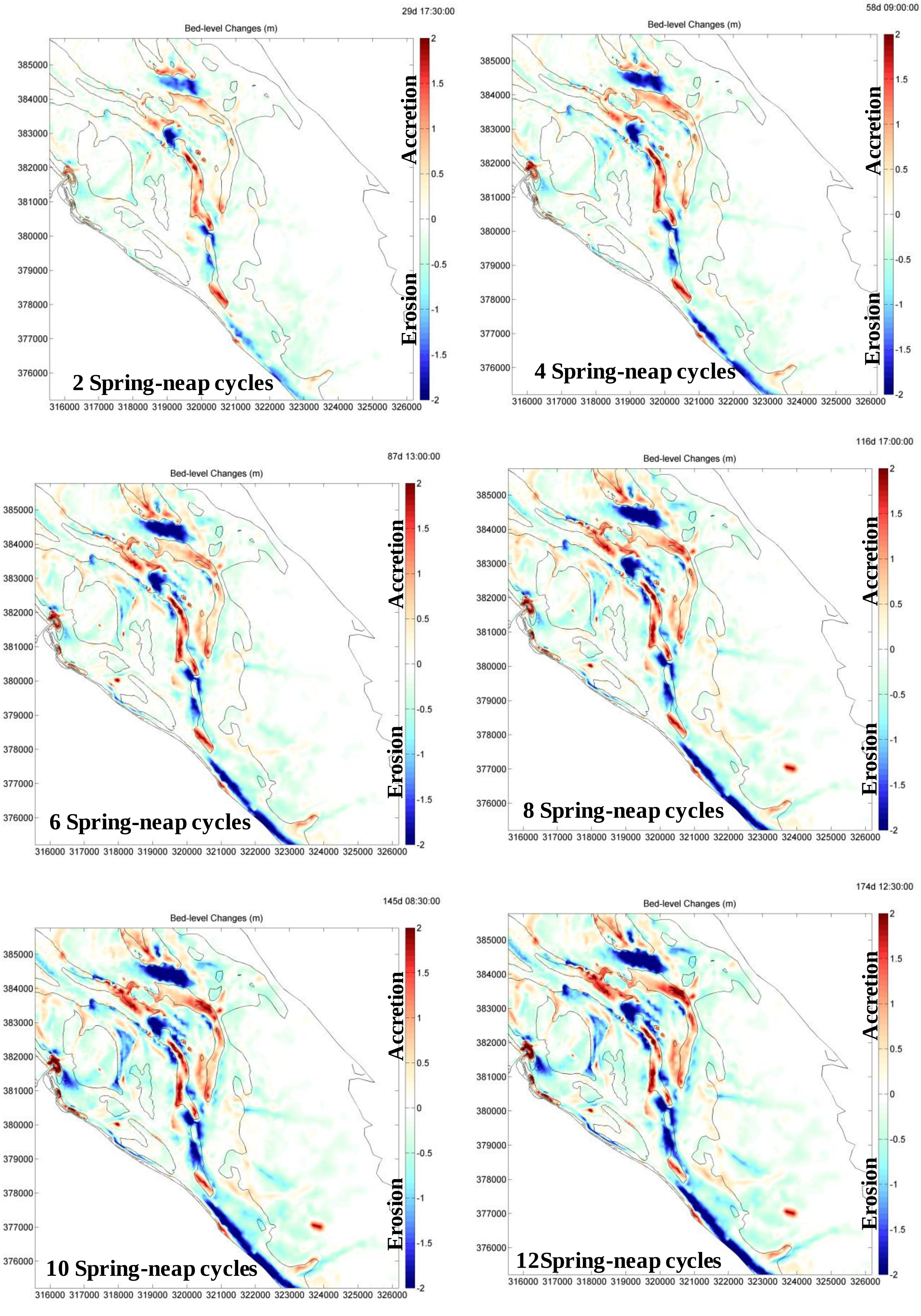

Figure 6.6 Different stages of morphological changes predicted over the simulation

Figure 6.7 displays points of data extraction, selected from each region (Figure 6.2). The trend of bed-level development and cumulative bed-level changes over the time (number of full spring-neap tidal cycles simulated) are presented in Figure 6.8 and 6.9 respectively. Each spring-neap cycle represents approximately 14.5 days.

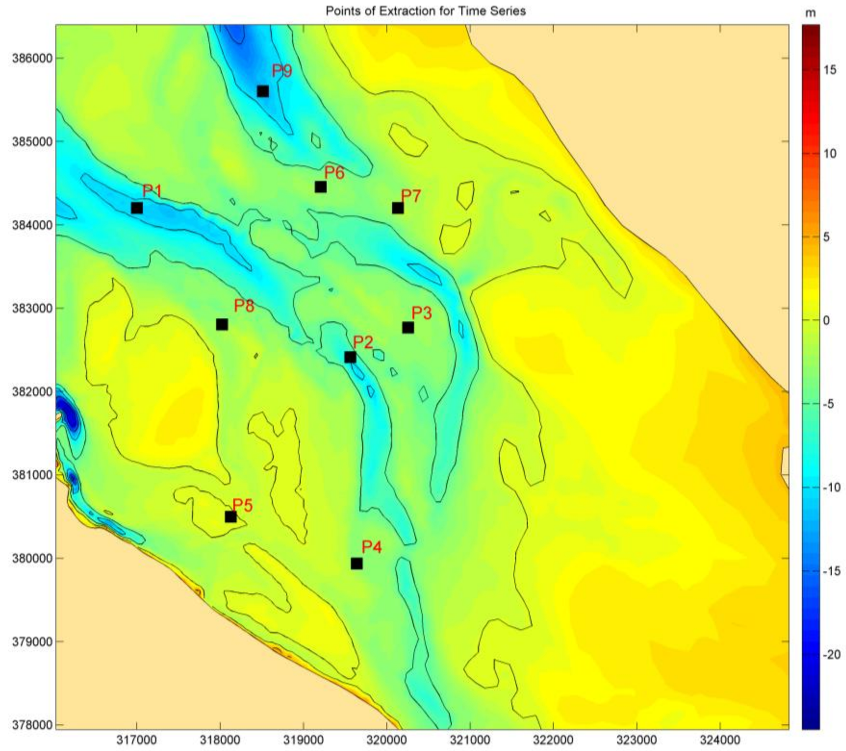

Figure 6.7 Locations of time series extraction

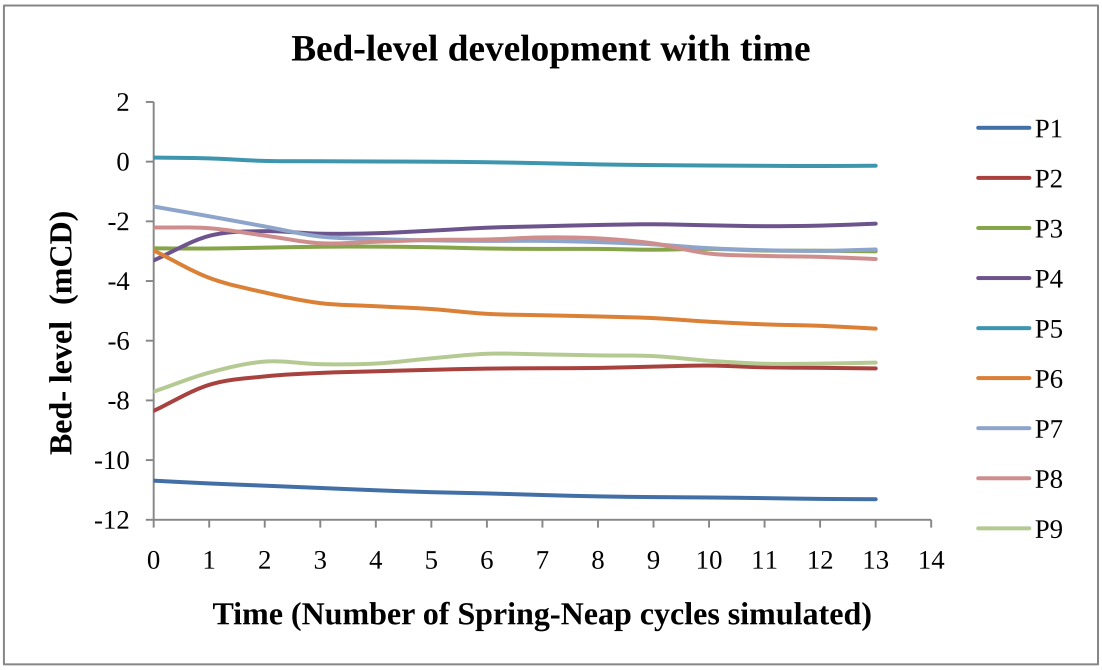

Figure 6.8 Bed-level developments with time

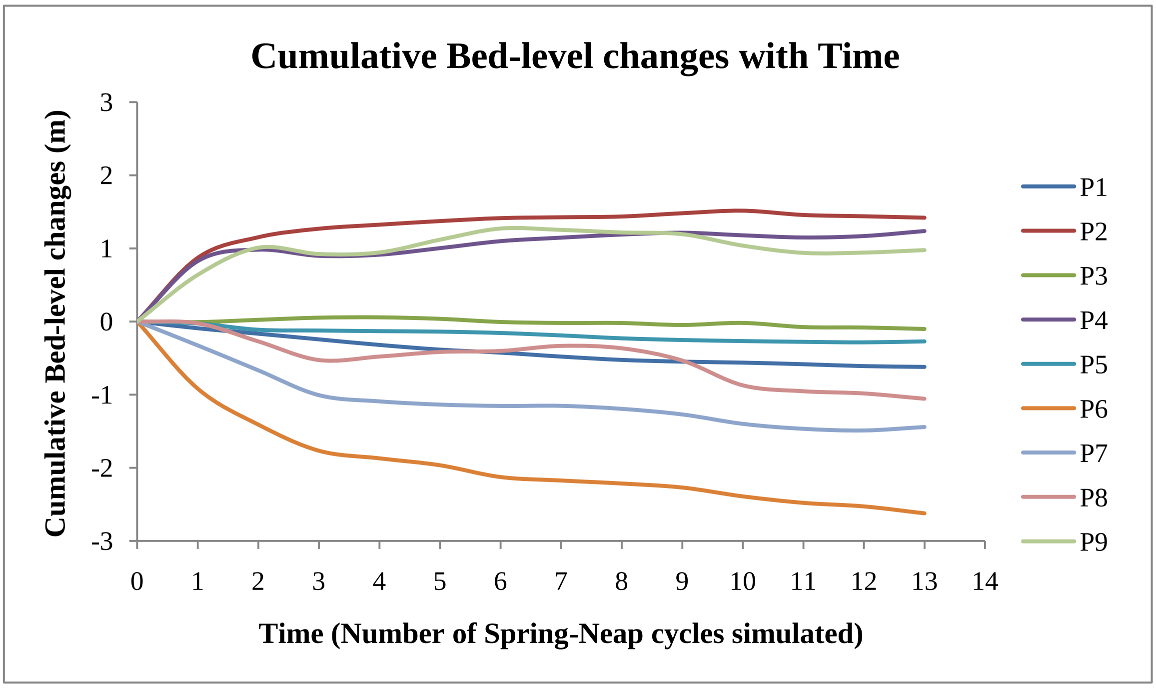

Figure 6.9 Cumulative bed-level changes with time

In figure 6.8, it is notable that bed-levels at P2, P4, P6, P7 and P9 indicates rapid changes during the first couple of spring-neap tidal cycles (~28 days). As shown in Figure 6.6, these locations are being energetic from the beginning of the simulation. Whereas at locations P1, P3 and P5 the changes are not significant as these locations slowly evolve with time. The bed-level at P6 (south of the Hilbre Channel) has been eroded up to 1.5 m within a month simulation which may not be the case in real situation. This effect also reflects in Figure 6.6 as well.

Cumulative bed-level changes at each location are shown in Figure 6.9. Apparently the model does initialisation at the beginning of the simulation which in turn leads to enormous changes in the bed-levels in the order of 1-2 m within first couple of spring-neap tidal cycles. These changes gradually decrease in the subsequent period of the simulation, and after the period of 10 spring-neap cycles remain constant, except at P6 where the bed erodes continuously throughout the simulation period. This implies even the simulation continues for the rest of the period (up to three years), hardly any variations from this trend is expected.

Fluctuations at P9 may be due to sediment exchanges between the Hilbre Channel and the adjacent shallower region after the initialisation, whereas the reason for the fluctuation at P8 is unclear.

6.4 Comparison of Model Predictions with the Observations

In principle, morphological simulation must be completed for the entire simulation period of 3 years and 4 months (80 spring-neap cycles) to compare the model results with the observations. However, due to various uncertainties associated with the application of morphological factor in this study (as discussed in section 5.6 and 6.3.4), model simulation was unable to complete within this study period.

Hence it was decided to use the available model results which, have been simulated for 6 months period (12 spring-neap tidal cycles) with the morphological factor 1 and morphodynamic time step 12.5 hrs, to make comparison with the observations. Here observations are extracted from the model bathymetry of 2006. Linearising the observed changes (Figure 6.1c) for the 6 months period gives morphological changes as shown in Figure 6.10a. Comparing these linerarised observations with the model predictions (Figure 6.10b) indicates that the model results seem to be over predicting the morphological changes when compared to observations. The main reason for this is, as demonstrated in section 6.3.3; the model does initialisation at the beginning of the simulation leads to higher morphological changes. Therefore, linearising the changes would completely misinterpret the model performance.

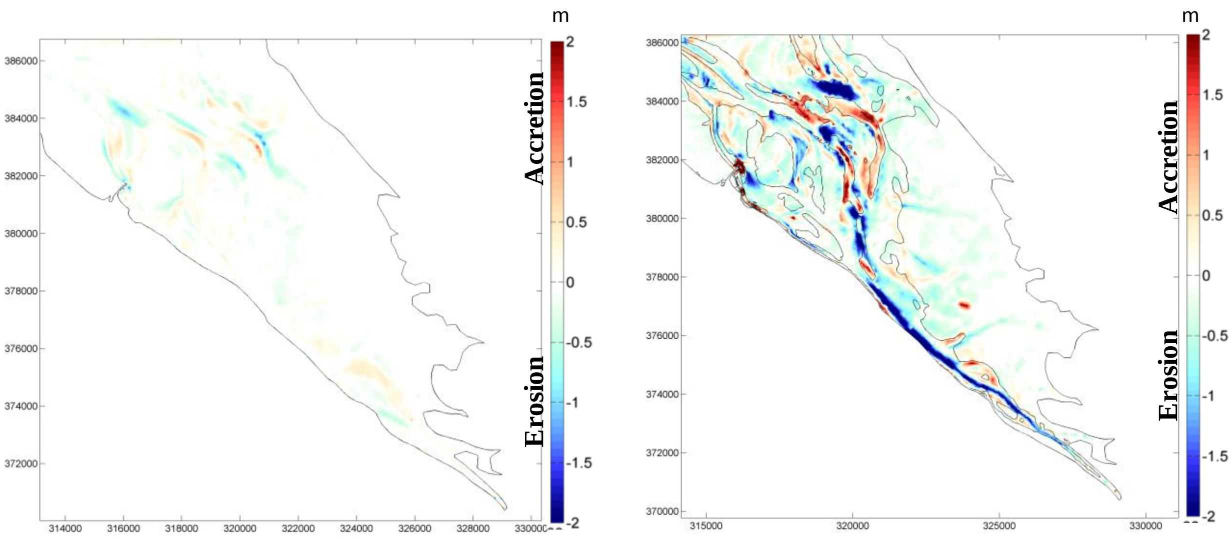

a.) Linearised observed changes

b.) Model predicted changes

Figure 6.10 Comparison of model predicted morphological changes after 6 months with the linearised observed changes

Model predictions are then compared with the complete observations (without linearising) quantitatively using the Brier Skill Score (BSS) approach discussed in 3.6.1. In this circumstance, it is anticipated that the model predictions might under predict the changes as the model results were obtained after 6 months simulation period only, this is almost 6 times lesser compare to the period of observed changes (more than 3 years). However, this comparison allows investigating whether the model at least does the prediction of morphological changes in the right direction.

Brier Skill Scores (BSS) are calculated based on the standard formula given by Sutherland et al. (2001) and Van Rijn's method (2003) which includes the measurement error. Therefore, in order to satisfy the conditions given in Equation (4.6), the data was filtered to exclude the points where the difference between the modelled and observed bed-level changes is less than the measurement error. From Equation 4.2 and 4.6 these can be written as;

$$BSS = 1 - \frac{\frac{1}{j}\sum_{j=1}^{j}(b_o - b_m)^2}{\frac{1}{j}\sum_{j=1}^{j}(b_o - b_i)^2} \qquad (6.1)$$

$$BSS_{vr} = 1 - \frac{\frac{1}{j}\sum_{j=1}^{j}(|b_m - b_o| - \delta)^2}{\frac{1}{j}\sum_{j=1}^{j}(b_i - b_o)^2} \qquad (6.2)$$

where b_o = observed bed-level (2006) ; b_m= model predicted bed-level; b_i = initial bed-level (2003); and, δ = measurement error (0.15 m)

The Brier Skill Sores of the model performance relative to the initial conditions are presented in Table 6.2. The different regions of the estuary are referred to Figure 6.2. (Extracted points at each region are shown in Appendix. A7)

From Table 6.2 both BSS and BSS_{vr} are positive in regions of A and B. According to the BSS classification Table 3.1, the model performance is reasonable in channels. Whereas, they are positive in the shallow areas between channels (E) and south of the Salisbury Bank (H), giving highest scores, and the model predictions are good in these regions. Both methods give negative scores in regions D, I and J particularly, region D gets higher negative score. This implies the model performance is very poor in region D, the reason is model behaves unrealistically, eroding the sand bank south of the Hilbre Channel, as it has already been noted in section 6.3. It is notable that Van Rijn's method gives improved skill scores compare to the standard method, though it falls into the same classification as the standard BSS does except in region L, where the BSS_{vr} indicates reasonable model performance. This might be including the measurement error in BSS_{vr} tending to reduce the numerator in Equation (6.2), so improving the BSS_{vr} values calculated.

Table 6.2 BSS for model performance relative to the initial conditions

Bed-level (mCD)	**Region**	**BSS**	**BSS_{vr}**
< -10m	A	0.19	0.33
-10 - -5m	B	0.13	0.28
-5 - 0m	C	-0.27	0.22
	D	-1.26	-0.83
	E	0.16	0.33
	F	-0.22	0.18
	G	-0.33	0.08
	H	0.37	0.57
	I	-1.30	-0.39
0 - 5m	J	-0.54	-0.03
	K	0.03	0.26
	L	-0.29	0.34

Scatter plots that compare the bed-level changes predicted by the model with the observed bed-level changes, are given in Appendix. A9.

Trends of the BSS with time have been examined at randomly selected locations (Figure 6.7) from each of the above regions (Figure 6.2), and shown in Figure 6.11. This plot shows how the Brier Skill Scores varies over the simulation. X-axis shows number of spring-neap cycles simulated during the modelling.

It should be borne in mind that the magnitude of the BSS values are not comparable with the ones shown in Table 6.2 as the trends shown in Figure 6.11 just represent the single location in each region whereas, the BSS values obtained in Table 6.2 are based on several numbers of points in each region.

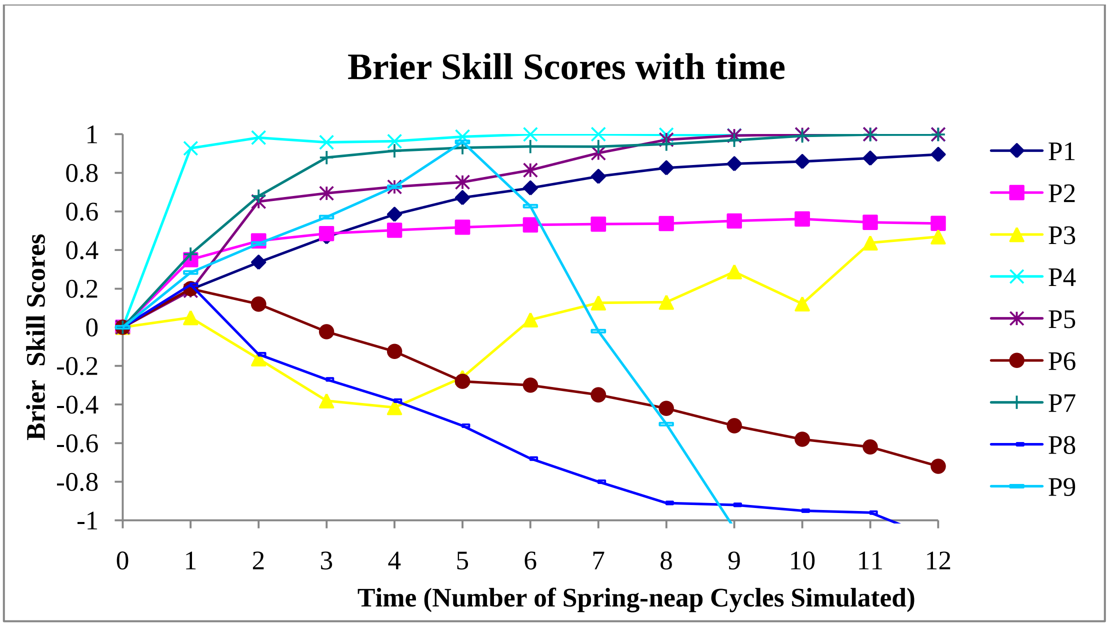

Figure 6.11 Trends of Brier Skill Score with time

In Figure 6.11, it can be seen that BSS values increases from zero at the at locations P1, P4, P5 and P7 and reaches close to 1 after the simulation over 12 spring-neap cycles (~175 days). This indicates the model predictions in those locations are getting closer with the observations when continuing the simulation over longer time period. This is consistent with the positive BSS values obtained in corresponded regions in Table 6.2. Though BSS tend to give positive values at locations at P2 and P3, it is hard to predict that the BSS values would reach close to 1 at these locations when continuing the simulation further long period.

In contrast, it can be definitely say that the model predictions at P6, P8 and P9 are away from the observations even the simulation continues further, BSS would have no possibilities to improve or getting positive values. The reasons for this can be either the model predictions are in wrong direction or over predicting the morphological changes at those locations. Following reasons can be said for the BSS trends at P6, P8 and P9.

- P6 – the reason is very clear that the model behaves unrealistically in that region as discussed before. Because of higher erosion in that region tend to gives negative BSS.
- P8 – At this location the model starts to over predict the changes after simulation of 1st spring-neap cycle.

- P9 – model predictions at this location is in the right direction until 5 spring-neap cycles (~70days) as the BSS gradually increases up to 1, and then BSS declines and gets negative values during rest of the simulation period. This is because the model starts to over predict the changes after ~70days simulation.

Visually examining the model predicted and observed morphology (Figure 6.12) gives following trends (channels are shown in same Figure);

- Model has connected the Hilbre Channel and the channel immediately south (C_1) by eroding the shallow area that was in between these two channels. The eroded material has been deposited into both deeper area of Hilbre channel and channel C_1. In reality, these two channels are not being connected and the channel (C1) tends to migrate eastward. This behaviour of the model leads to huge uncertainty in reproducing the observed morphological changes.
- The shallower area along east side of the Salisbury Bank has been deepened and it has stretched further down in the model. Whereas, the observations in that region does not show such behaviour apparently.
- Salisbury Channel has connected with the channel immediately south (C2) in both model and observed bathymetry. Similarly, the channels C1 and C2 have converged in both model predicted and observed morphology. But the in the model converging point is slightly further southward and unlike the natural shape channels are becoming straighten point.

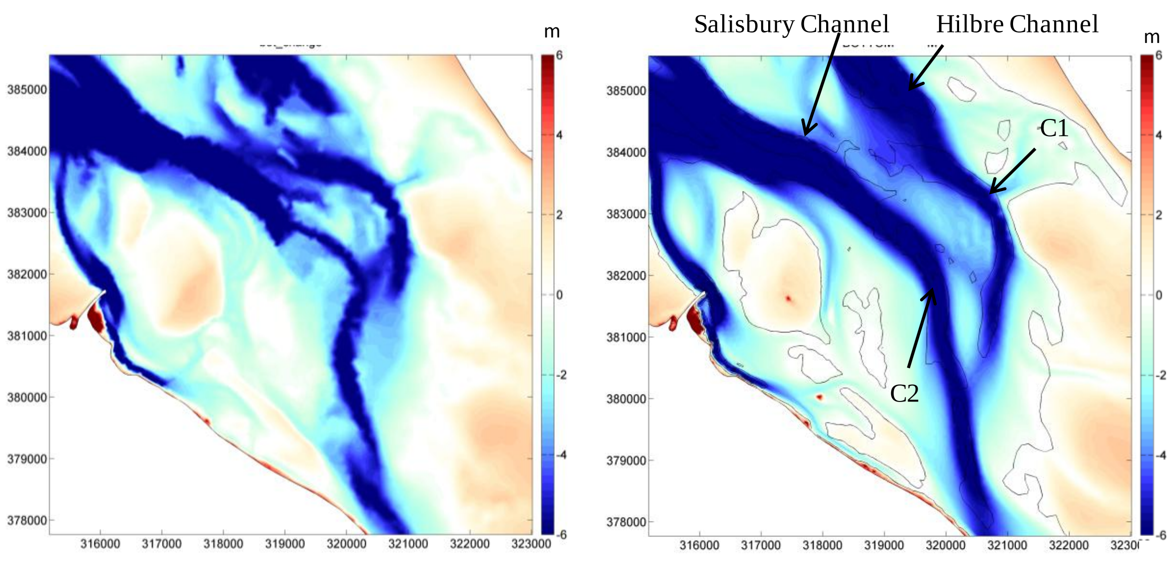

a.) Observed morphology b.) Model predicted morphology

Figure 6.12 Observed and model predicted morphology

6.5 Comparison of morphological changes between model results

Morphological simulations were carried out for different modelling scenarios given in Table 6.3. This section presents the results and compares between model results to assess the performance of the model for different tidal conditions, morphological factor and morphological time steps.

Table 6.3 Different Modelling scenarios

Scenario No.	Tides	Morphological Factor	Morphological time step (hrs)	Simulation period (days)
1	Spring-neap tide	1	12.5	70
2	Morphological tide	1	12.5	70
3	Spring-neap tide	2	12.5	70
4	Spring-neap tide	1	12.5	14
5	Spring-neap tide	1	1	14

6.5.1 Different types of boundary conditions

This section compares the model results obtained from first two scenarios shown in Table 6.2 in order to examine the model performance of morphological tide relative to the spring-neap tide. Figure 6.13 shows the bed-level changes obtained after simulation of 5 spring-neap cycles (~70 days) for the spring-neap and morphological the tides. All the other parameters were kept to be same in the model.

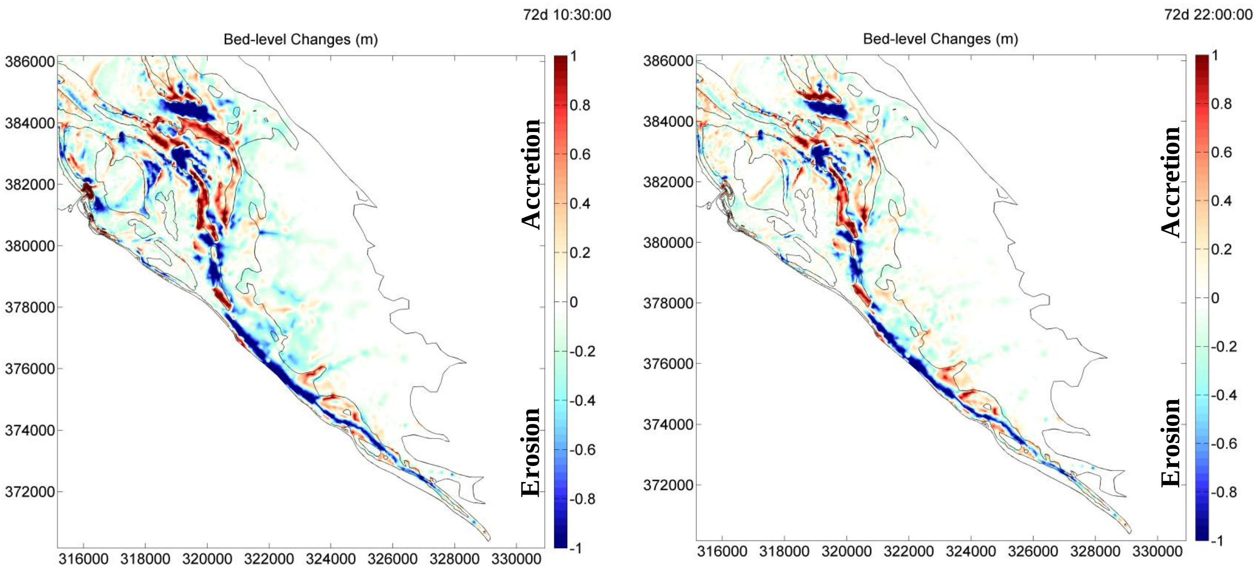

a.) Spring-neap tides b.) Morphological tide

Figure 6.13 Comparison of Bed-level changes for different tidal conditions

Figure 6.13 shows morphological tides produce the overall patterns of bed-level changes as the over the spring-neap tides, but morphological changes are lower in magnitude. Particularly, erosion on the south of the Hilbre Channel and along east side of the Salisbury bank is slightly lower in the case of morphological tide compared to the other case. One of the major differences is, morphological tide has produced very little accretion on the channel immediately south of the Hilbre Channel whereas; there is relatively very high accretion predicted in the spring-neap tide case.

In principle, the sediment transport rate is high during the spring tide of the tidal cycle and much of the morphological changes are predominantly due to spring tide. Alternatively, morphological tide has the tidal range lower than the spring-neap tidal range, and gives constant forcing throughout the modelling loosing the dynamism. This might be the reason for the above differences in predicted morphology.

The morphological changes in both cases have been compared at different regions (Figure 6.2) with the aid of scatter plots shown below.

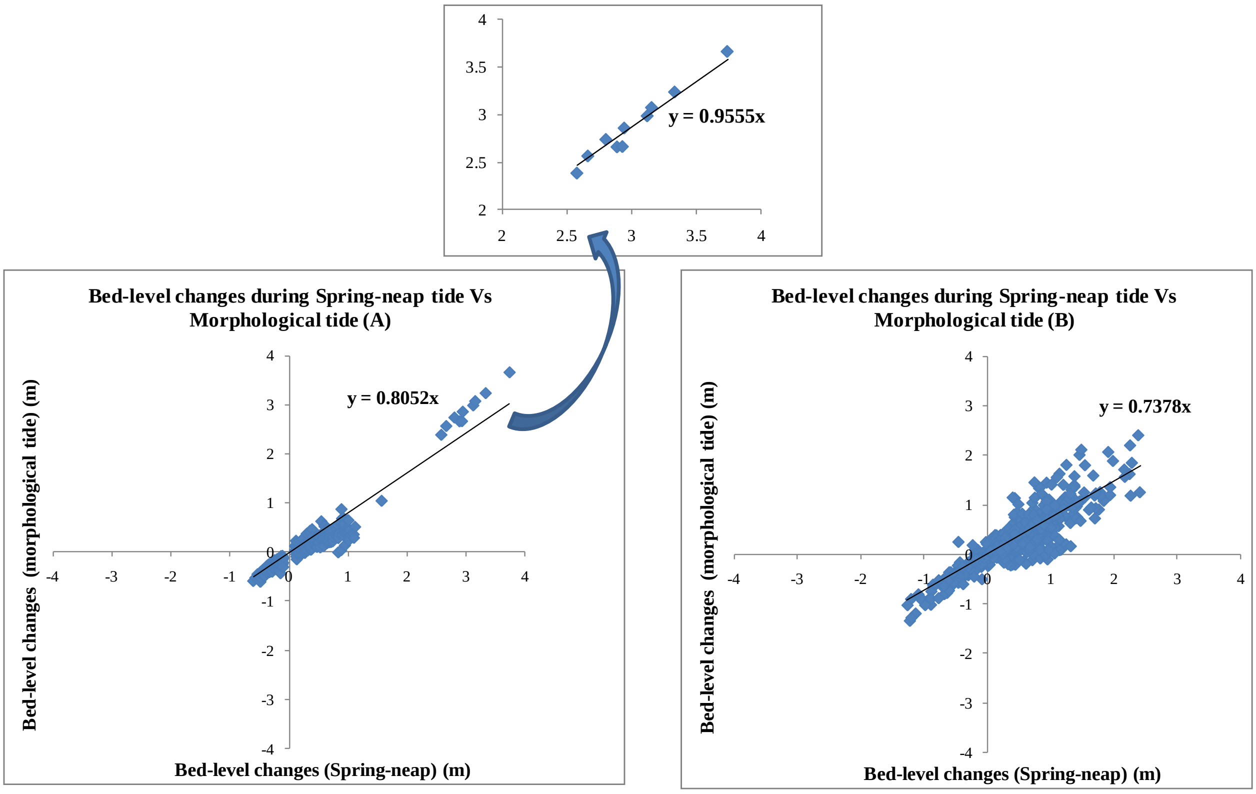

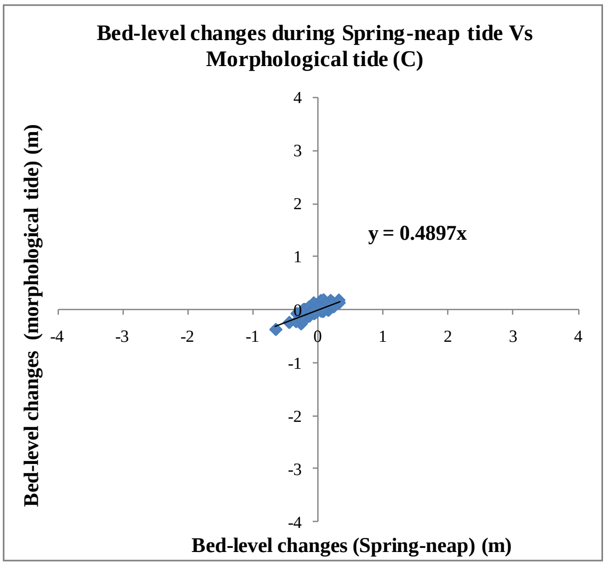
Bed-level changes during Spring-neap tide Vs Morphological tide (C)
y = 0.4897x
Bed-level changes (morphological tide) (m)
Bed-level changes (Spring-neap) (m)

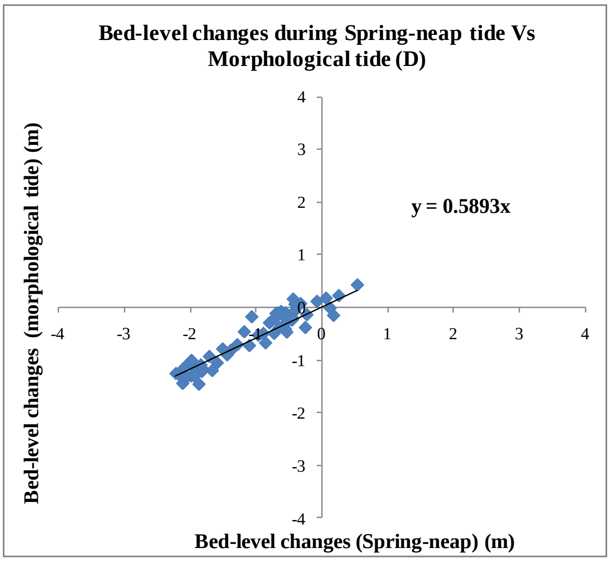
Bed-level changes during Spring-neap tide Vs Morphological tide (D)
y = 0.5893x
Bed-level changes (morphological tide) (m)
Bed-level changes (Spring-neap) (m)

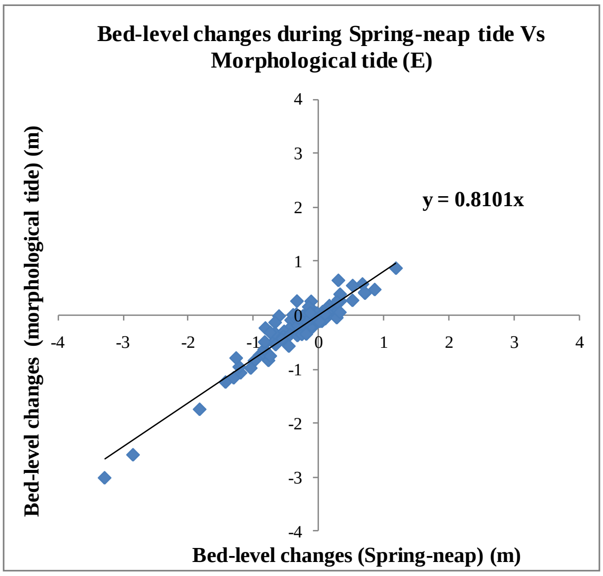
Bed-level changes during Spring-neap tide Vs Morphological tide (E)
y = 0.8101x
Bed-level changes (morphological tide) (m)
Bed-level changes (Spring-neap) (m)

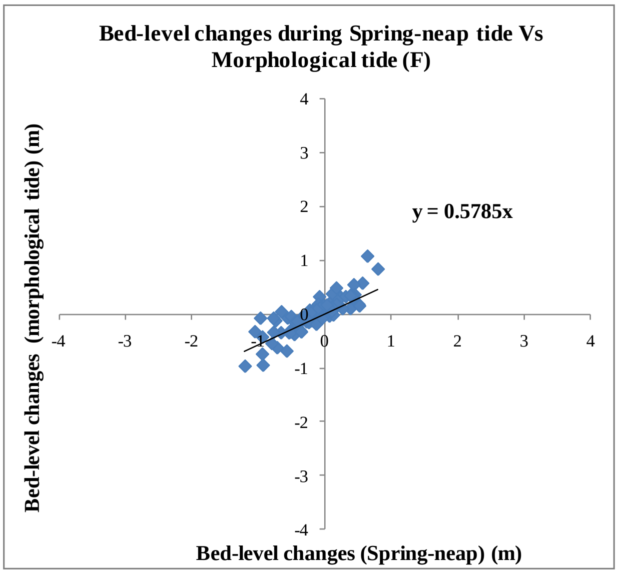
Bed-level changes during Spring-neap tide Vs Morphological tide (F)
y = 0.5785x
Bed-level changes (morphological tide) (m)
Bed-level changes (Spring-neap) (m)

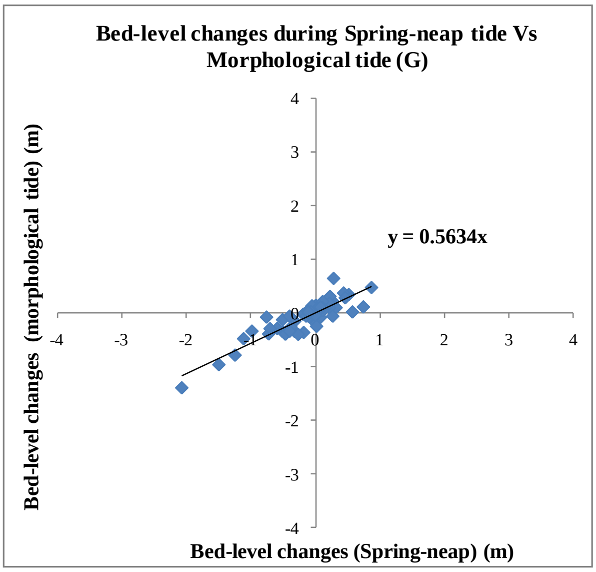
Bed-level changes during Spring-neap tide Vs Morphological tide (G)
y = 0.5634x
Bed-level changes (morphological tide) (m)
Bed-level changes (Spring-neap) (m)

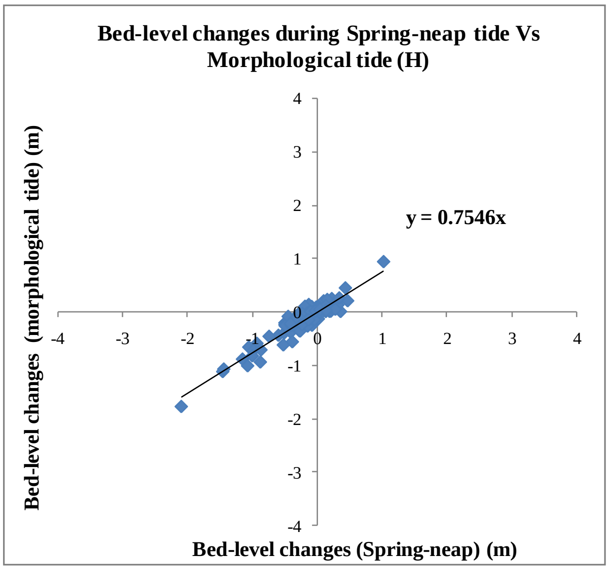
Bed-level changes during Spring-neap tide Vs Morphological tide (H)
y = 0.7546x
Bed-level changes (morphological tide) (m)
Bed-level changes (Spring-neap) (m)

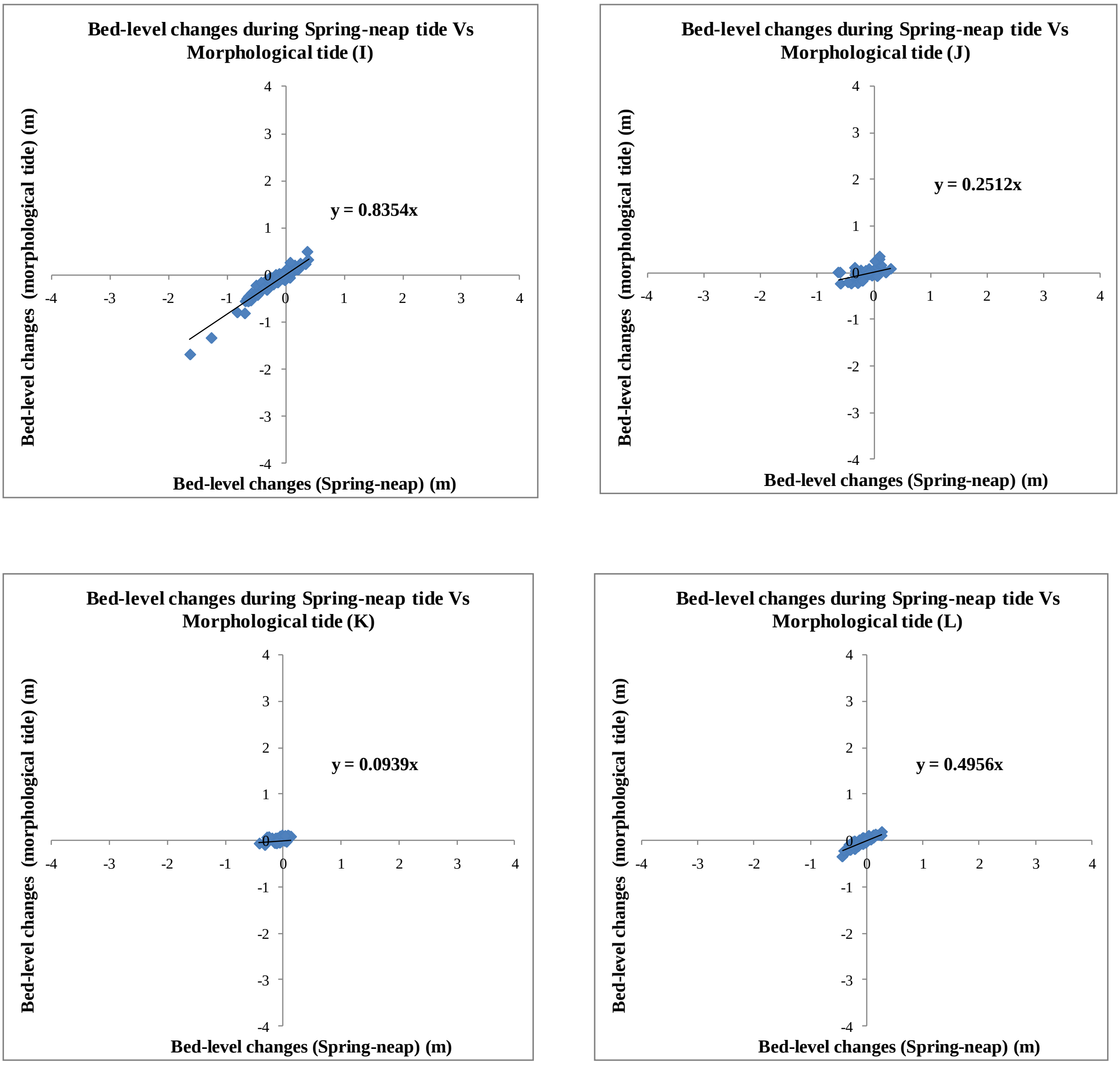

Figure 6.14 Scatter plots of bed-level changes for spring-neap and morphological tides

There is a good agreement obtained for the predicted bed-level changes between morphological and spring-neap tide cases at regions A, E, H and I with the correlation coefficient more than 0.8. Interestingly, in deep channels (A), it gives very good correlation when the changes are more than 2m (as shown Figure 6.13 for region A). Similarly, at region E there is a good relationship between the predicted morphological changes by both cases. In contrast, morphological tide predictions are poor at shallower regions (C, D, F and G) and very poor at sand banks and mudflats (J, K and L). The plot relevant to region D implies that the morphological tide prediction are almost 40% lesser than the predicted by spring-neap tide. Moderate agreement has been obtained at region B, where the bed-level changes are highly scattered. This is consistent with the Figure 6.13, as the accretion on the channels (adjacent to the banks) is not being reproduced in the morphological tide case.

Brier Skill Score (BSS) assessment at each of the above regions was performed assuming the bed-levels predicted by the spring-neap tide represents the ideal case. Following equation can be written for this case based on equation (4.2). In this case, the skill scores compare the mean square difference between morphological and spring-neap predicted changes with the mean square changes predicted by spring-neap tide.

$$BSS = 1 - \frac{\frac{1}{j}\sum_{j=1}^{j}\sum (b_{mor} - b_{spnp})^2}{\frac{1}{j}\sum_{j=1}^{j}(b_i - b_{spnp})^2} \qquad (6.3)$$

where, b_{mor} - Bed-level predicted by morphological tide; b_{spnp}- Bed-level predicted by the spring-neap tide; and b_i – Initial bed-level (2003)

Table 6.4 Brier Skill Scores for performance of the morphological tides

Bed-level (mCD)	Region	Brier Skill Score
< -10	A	0.89
-10 - -5	B	0.82
-5 – 0	C	0.68
	D	0.81
	E	0.91
	F	0.67
	G	0.74
	H	0.89
	I	0.92
0 - 5	J	0.29
	K	0.12
	L	0.72

From Table 6.4, BSS values shows agreement with the results obtained in scatter plots except at region D, where it gives very good scores. The reason may be BSS values mainly depend on the denominator of the Equation (6.3), when the denominator (actual changes) is relatively larger than the numerator (difference between the predictions), it tends to give higher scores. In this case bed-level changes obtained at D during the spring-neap tide $(b_i - b_{spnp})$ are relatively larger than $(b_{mor} - b_{spnp})$. Therefore, Brier Skill Score gives relatively higher value at this region D despite there can be seen considerable differences between morphological changes produced by spring-neap and morphological tides.

6.5.2 Different Morphological Factors

In this section, the morphological changes obtained from 1st and 3rd scenarios in Table 6.3 are compared in Figure 6.14. This examines the differences in morphological changes when applying morphological factor (MF) 2 when compared to results from factor 1. The results are obtained after simulation over 5 spring-neap cycles (~70 days).

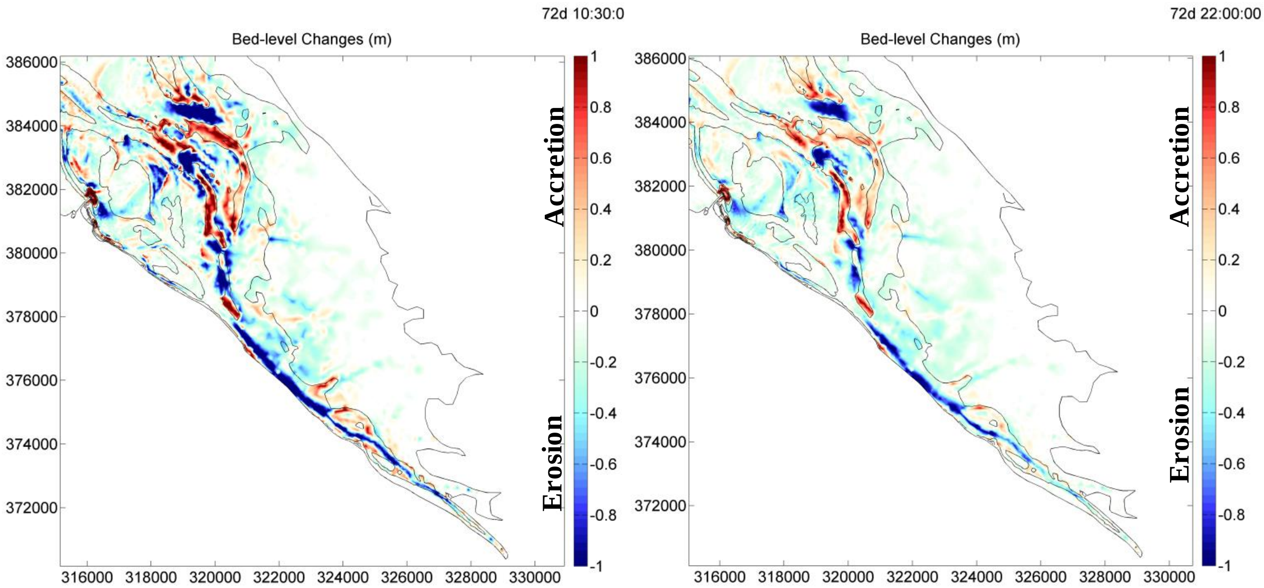

a.) Morphological changes for MF 1 b.) Morphological changes for MF 2

Figure 6.15 Comparison of Morphological changes for different morphological factors

It can be clearly seen from Figure 6.14 that the overall erosion and accretion patterns in the case of MF 2 are identical to the case of MF 1. However, morphological changes result from MF 2 is lower in magnitude. Particularly, accretion on south of the Hilbre Channel is significantly lower in the case of MF 2. Scatter plots at key regions (A, B, D, E) compares the bed-level changes obtained in both cases (refer Figure 6.2 for regions) are shown in Figure 6.15.

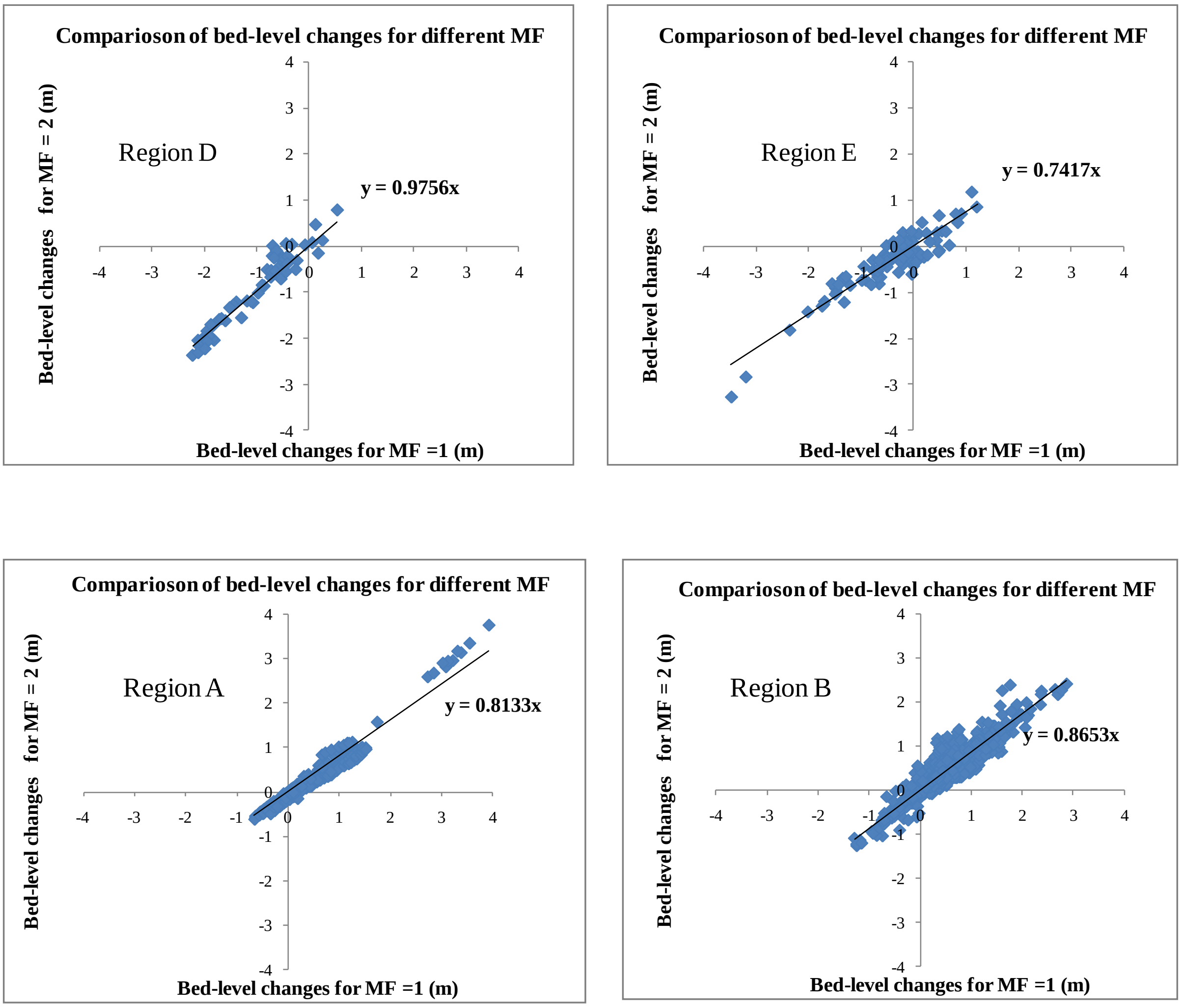

Figure 6.16 Scatter plots of bed-level changes for different morphological factors

In Figure 6.15, scatter plots reflect the above discussion as the correlation coefficients are below 1. This also implies that morphological factor (MF) of 2 predicts the bed-level changes considerably lower than those predicted by MF 1. This behaviour is also shown by calculating Brier Skill Scores at all the regions (Table 6.5). BSS values indicate there is a excellent agreement exist between the predictions of MF 1 and 2 except shallower sand banks and mudflats. BSS values always stand less than unity, which means MF 2 is predicting lower erosion or accretion.

In this case BSS is given by;

$$BSS = 1 - \frac{\sum(b_{MF1} - b_{MF2})^2}{\sum(b_i - b_{MF1})^2} \qquad (6.4)$$

where, b_{MF1} - Bed-level predicted with MF1; b_{MF2} - Bed-level predicted with MF2; and b_i – Initial bed-level (2003)

Table 6.5 Brier Skill Scores for performance of the morphological factor of 2

Bed-level (mCD)	Region	Brier Skill Score
< -10m	A	0.91
-10 - -5m	B	0.89
-5 - 0m	C	0.75
	D	0.97
	E	0.78
	F	0.79
	G	0.93
	H	0.86
	I	0.94
0 - 5m	J	-0.25
	K	-1.26
	L	0.79

Although morphological factor 2 predicts the overall pattern similar as the factor 1 does, the reason for lower in magnitude is unclear. More investigation is required to identify the main cause that lowers the morphological changes in the MF 2 case compared to the case of MF 1.

6.5.3 Different Morphological Time Step

The scenarios 5 and 6 in Table 6.3 are considered in this section. Figure 6.16 compares the morphological changes obtained for 1 hr and 12.5 hrs morphological time steps. On the whole, although morphological pattern is similar in both cases, yet notable differences in region south of the Hilbre Channel can be seen. Morphological time step 1 hr has shown lower erosion in that region and slightly lower accretion to the channel immediately down. Figure 6.17 compares the bed-level changes modelled over a spring-neap cycle obtained at X in both cases (the tidal signal is shown below in the same Figure 6.17).

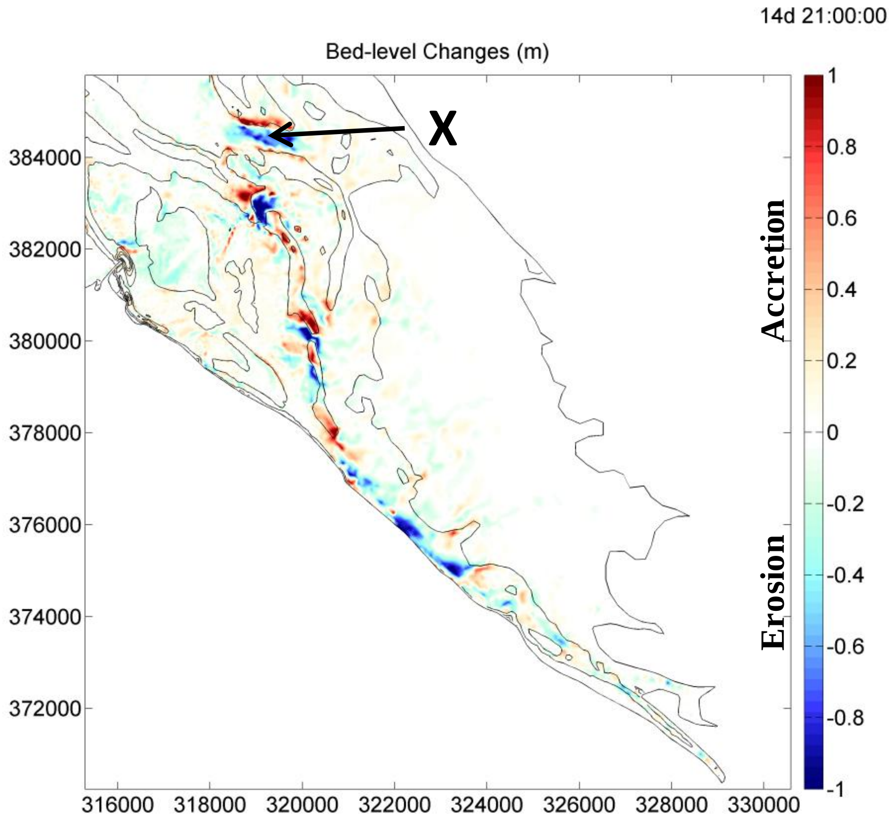

a.) Morphological changes ($\Delta t_{mor} = 1$ hr)

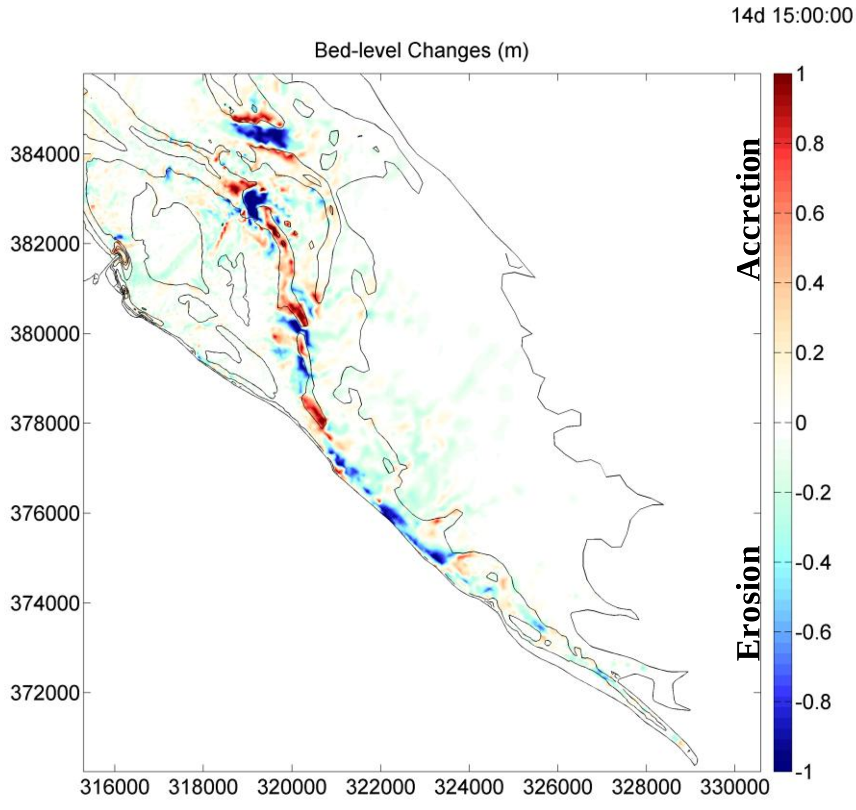

b.) Morphological changes ($\Delta t_{mor} = 12.5$ hr)

Figure 6.17 Comparison of morphological changes for different morphological time steps

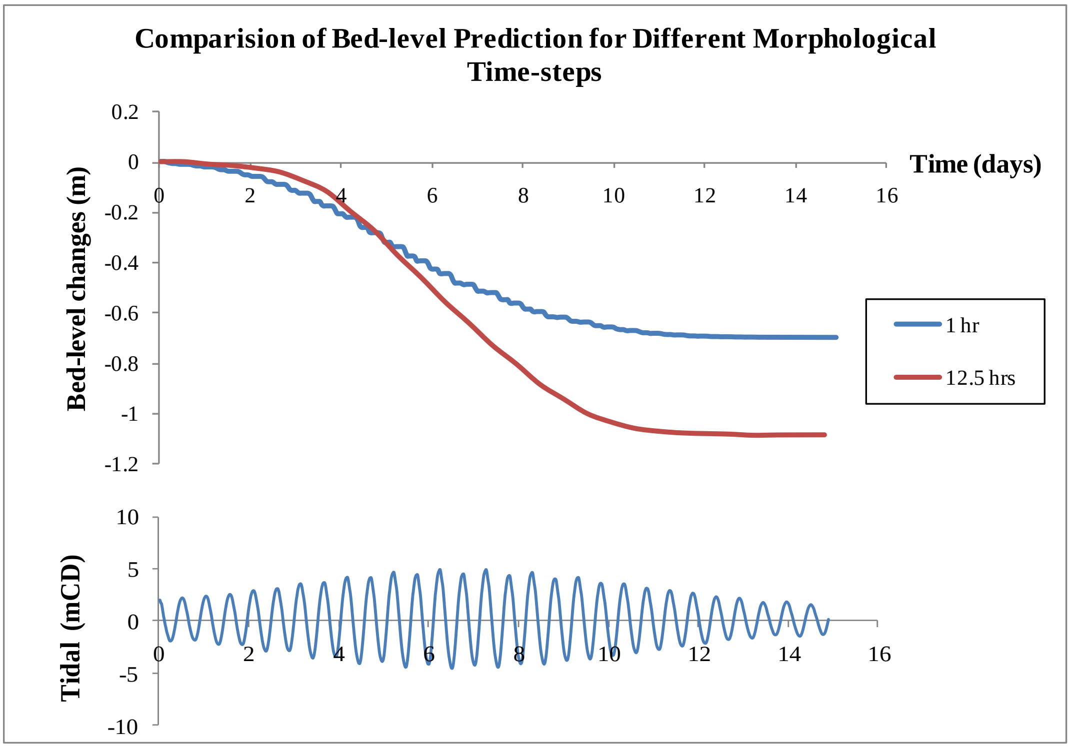

Figure 6.18 Cumulative bed-level changes over a spring-neap cycle

In Figure 6.17 it is clearly visible that bed-level changes correspond to 1 hr time step is approximately 0.4 m lower than that of 12.5 hrs at X during the spring tide. This differences shown above when using the higher morphological time step within a spring-neap cycle (14.8 days), simulation over several months to years might yield in larger variations. Even though longer time step reduces the computational time effectively in long-term morphological simulations there is a disadvantage of getting excessive erosion/accretion. Morphological time step 1 hr indicates the bed is updated more (~ 12 times) frequently and changes are much smoother compared to longer time step. However, smaller time step certainly leads in much longer computational time in long-term morphological simulations. Therefore, an optimum time step that gives stable morphological changes with reasonable computation time has to be determined by conducting sensitivity tests.

6.6 Sensitivity test for different grain-sizes

The sediment grain size used throughout the present modelling study is 0.2 mm, which was assumed to be uniform over the entire estuary. However, in the data review a scatter of sediment sizes ranging from 0.15 to 0.50 mm was observed.

Accordingly, sensitivity tests were carried out by carrying out the morphological modelling over 2 spring-neap cycles (~ 28 days) for three different grain sizes of 0.1, 0.2 and 0.3 mm. Figure 6.18 compares the morphological changes obtained for all three cases.

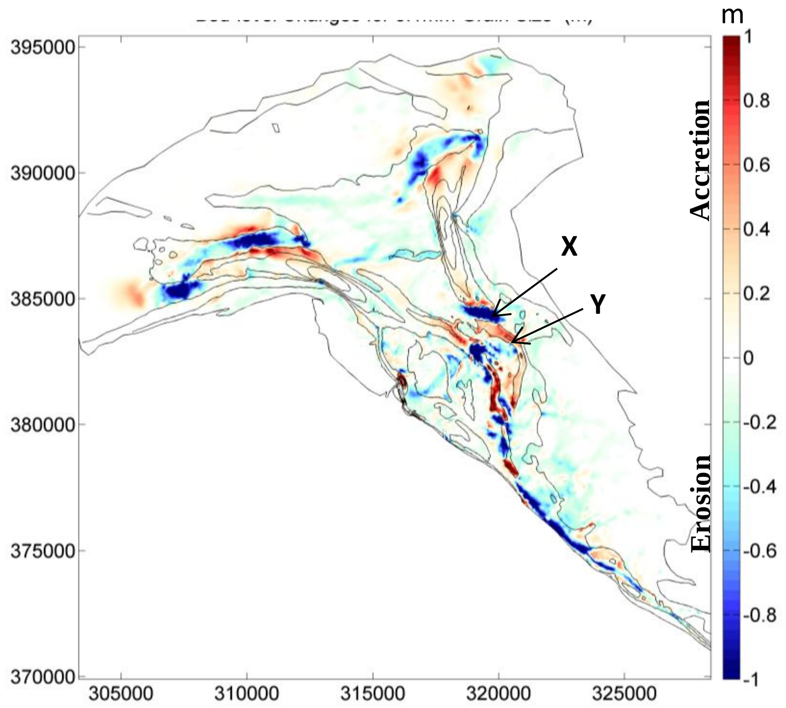

a.) Morphological changes for grain size 0.1 mm (m)

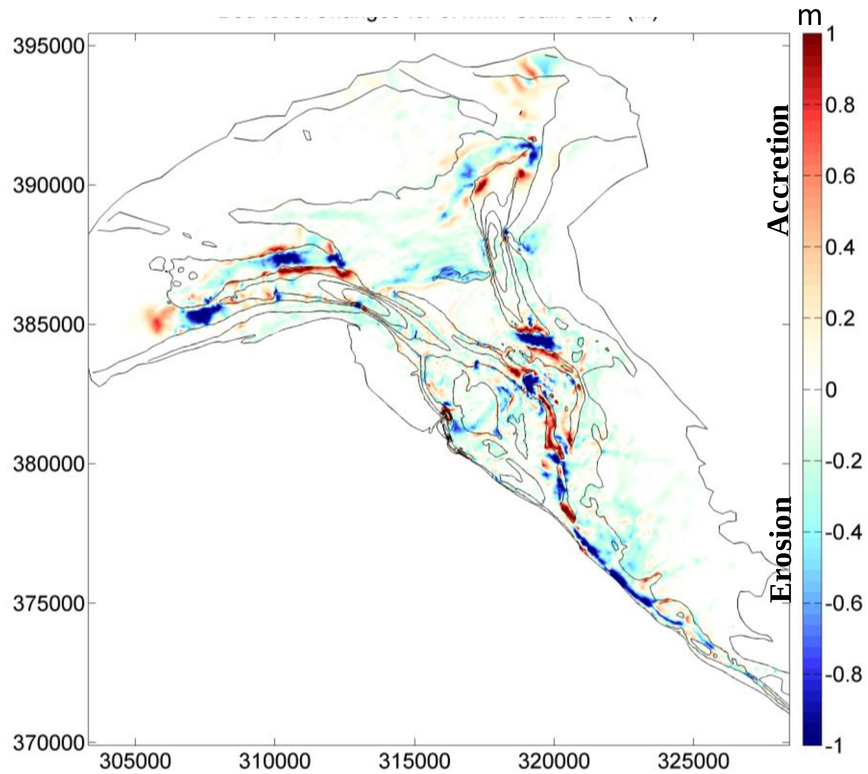

b.) Morphological changes for grain size 0.2 mm

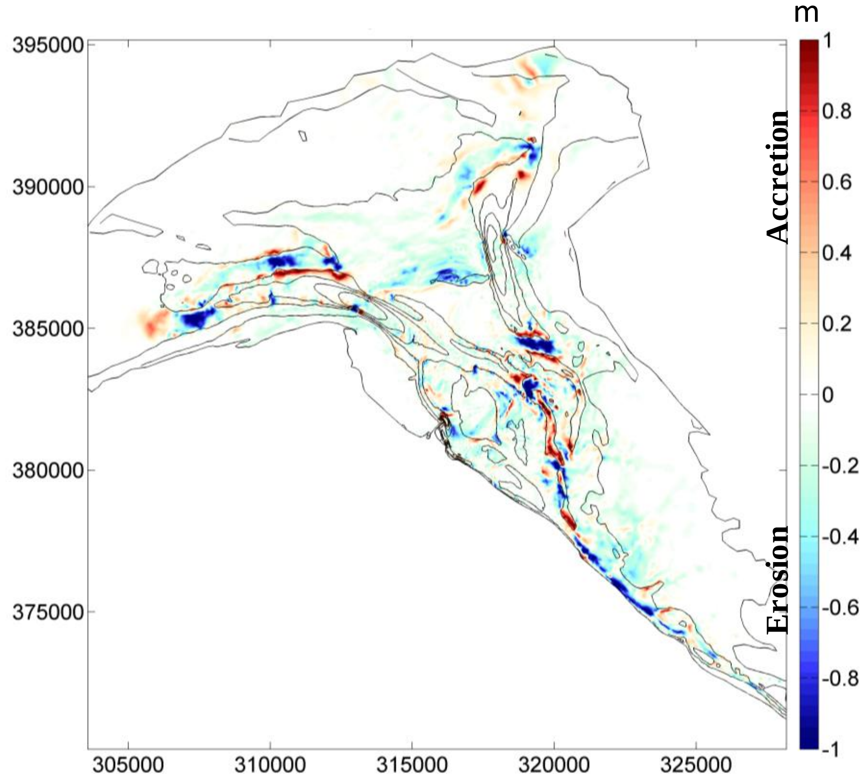

c.) Morphological changes for grain size 0.3 mm

Figure 6.19 Comparison of morphological changes for different sediment grain sizes

This indicates that the overall qualitative pattern of erosion and deposition is unchanged for all three grain sizes, but that the magnitudes of these changes vary with grain size. Particularly, finer grain size 0.1 mm gives more energetic compare to other two cases, whereas there is not much deviation can be seen apparently between the cases of 0.2 and 0.3 mm. Time series of bed-level changes with time obtained at two locations (X and Y shown in Figure 6.18a) in most energetic regions are shown in Figure 6.19 (Tidal signal is shown in the same figure), where X and Y represent the erosion and accretion respectively.

Both erosion and accretion pattern shown in Figure 6.19a and 6.19b indicate that finer grain (0.1 mm) larger deviation from 0.2 mm case than coarser grain (0.3 mm). This is mainly due to the non-linear relationship exist in the sediment transport relation with the grain sizes. Finer grain gives at least 40% erosion/accretion more than the median grain (0.2 mm), whereas the coarser grain tends to predict only ~15 – 20% lower than the median grain at locations X and Y. However these percentages may vary over the space and time. Overall, this comparison reveals that using coarser grain sizes (> 0.2 mm) does not have significant effect where, finer grain sizes (< 0.2 mm) tend to be more dynamic and increase the morphological changes significantly.

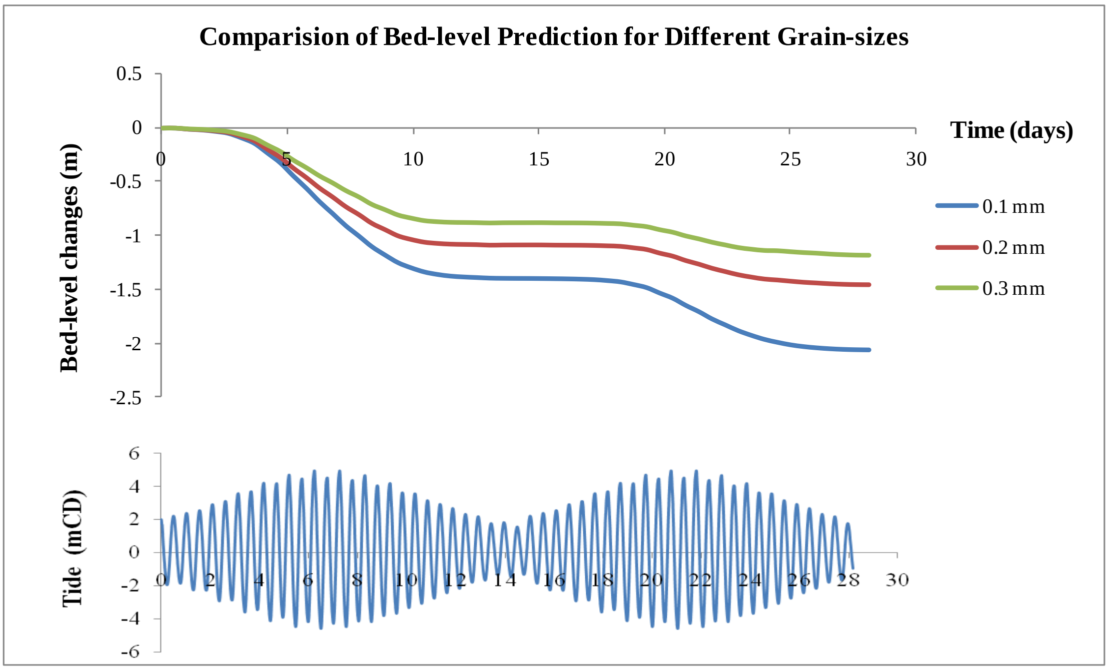

a.) Comparison of bed-level changes for different grain sizes at X

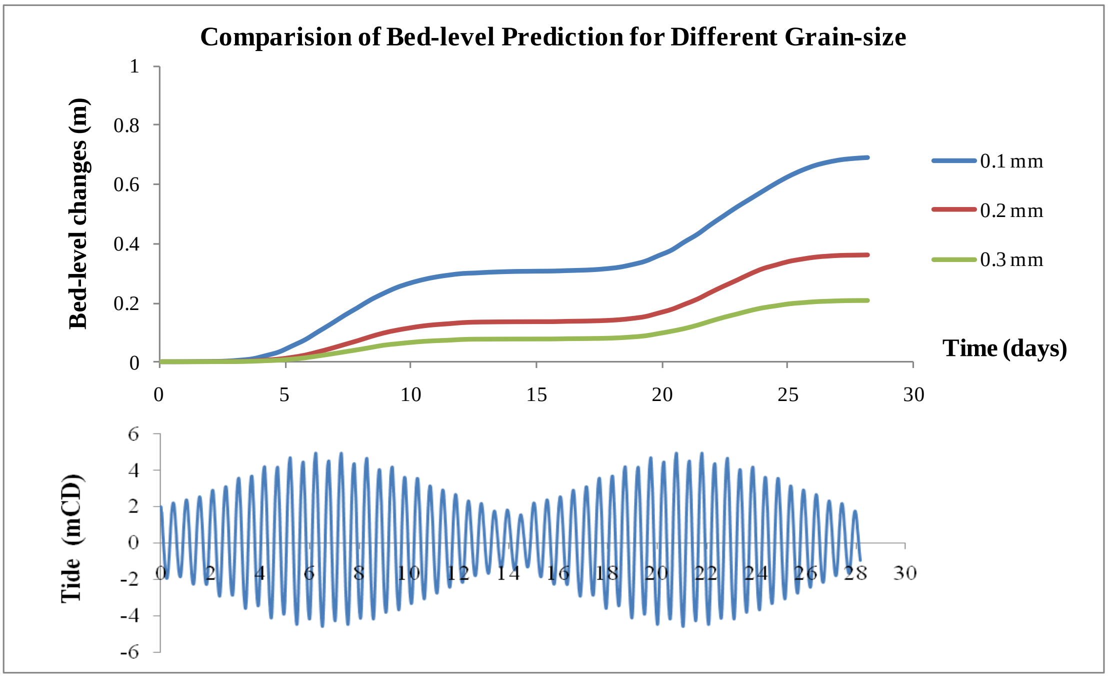

b.) Comparison of bed-level changes for different grain sizes at Y

Figure 6.20 Comparison of bed-level changes for different grain sizes at X and Y

6.7 Discussion and Summary

Morphological simulation was performed using coastal area numerical modelling system, PISCES over 12 spring-neap cycles (~174 days) with the morphological time step of 12.5 hrs. Analysis of bed development over the time shows, morphological changes are rapid during the first couple spring-neap cycles giving bed-level changes up to 1 m. These changes are then stabilised after around 10 cycles of simulation. However, model behaviour during the initialisation highly affects the end results at this stage; it is hard to ensure that this behaviour would balance the situation when continuing the simulation over rest of the period.

Even though complete morphological simulation was not achieved, the available model results for ~6 months of simulation have been compared with the observations qualitatively. Detailed Brier Skill Score (BSS) assessment at selected regions of the estuary (Figure 6.20) reveals that the model performs poorly in most of the shallower regions and fairly good agreement was obtained in deeper and some of the shallower regions. Table 6.19 gives the summary of comparison between model predicted and observed morphological changes. BSS values shown in Figure 6.20 indicate whether the model predictions are closer to the observed changes in that region. It should be borne in mind that, even though the BSS value indicates model prediction are good, it does not imply that all the morphological features are reproduced correctly in the model.

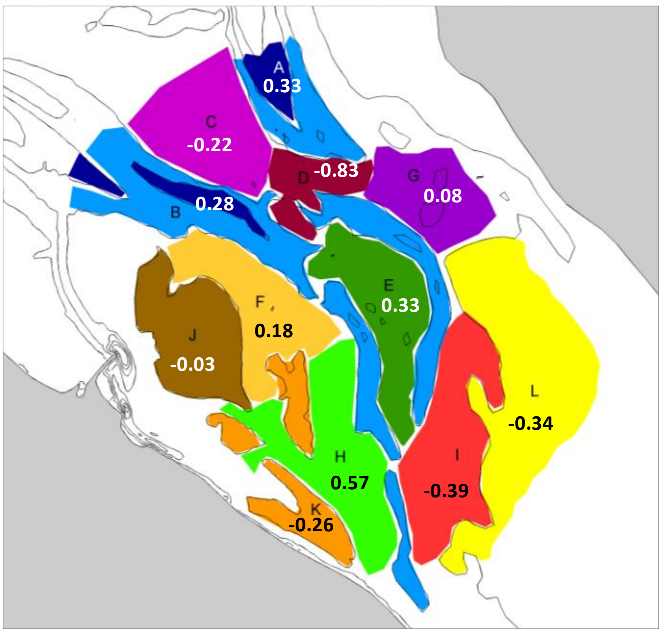

Figure 6.21 BSS_{vr} at different regions of the Estuary

Table 6.6 Summary of comparison between model prediction and observed morphological changes

Region	Actual changes (2003- 2006)	Model Predicted changes (after 170 days simulation)	BSS
A	Predominantly erosion with little accretion on the edges of the channel	higher accretion of channels adjacent to sand banks, erosion is much lower	Fair
B	Predominantly erosion except the channel east of the Salisbury bank, undergone significant accretion	Considerable erosion on the south tip of Welsh channel, massive deposition on the channel east of the region E	Fair
C	Patches of accretion	Erosion of the sand bank on the region of convergent of the Hilbre and Welsh channels	Poor
D	Small patches of erosion and accretion on the south tip of Hilbre Channel	As the Hilbre Channel connects with the small channel down, massive erosion of sand bank	Very Poor
E	Highly energetic, along east side of bank accretion and west side erosion	Relatively less energetic, but erosion on the east side is similar to actual situation	Good
F	Notable erosion along east Salisbury bank and more accretion on south-east	Significant erosion along east side of Salisbury bank, accretion on south east is poorly predicted	Fair
G	Mainly accretion	Predominantly erosion	Poor
H	Scattered erosion and accretion patches	Relatively very lower erosion and accretion	Good
I	Not very energetic except higher erosion on the smaller area north east of this region due to the extension of channel	Minor erosion along the north edge	Poor
J	High accretion on the north tip and high erosion on the south tip, no significant change in the middle	Erosion on the south half	Poor
K	Scattered erosion and accretion patches	Predominantly erosion, but lower	Poor
L	Considerable erosion on the south and very little accretion patches on north	No significant changes except small patches of erosion penetrating through the mudflats	Poor

In addition to the above modelling assessment, there were different modelling scenarios (Table 6.3) carried out and results were compared quantitatively. The bed-level changes obtained in each model were compared under three categories in order to assess the model performance for;

- Different types of tidal conditions (morphological tides compared with spring-neap tidal conditions)
- Morphological factor (MF) (MF 2 compared with MF 1)
- Morphological time steps (1 hr compared to 12.5 hrs time step)

The analysis of above results indicates that the overall pattern of the erosion and accretion is unchanged, but they vary in magnitude. The region (D) south of the Hilbre Channel is being very energetic in all the cases.

Generally, morphological tides predict morphological changes are lower in magnitude than spring-neap tide. However, morphological tides predictions give good agreement with the spring-neap tides in channels, particularly very good relations were obtained when the magnitude of the morphological changes are more than 2 m. whereas, they give poor relations in shallower sand banks and mudflats. As the sediment transport occurs mainly during the spring tide, which is the main trigger for the morphological changes, using the spring tide that has rather higher tidal range would increase the magnitude of morphological changes.

The model has shown instabilities when applying morphological factor anything higher than 5, however a simulation was performed with the MF 2 over 5 spring-neap cycles. Although MF 2 gives similar morphological changes as over the simulations with MF 1, they are lower in magnitude. One of the main causes for these differences can be explained as follows; when applying MF 2 it multiplies the changes after each morphological time step completed, thus after a simulation over one tidal cycle it has in fact modelled over 2 tidal cycles. Accordingly, after simulation over 2 ½ spring-neap cycles, it has modelled over 5 spring-neap cycle. This means simulation did not cover the entire spring tide in the MF 2 case, this may cause lower transport occur in the model compared with MF 1 case where simulation covers 5 full spring-neap cycles.

Morphological model updates the bed on the time scale of hydrodynamic forcing, which the period of tide (~12.5 hrs). This was chosen as the optimum morphological time step that gives reasonable computation time. However, a comparison was made with the 1 hr time step after simulation over one spring-neap cycle. Erosion and accretion pattern is generally unchanged, whereas morphological time step 1 hr tends to produce the bed-level changes rather lower and smoother than when using 12.5 hrs time step as the bed is updated more frequently (It is also explained in Appendix A.6). Yet, in long-term simulations, updating the bed more frequently (1 hr time step) would yield in excessive running time, thus higher morphological factors might require accelerating the computation. This will eventually cause for instabilities to occur in the model.

7. CONCLUSIONS AND RECOMMENDATIONS

Morphological modelling of the Dee Estuary has been carried out using the process based model, PISCES, developed by HR Wallingford, in order to achieve the main goal of this study. Comprehensive bathymetric data sets covering an entire estuary, collected by Environmental Agency in 2003 and 2006, have been used to evaluate the model. Morphological modelling simulation over the period of three years is computationally expensive and challenging to achieve within the limited time period. Also the Dee Estuary consists of complex bathymetry and huge intertidal area with larger tidal ranges making the system even more challenging one to model.

Much effort have been taken to apply various input reduction techniques which are often being used in long-term morphological modelling, such as morphological tide and morphological factor, in order to have a reasonable computation time. However, application of the morphological factor to the present model has resulted in huge instabilities in the intertidal area and consequently cause for model failure. This indicates, even though morphological factor accelerates the morphodynamic simulations drastically, it leads to wrong description of the physical processes, as erosion and deposition processes are extrapolated.

Due to various uncertainties and failures associated with the model, the simulation was not only been carried out partially (for 6 months) instead of over the three-year period. The results are therefore a measure of whether the model performs in right direction in achieving the observed morphological patterns. Model results were evaluated against the observations using quantitative assessment method, Brier Skill Score (BSS), combination with scatter plots.

Quantitatively, model performs reasonably well in deeper areas and some of the shallower regions, whereas it is poor in most of the shallower banks and mudflats. Qualitatively, the model behaves poorly as it tends to connect the channels and becoming more ebb dominant, whereas naturally channels show tendency of bending and migrating. Significant morphological changes were noted during the initialisation of the model, which had greatly affected the morphological changes of the end results obtained. Thereafter, the model reached a stable condition where there were no significant morphological changes observed as during the initialisation. Therefore, it is hard is hard to ensure that the effect of initialisation would be balanced with the time when continuing the simulation over rest of the period.

In addition, several modelling scenarios were performed and results were compared quantitatively in order to assess the model performance for the morphological tide, and different morphological factors and morphological time steps. The overall morphological patterns were unchanged in all the cases, but they varied in magnitudes. Bed-level changes predicted by the morphological tides were in good agreement with those predicted by spring-neap tides in channels, particularly when the changes are more than 2 m. Whereas, they are poor to moderate in shallow regions. Morphological factor (MF) 2 produces similar morphological changes as with MF 1, except in some of the shallower regions.

Even though much effort have been taken to assess the model quantitatively in various ways, due to incompleteness of the model simulation and various uncertainties with the model, conclusions could not be drawn objectively, however above judgement was made subjectively based on the qualitative assessments and visual inspection of the model results. In conclusion, present morphological model, PISCES, is not very effective in studying long-term estuarine morphological behaviour as the model consists of several uncertainties and cannot reproduce the observed morphological behaviour. Further research is required to identify the issues and take necessary steps to improve the model performance to be able to model even complicated morphology.

Recommendations for further work

A proper description of the wetting and drying procedure has to be included in the model. Particularly, when modelling the estuaries, the intertidal area in the model falls dry and becomes wet during the tidal cycle. This causes the cells become dry when the water depth decreases below a threshold value (minimum water depth). Particularly, in long-term simulation this creates huge instabilities when applying morphological factors.

When examining the results, it was identified that instability of the model has initiated along the south west of the model boundary, where the bathymetry was not well defined. Improving the mesh resolution of the present model bathymetry at these regions might give improved results, but in that case sufficient time must be allowed for the modelling, as it will increase the computation time further.

Although, morphological tide used in this study produced overall morphological changes similar to the spring-neap tide, they were lower in magnitude. Hence, selection of representative tide that has the tidal range rather higher than the present one is required to accelerate the morphological changes. Several sensitivity tests must be conducted with the morphological model to ensure the tide is representative.

Selecting the maximum morphological time step that satisfies the stability criterion is challenging, as it required calculating the celerity of the bed over the entire model domain. Therefore, it must be incorporated in the programme coding/ there must be a method formed that allows user to simply check the stability requirement for the model when selecting the morphological time step.

PISCES, uses a single grain size for morphodynamic modelling, in fact cannot be used to model the entire estuary due to the varying grain size. Sediment transport module of the modelling system uses Van Rijn's sediment transport formula, which is developed mainly for rivers, where the sediments are more narrowly graded than in estuaries. Therefore, it may be best to develop a power law relation for the sediment transport based on the field measurements of sediment fluxes at particular site.

This study was undertaken assuming that tide is the main forcing factor that causes for the morphological changes of the estuary. However, this excludes the seasonal variations and storms which may have affected the estuarine morphological evolution. Detail investigations and several sensitivity tests required to find out what is the main trigger for the morphological evolution of the Dee Estuary during the period of 2003 and 2006.

REFERENCES

Allen, G.P., Salmon, J.C., Bassoullet, P., Du Penhoat, T., and De Grandpre, C., 1980. Effects of tides on mixing and suspended sediment transport in macrotidal estuaries. *Sediment Geology*. 26, pp. 69-90.

Aubrey, D.G., and Speer, P.E., 1985. A study of non-linear tidal propagation in shallow inlet/estuarine systems, part 1: observations. *Estuarine, Coastal and Shelf Science,* 21, pp. 185–205.

Bokuniewicz, H., 1995. In Perillo, G.M.E. (2n ed.), Geomorphology and sedimentology of estuaries. Developmets in Sedimentology. 53.

Bolanos, R., and Souza, A., 2010. Measuring hydrodynamics and sediment transport processes in the Dee estuary. *Earth System Science*. 3, pp. 79-107.

Brown, J., Colling, A., Park, D., Philips, J., Rothery, D. and Wright, J., 1999. *Waves, Tides and Shallow Water Processes* (2nd ed.). Oxford: Pergamon Press and The Open University.

Brown, J.M., and Davies, A.G., 2010. Flood/ebb tidal asymmetry in a shallow sandy estuary and the impact on net sand transport. *Geomorphology.* 114, pp.431–439.

Brown, J.M., and Davies., 2009. Methods for medium-term prediction of the net sediment transport by waves and currents in complex coastal regions. *Continental Shelf Research.* 29, pp. 1502–1514.

Cameron, G., and Pritchard, D., 1963. Estuaries. in Hill, M., (ed.), *The Sea*, vol 2, pp. 306-324. Wiley Interscience, New York.

Carter, R.W.G., 1998. *Coastal Environments: An Introduction to the Physical, ecological and Cultural Systems of Coastlines*. Academic Press Limited. London. pp. 617.

Chesher, T.J., Wallace, H.M., Meadowcroft, I.C., and Southgate, H.N., 1993. PISCES, A Morphodynamic Coastal Area Model. First Annual Report, HR Wallingford Report SR 337.

Cowell, P. J., Stive, M. J. F., Niedoroda, A. W., de Vriend, H. J., Swift, D. J. P., Kaminsky, G. M., and Capobianco, M., 2003a. The coastal-tract (part 1): A conceptual approach to aggregated modelling of low-order coastal change. *Journal of Coastal Research*, 19 (4), pp. 812-827.

d'Angremond, K., And Pluim-Van der Velden, E.T.J.M., 2001. Introduction to Coastal Engineering. Delft: VSSD.

Davies, A.G., van Rijn, L.C., Damgaard, J.S., van de Graaff, J., and Ribberink, J.S., 2002. Intercomparison of research and practical sand transport models. *Coastal Engineering,* 46, pp. 1–23.

De Vriend, H.J., (1996), Mathematical modelling of meso-tidal barrier island coasts. Part I: Empirical and semi-empirical models, in Liu, P.L.F., (ed.), *Advances in coastal and ocean engineering*, vol. 2, pp. 115-149. World Scientific, Singapore.

De Vriend, H.J., 1996. Mathematical modelling of meso-tidal barrier island coasts: part II. Empirical and semi empirical models. In: Liu, P.L.F., (Ed.), *Advances in Coastal and Ocean Engineering,* vol. 2, pp. 151-197. World Scientific, Singapore.

De Vriend, H.J., Capobianco, M., Chesher, T., De Swart, H.E., Latteux, B., and Stive, M.J.F., 1993b. Approaches to long term modelling of coastal morphology: a review. Coastal *Engineering.* 21 (1-3), pp. 225-269.

Dennis, J.M., Spearman, J.R., and Dearnaley, M.P., 2000. The development of Regime models for prediction of the long term effects of civil engineering activities of estuaries. *Physics and Chemistry of the Earth (B),* 25, pp. 45-50.

Di Silvio, G., 1989. Modelling the morphological evolution of tidal lagoons and their equilibrium configurations. XXII Congress of the IAHR, Ottawa, Canada.

Dronkers, J., 1986. Tidal asymmetry and estuarine morphology. *Netherlands Journal of Sea Research (NJSR)*. 20, pp. 117–131.

Elias, E.P.L., Cleveringa, J., Buijsman, M.C., Roelvink, J.A., Stive, and M.J.F., 2006. Field and model data analysis of sand transport patterns in Texel tidal inlet. *Coastal Engineering,* 53 (5–6), pp. 505–529.

Engineering and Design Photogrammetric Mapping, 1993. Engineer Manual. chapter 1. No. 1110-1-1000 31.

Fairbridge, R.W., 1980. The estuary: its definition and geo-dynamic cycle. In: Woodroffe, C. D., 2002. *Coasts: Form, processes and evolution*. Cambridge University Press, Cambridge.

Friedrichs, C.T., and Aubrey, D.G., 1998. Non-linear tidal distortion in shallow well-mixed estuaries: a synthesis. *Estuarine, Coastal and Shelf Science.* 27, pp. 521-545.

Guenther1, G.C., Cunningham, A.G., LaRocque, P.E., and Reid, D.J., 2000. Meeting the accuracy challenge in airborne LiDAR bathymetry. *Proceedings of EARSeL-SIG-Workshop LIDAR.*

Hayes, M.O., (1975), Morphology of sand accumulation in estuaries: an introduction to the symposium, in Estuarine research II, edited by L.E. Cronin, Academic Press, New York, pp. 3-22.

Hibma, A., Stive, M.J.F., and Wang, Z.B., 2004. Estuarine morphodynamics. *Coastal Engineering*. 51, pp. 765-778

HR Wallingford (2004). Dee Estuary Modelling. Phase 1 Model set-up and calibration. HR Wallingford Report EX5081, Release 1.0 December 2004.

HR Wallingford (2005). Dee Estuary Modelling. Phase 2 Assessment of the impact of a dredged navigation channel to the Port of Mostyn. HR Wallingford Report EX5097, Release 2.0 May 2005.

HR Wallingford (2007). Dee Estuary Modelling. Port of Mostyn EIA 2007 Hydraulic Modelling Studies. HR Wallingford Report EX5514, Release 1.0 April 2007.

Huthnance, J.M., 1982. On the formation of sand banks of finite extent. *Estuarine, Coastal and Shelf Science.* 15, pp. 277-299.

Huthnance, J.M., Karunarathna, G., Lane, A., Manning, A.J., Norton, P., Reeve, D., Spearman, J., Soulsby, R.L., Townend, I.H., and Wright, A., 2007. Development of Estuary Morphological Models. The Institute of Mathematics and its Applications.

Kang, J.W., and Jun, K.S., 2003. Flood and ebb dominance in estuaries in Korea. *Estuarine, Coastal and Shelf Science*. 56, pp. 187-196.

Kang, J.W., Jun, K.S., 2003. Flood and ebb dominance in estuaries in Korea. *Estuarine, Coastal and Shelf Science*. 56, pp. 187–196

Karunarathna, H., and Reeve, D.E., 2008. A Boolean approach to prediction of long-term evolution of estuary morphology. *Journal of Coastal Research* 24 (2), pp. 51-61.

Karunarathna, H., Reeve, D., and Spivack, M., 2008. Long-term morphodynamic evolution of estuaries: An inverse problem. *Estuarine, Coastal and Shelf Science*, 77, pp. 385-395.

Lanzoni, S., and Seminara, G., 1998. On tide propagation in convergent estuaries. *Journal of Geophysical Research*. Vol. 103 (C13), pp. 793-812.

Lanzoni, S., Seminara, G., 2002. Long-term evolution and morphodynamic equilibrium of tidal channels. *Journal of Geophysical Research*. 107 (C1).

Latteux, B., 1995. Techniques for long-term morphological simulation under tidal action. *Marine Geology*. 126 (1–4), pp. 129–141.

Lesser, G.R., Roelvink, J.A., Van Kester, J.A.T.M., and Stelling, G.S., 2004. Development and validation of a three-dimensional morphological model. *Coastal Engineering*. 51, pp. 883–915.

Lesser, G.R., Roelvink, J.A., Van Kester, J.A.T.M., and Stelling, G.S., 2004. Development and validation of a three-dimensional morphological model. *Coastal Engineering*. 51, pp. 883-915.

Marker, M.E., 1967. The Dee Estuary: Its progressive silting and salt marsh development. *Transactions of the Institute of British Geographers*. 41, pp. 65–71.

Moore, R.D., Wolf, J., Souza, A.J., and Flint, S.S., 2009. Morphological evolution of the Dee Estuary, Eastern Irish Sea, UK: a tidal asymmetry approach, *Geomorphology*, 103, pp. 588–596.

Nicholson, J., Broker, I., Roelvink, J.A., Price, D., Tanguy, J.M., and Moreno, L., 1997. Intercomparison of coastal area morphodynamic models. *Coastal Engineering*. 31, pp. 97–123.

Olds, S., and Davison, A., 2009. Port of Mostyn Breakwater Quay Development Environmental Statement. Port of Mostyn Ltd.

Prandle, D., 2004. How tides and river flows determine estuarine bathymetries. *Progress in Oceanography*. 61, pp. 1–26.

Prandle, D., 2009. *Estuaries: Dynamics, Mixing, Sedimentation and Morphology*. Cambridge University Press.

Robins, P.E., and Davies, A.G., 2010. Morphodynamic processes in shallow estuaries: Influence of tidal flats and channels on sand transport. *River, Coastal and Estuarine Morphodynamics.* Taylor and Francis Group, London.

Roelvink, J.A., 2006. Coastal morphodynamic evolution techniques, *Journal of Coastal Engineering*, 53, pp. 177-187.

Rossington, S.K., 2008. Modelling Large-Scale Estuarine Morphodynamics Using Equilibrium Concepts: Responses to Anthropogenic Disturbance and Climatic Change. PhD Thesis. University of Southampton.

Soulsby, R.L., 1997. Dynamics of Marine Sands: A Manual for Practical Applications. Telford, London.

Stive, M.J.F., Capobianco, M., Wang, Z.B., Ruol, P., and Buijsman, M.C., 1998. Morphodynamics of a tidal lagoon and the adjacent coast. In: Dronkers, J., Scheffers, M. (eds), Physics of estuaries and coastal seas. Balkema, Rotterdam.

Sutherland, J., Walstra, D.J.R., Chesher, T.J., Van Rijn, L.C., and Southgate, H.N., 2004. Evaluation of coastal area modelling systems at an estuary mouth. *Coastal Engineering.* 51, pp. 119–142.

TELEMAC-2D Software, Version 5.2, User Manual (2002). EDF-DRD.

Valle-Levinson, A. (ed.), 2010. *Contemporary Issues in Estuarine Physics*. Cambridge University press.

Van der Wegen, M., 2005. Long-term morphodynamic equilibrium in alluvial estuaries. PhD proposal. Delft University of Technology, Netherlands.

Van der Wegen, M., 2010. Modelling morphodynamic evolution in alluvial estuaries. PhD thesis, UNESCO-IHE & Delft Technical University, Delft. CRC Press/Balkema. ISBN 978-0-415-59274-1.

Van Goor, M.A., Zitman, T.J., Wang, Z.B., and Stive, M.J.F., 2003. Impact of sea-level rise on the morphological equilibrium state of tidal inlets. *Marine Geology*. 202, pp. 211-227.

Van Rijn, L.C., Walstra, D.J.R., Grasmeijer, B., Sutherland, J., Pan, S., Sierra, J.P., 2003. The predictability of cross-shore bed evolution of sandy beaches at the time scale of storms and seasons using process-based profile models. *Coastal Engineering.* 47, pp. 295– 327.

Walton, T. L. Jr., 2002. Tidal velocity asymmetry at inlets. ERDC/CHL CHETNIV-47. U.S. Army Engineer Research and Development Center.

Wang, Z.B., Louters, T., and De Vriend, H.J., 1995. Morphodynamic modelling for a tidal inlet in the Wadden Sea. *Marine Geology*. 126, pp. 289–300.

Woodroffe, C. D., 2002. *Coasts: Form, processes and evolution*. Cambridge University Press, Cambridge.

Appendix. A1 Data coverage for the Dee Estuary bathymetry

Data comes from various surveys that covers the entire estuary has shown below.

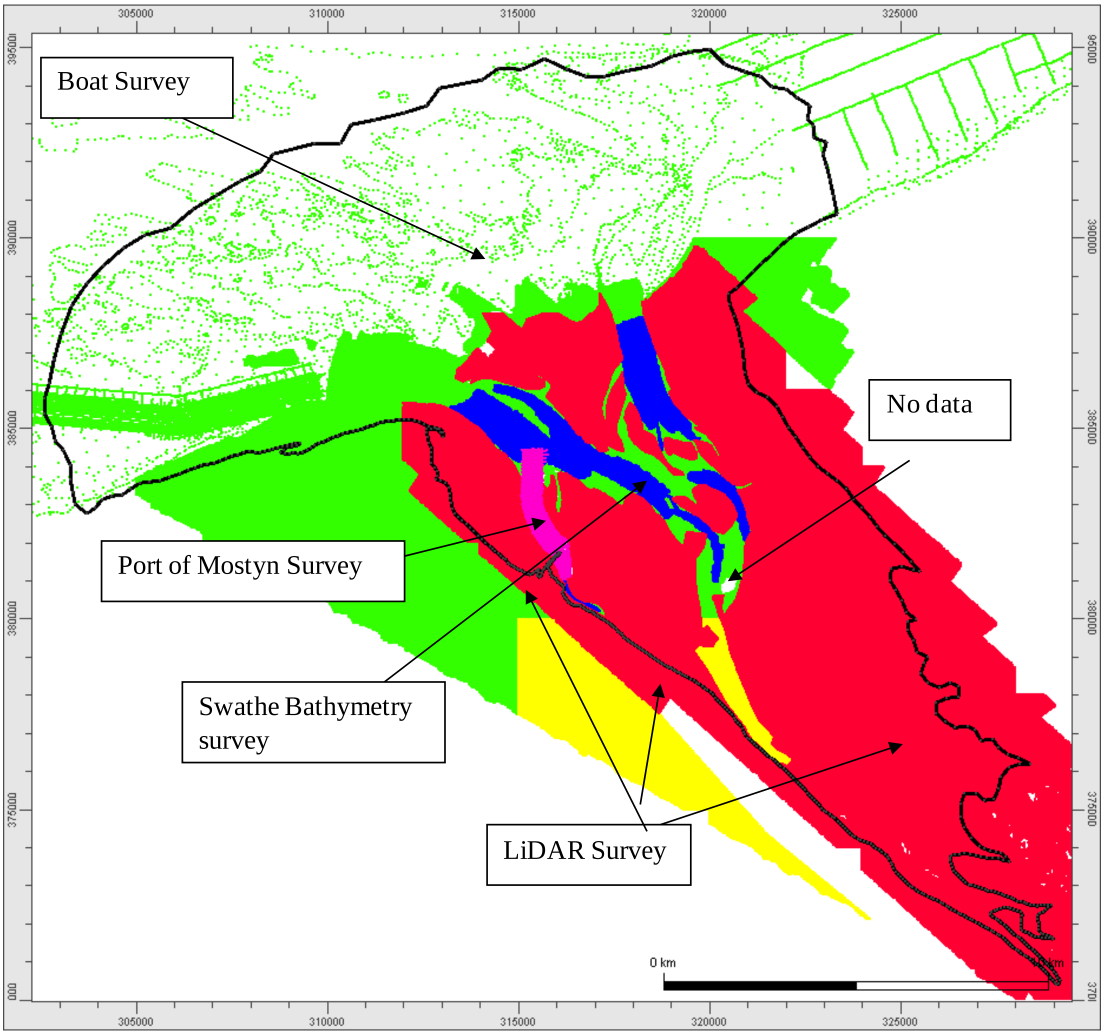

Figure A1.1 Data coverage for Dee Estuary bathymetry

Appendix. A2 Derivation of tidal boundary conditions

Calibrated regional flow model of the Irish Sea is used to drive a local model (in this case with boundaries in Liverpool Bay) in previous HR Wallingford (2004) studies. Water levels obtained at 11 points of the Liverpool Bay model is shown in Figure A2.1.

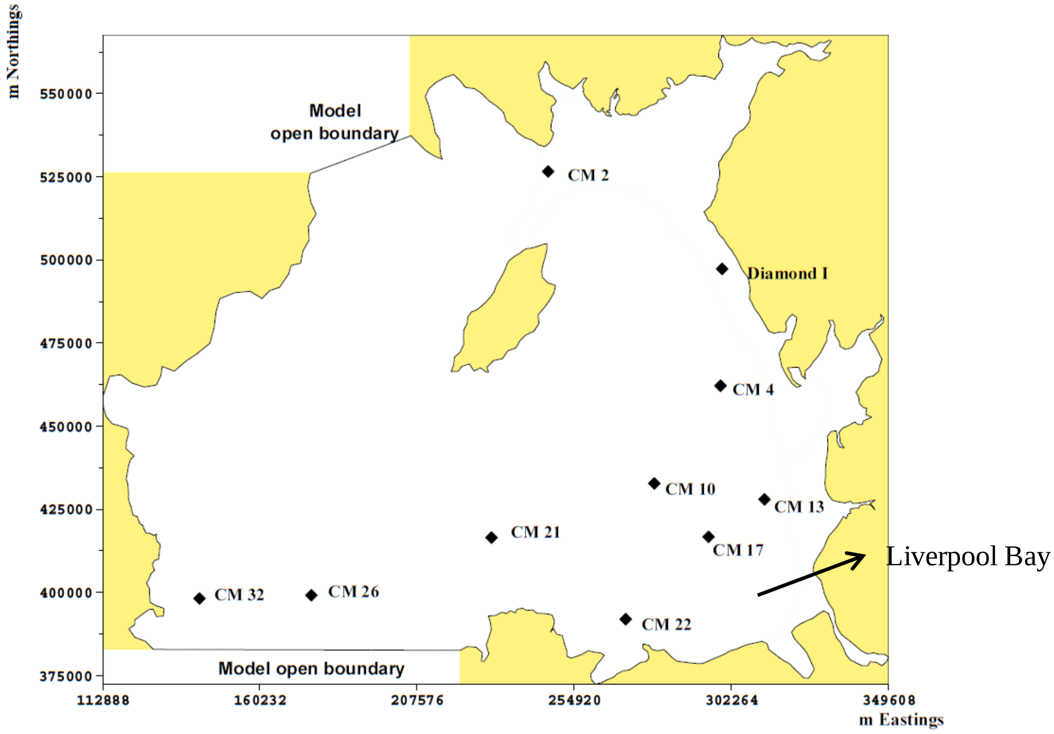

Figure A2. 1 Irish Sea Regional Model

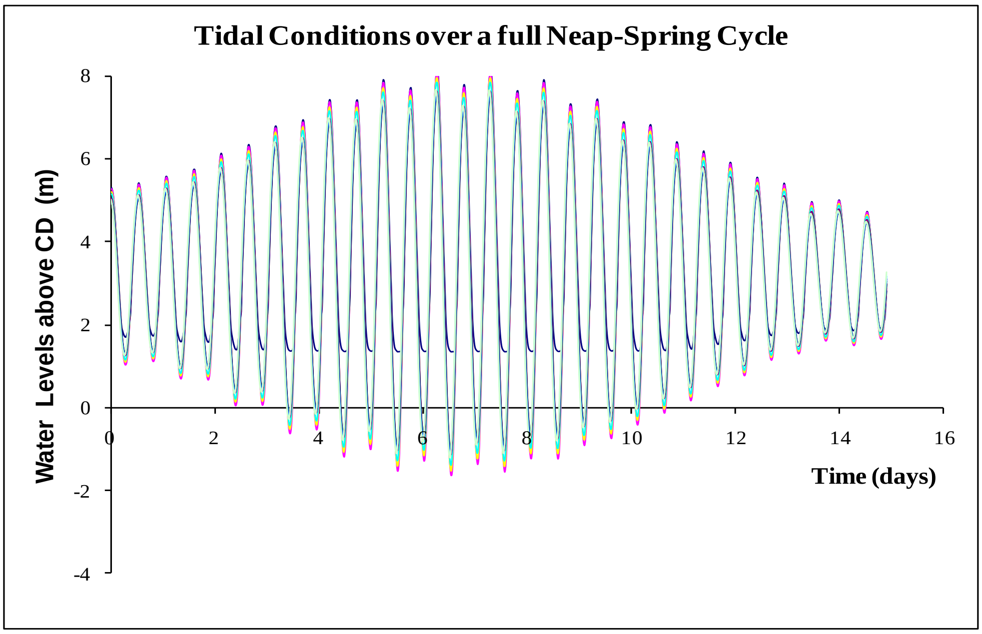

Figure A2.1 Tidal water levels over a full spring-neap cycle for the Liverpool Bay Model

Above water levels were imposed at the open boundary of the Liverpool bay model and flow model was simulated over a spring-neap cycle which gives the boundary conditions for the Dee Estuary model at 59 locations.

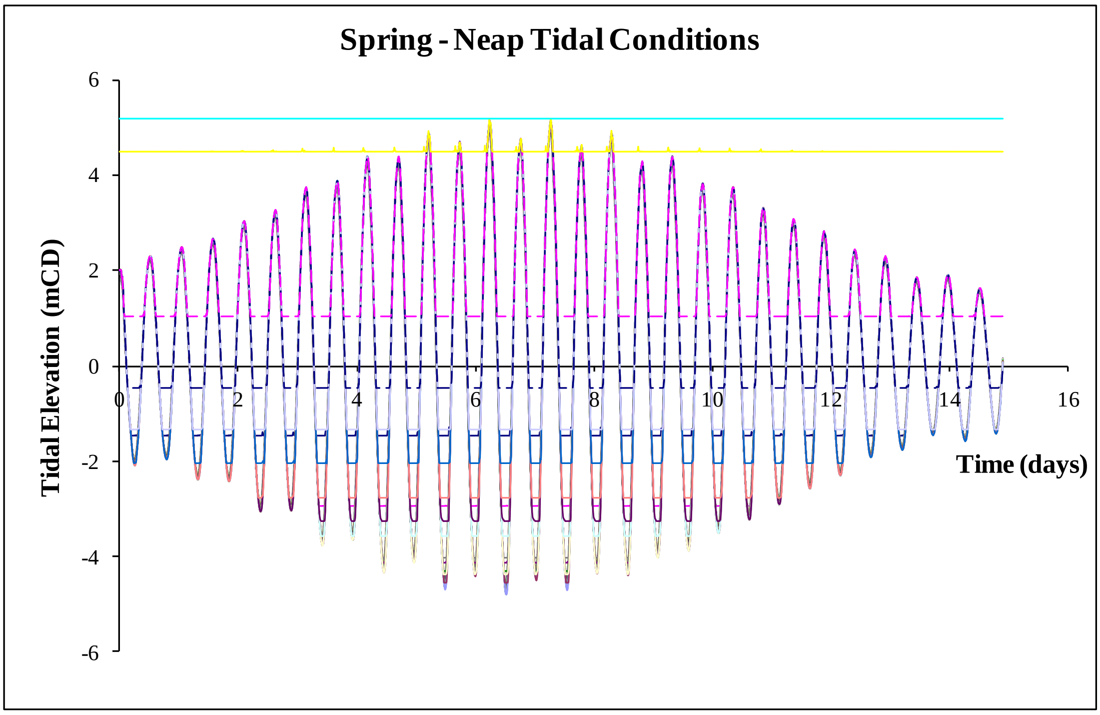

Figure A.3 Spring-neap Tides for the Dee Estuary Model

It can be seen that the water levels at all the points are not coinciding each other. This is because of varying topography at the model boundary and thus not all the points are getting flooded and ebbed during the tidal cycle.

Morphological tides;

Morphological tides were established for the Liverpool Bay model during the previous studies (HR Wallingford, 2005) is shown in Figure A2.4. Again same procedure was followed to obtain the morphological tides for the Dee Estuary model (Figure A2.5)

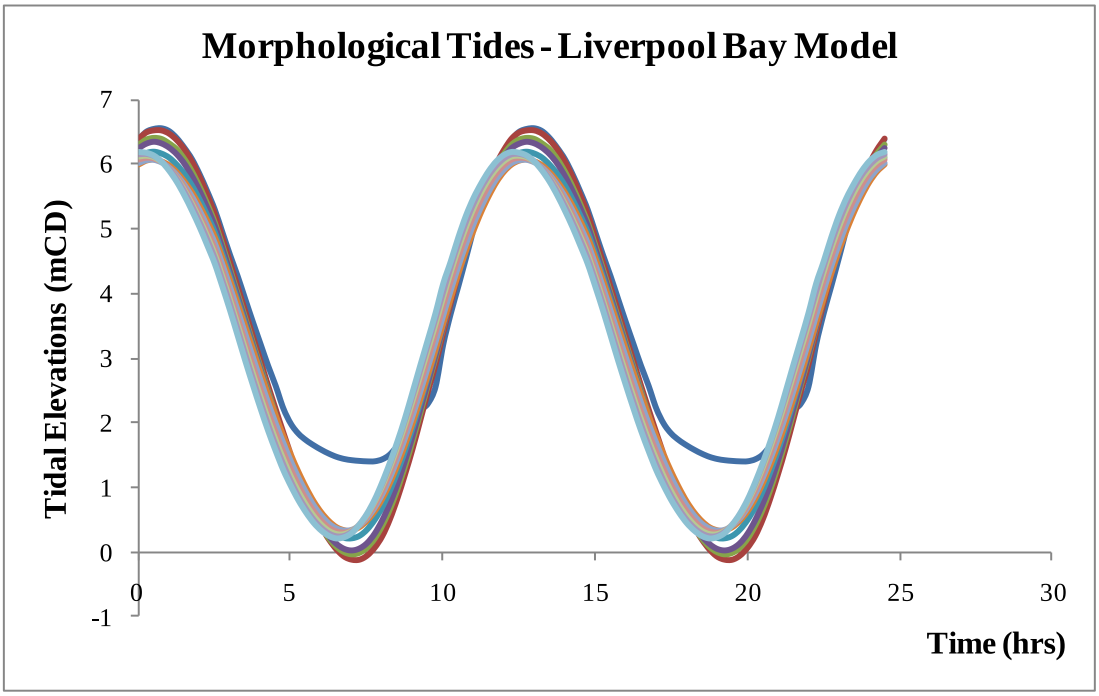

Figure A2.4 Morphological tides for the Liverpool Bay Model

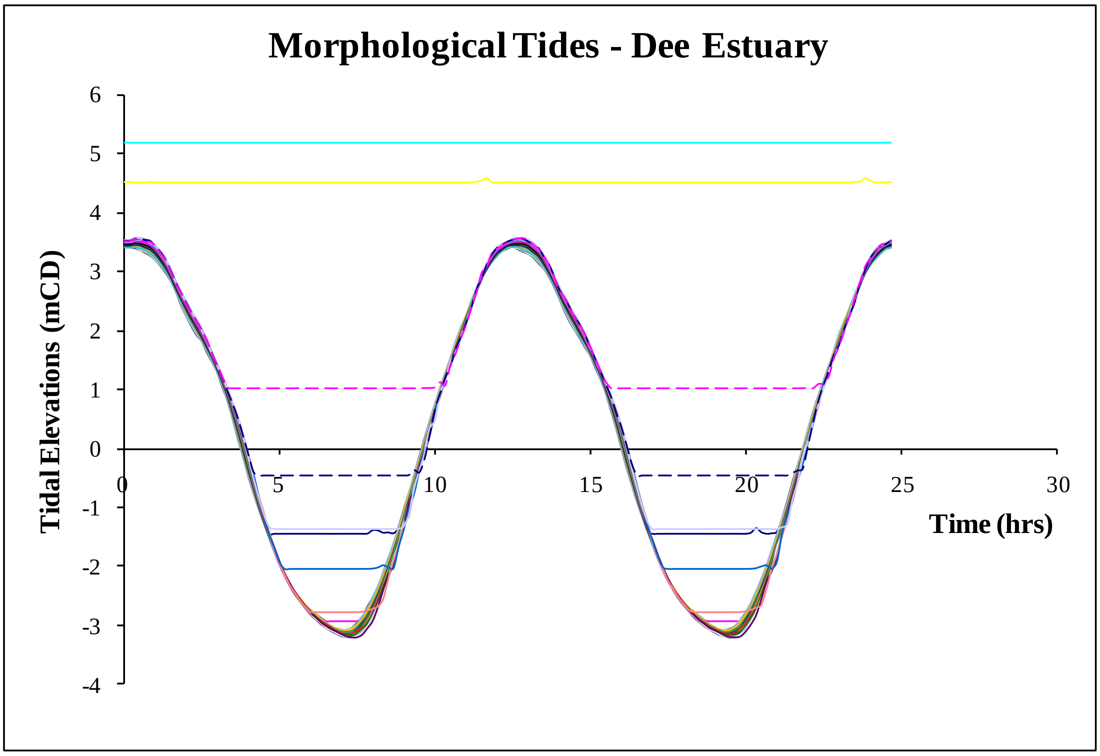

Figure A2.5 Morphological Tides for the Dee Estuary Model

Appendix. A3 Description of Chart Datum (CD) and Ordinary Datum (OD)

Chart datum is generally used by many marine charting agencies, including the United Kingdom.

Definition (CD):

A chart datum is the level of water that charted depths displayed on a nautical chart are measured from. A chart datum is generally a tidal datum; that is, a datum derived from some phase of the tide. Common chart data are lowest astronomical tide and mean lower low water (www.wikipedia.org).

Chart datum is generally kept below Mean Sea Level (MSL) considering the safety factors for navigators.

Definition (OD):

Ordnance Datum is a vertical datum used by an ordnance survey as the basis for deriving altitudes on maps. Usually mean sea level (MSL) is used for the datum (www.wikipedia.org).

Appendix. A4 Sample steering files in morphological modelling

Flow model (TELEMAC 2D):

```
/---------------------------------------------------------------------/
FORTRAN FILE                : './files/princidee_dem003.f'
BOUNDARY CONDITIONS FILE    : './files/geom_dem01.cli'
GEOMETRY FILE               : './files/geom_dem01.sel'
RESULTS FILE                : './initial/resdee_dem003'
/
RELEASE                     : V5P8
/---------------------------------------------------------------------/
COMPUTATION CONTINUED : YES
VARIABLES FOR GRAPHIC PRINTOUTS : 'U,V,S,H,B'
TIME STEP = 2.5
NUMBER OF TIME STEPS = 19440
GRAPHIC PRINTOUT PERIOD = 360
LISTING PRINTOUT PERIOD = 360
/---------------------------------------------------------------------/
FRICTION COEFFICIENT = 0.01
TURBULENCE MODEL = 2
NON-DIMENSIONAL DISPERSION COEFFICIENTS = 6. ; 0.6
VELOCITY DIFFUSIVITY = 10E-6
INITIAL CONDITIONS : 'CONSTANT ELEVATION'
INITIAL ELEVATION = 2.0
/---------------------------------------------------------------------/
TYPE OF ADVECTION : 1;5;2;1
LAW OF BOTTOM FRICTION : 5
SOLVER ACCURACY = 1.E-4
MAXIMUM NUMBER OF ITERATIONS FOR SOLVER = 200
OPTION FOR LIQUID BOUNDARIES = 2
/---------------------------------------------------------------------/
CORIOLIS : YES
CORIOLIS COEFFICIENT = 1.2E-4
/---------------------------------------------------------------------/
PRESCRIBED ELEVATIONS = 0.0;0.0
PRESCRIBED FLOWRATES  = 0.0;0.0
/---------------------------------------------------------------------/
MASS-BALANCE : YES
/---------------------------------------------------------------------/
&ETA
&FIN
```

Sediment transport model (SANDFLOW 2D)

```
FLOW RESULTS FILE = ./initial/resdee_dem003
OUTPUT FILE = ./ressand_dem003
LOG FILE = ./sand_dem003.log
BOUNDARY CONDITIONS FILE = ./files/geom_dem01.cli
END FILE = ./sand_dem003.end
START TIME = 0
COMPUTATION CONTINUED = NO
NUMBER OF TIMESTEPS = 4500
TIMESTEP = 10.0
STORAGE INTERVAL = 180
TYPE OF ADVECTION = 1
DIFFUSION STEP = yes
DIFFUSION = 2.0
ALPHA = 1.0
INITIAL SUSPENDED SAND = 0.0
INITIAL SAND DEPOSITS = 100000.0
TEMPERATURE = 10.0
SALINITY = 34.0
LOOKUP U MAX = 2.0
LOOKUP H MAX = 20.0
FRICTION = 0.017
LAW FOR SATURATION CONCENTRATION = 1
FORCE SATURATION = no
LOOKUP H STEPS = 21
LOOKUP U STEPS = 21
GRAIN SIZE = 200
MIXING FACTOR = 1.0
/SUSPENDED LOAD = YES
/BED LOAD = YES
&ETA
&FIN
```

Morphological model (PISCES)

```
Perform Initial Runs             : yes
Restart of existing run          : no
Initial Flow File                : new_flow.res_0_0
Initial Sand File                : new_sand.res_0_0
Restart time step                : 0
Wave Forcing                     : no
Cas File Flow                    : casdf_gen.str
Steering File Sand               : sand_gen.str
Flow Boundary Condition          : bc_sprnp_3yrs.txt
Flow BC Comment lines            : 0
Flow BC Columns                  : 59
Maximum Water Level              : 30
Start Time                       : 3600
Number of time steps             : 2102
Morphological Factor             : 1
Period of each time step         : 45000
Flow Overlap                     : 3600
Number of Smoothings             : 0
Number of Continuity Updates     : 0
Combine results in single file   : yes
Print interval for results       : 1
```

Appendix. A5 Thompson boundary conditions

Flow model gives a sudden velocity jet with very high velocities at the northern model boundary as can be seen in Figure A5.1 when updating the bed. The reason is developing higher flow gradient when higher water levels enter the model boundary during spring tide due to the Bernoulli's effect.

To avoid this there is an option in TELEMAC model called Thompson's boundary conditions was activated during the modelling. This option is used when only water levels at several points are known. Thompson's method uses the characteristics method to calculate the missing values, thus TELEMAC-2D will compute the velocity at the boundary in the case of prescribed elevation. Hence inconsistencies in the flow occurred at the boundary was removed effectively by using this method.

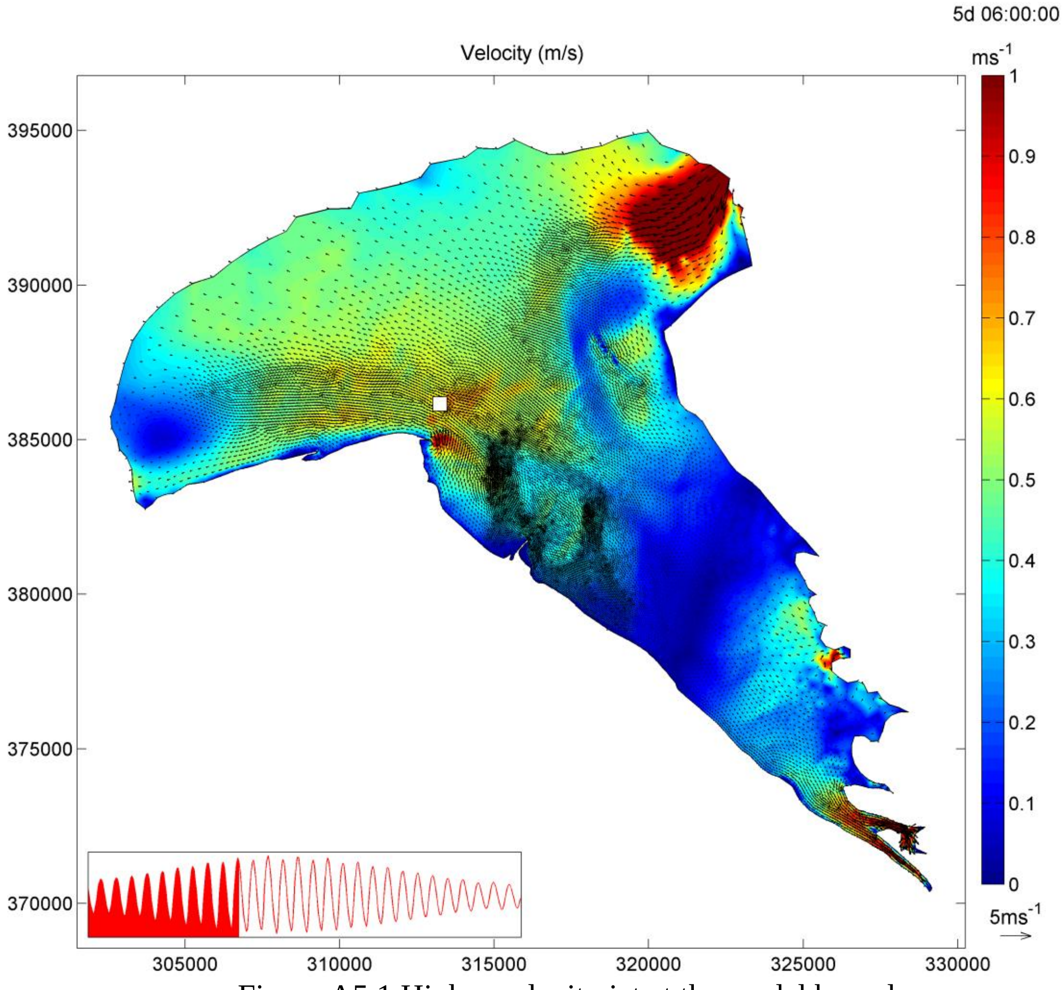

Figure A5.1 Higher velocity jet at the model boundary

Appendix. A6 Illustration of the morphological time step

Figure A6.1 illustrates how the morphological time step 1 hr works in the morphodynamic modelling. The vertical axis indicates the consequent morphological time loop. The morphological simulation starts from 1 hr, where the flow computation starts 0.5 hr before the sediment transport calculation. This flow overlap time step assist in removing any initialisation problems at each loop. Bed updating takes place after completing of the sediment transport calculations. Consequently the next time loop starts with the flow overlap. The corresponding tidal signal is show on the bottom of the same figure.

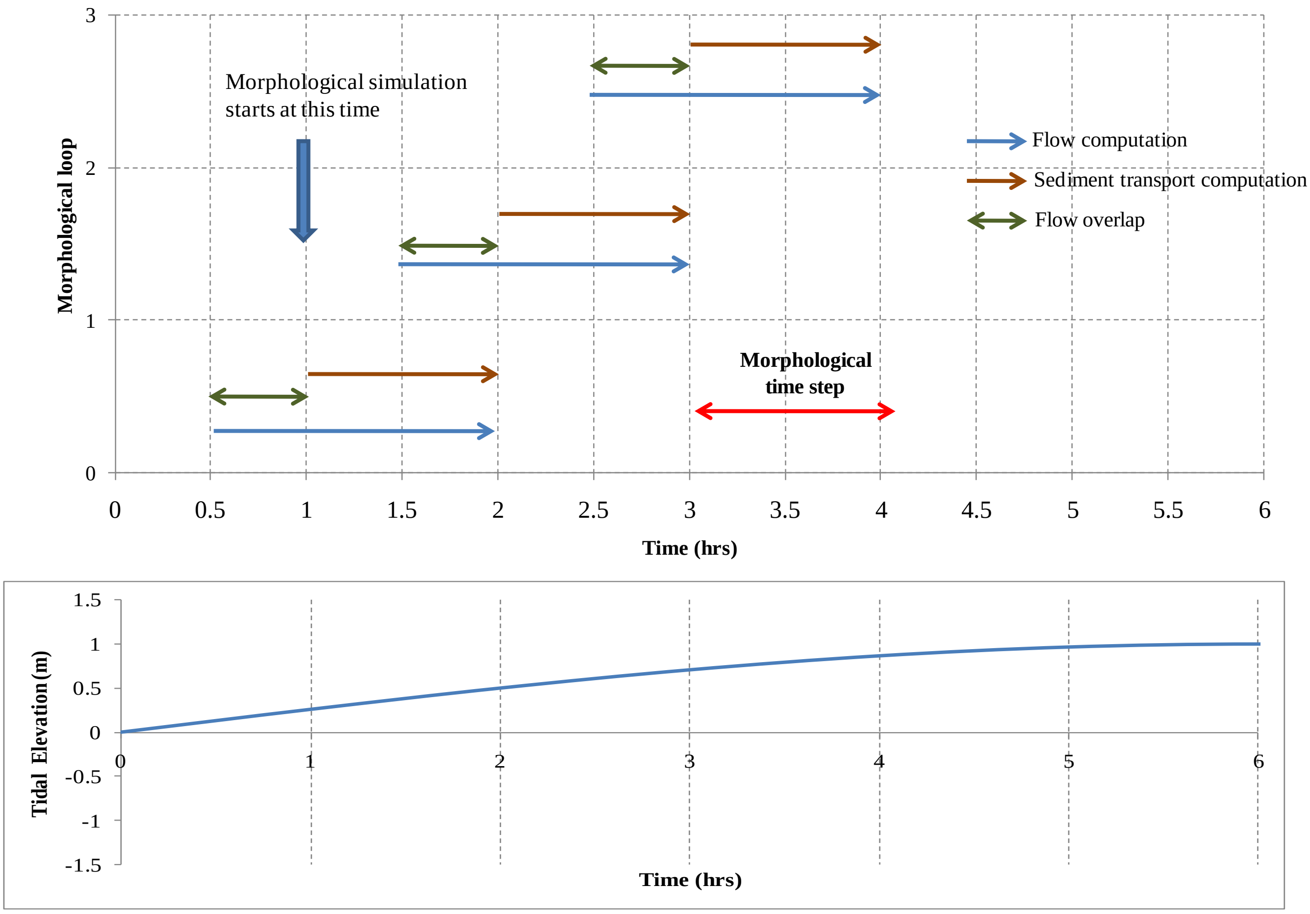

Figure A6.1 Illustration of morphological time step 1 hr

Similarly, this mechanism for the morphological time step 12.5 hrs, which is the period of a tide, is shown schematically in A6.2. The flow overlap is kept as 1 hr in this simulation. It can be noted that the overlap time in this case is only 1/12th of the morphological time step whereas in the previous case (1 hr time step) it is half of that corresponding morphological time step. This is the reason why the simulation results with the 1 hr time step were found to be smoother than the 12.5 hrs time step one.

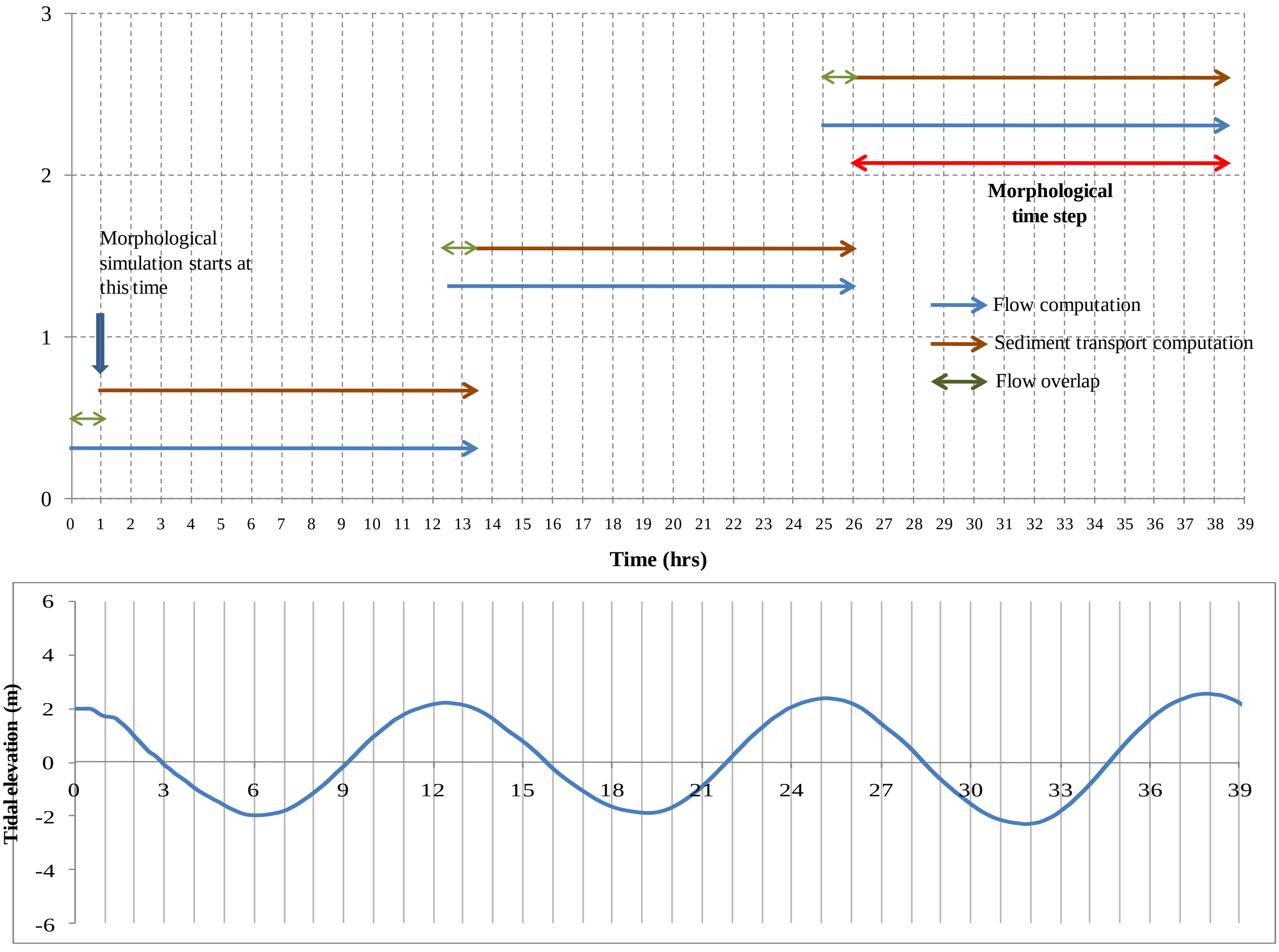

Figure A6.2 Illustration of morphological time step 12.5 hrs

Figure A6.3 Shows, when applying morphological factor of 5 to the above case (12.5 hrs time step). The tidal signal is shown on the bottom of the same figure. Here also the flow overlap time was kept to be 1hr. Morphological computation starts 1 hr after the flow calculations, where the flow computation takes place over a tidal period and consequently it will fed to the sediment transport model, in which the sediment transport simulation done. Subsequently bed updating takes place and then the morphological changes are multiplied by a factor of 5. Thus in fact it modelled over 5 tides after simulation over one tide (1st tide). As shown in figure A6.3, it skip the time of rest of the period (4X12.5 hrs) and again starts at 63.5 hrs using the 2nd tide.

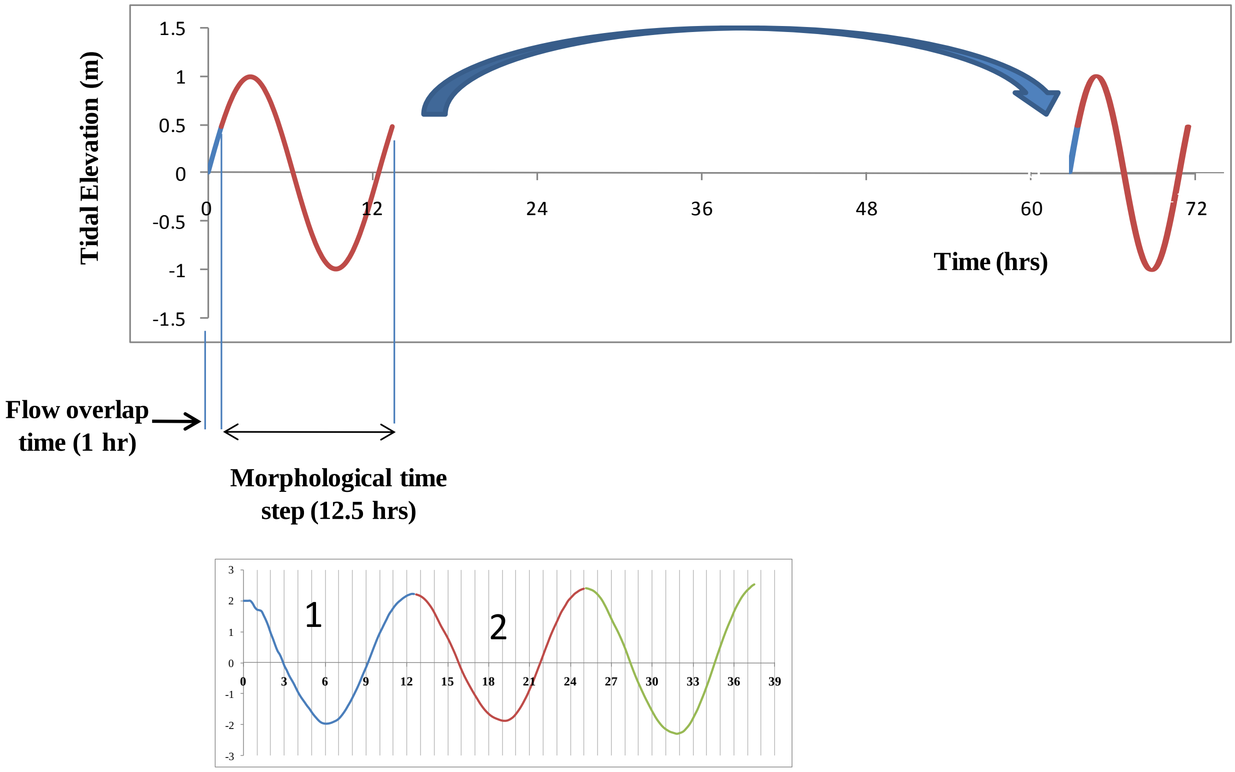

Figure A6.3 Illustration of morphological time step with the morphological factor

Appendix. A7 Issues with the Morphological model

There were several uncertainties identified during the present modelling studies. These are briefly explained here with figures.

Instabilities when using morphological factor (MF) 10 ;

Instabilities were found when the simulation enter the spring tide, thus there was huge sediment transport occurred when the model updates the bed. Initially, the cells started to get dry and with the time it propagated to the entire area and cause for failure in continuing the simulation as shown in below Figure A6.1. And also it increased the risk of cells in the model becoming permanently ‘dry’ when continuing the simulation over long period.

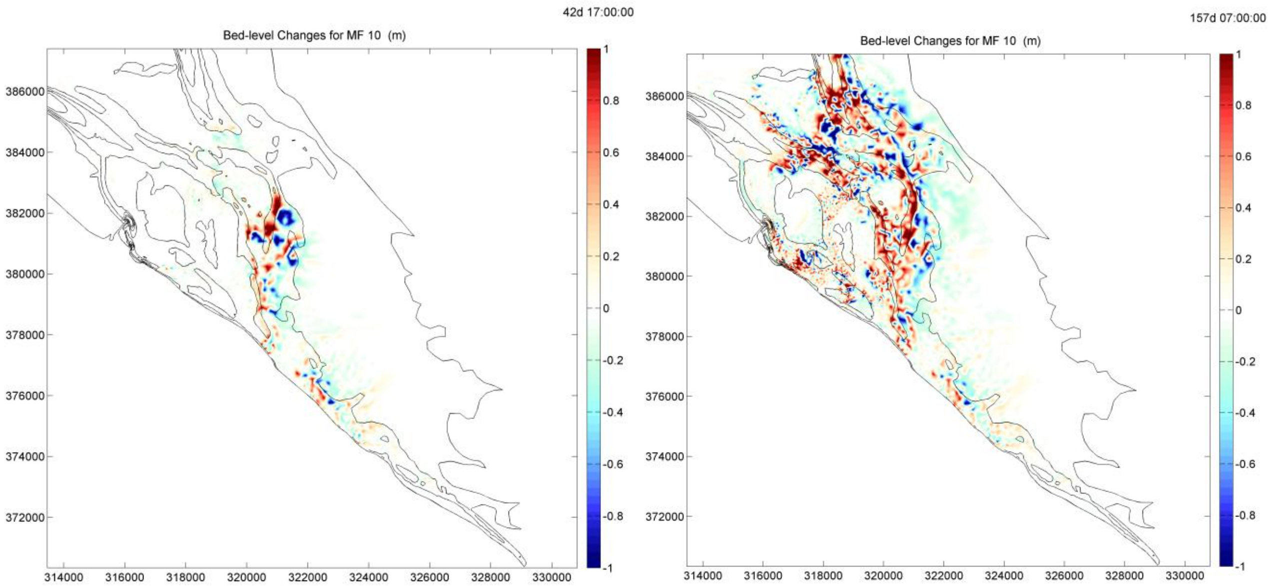

Figure A6.1 Instabilities arise from south of the estuary propagate to the entire area

This is partly because of the huge intertidal area in the model gets wetting and drying during the tidal cycle. And also the present model doesn’t incorporate this wetting and drying when doing the calculations.

Uncertainties with the morphological factor:

An attempt was made to run the same model as discussed above with 1 hr time step (which gives frequent bed updating compared to 12.5 hrs time step), and morphological factor 10. Surprisingly, the morphology did not show any significant evolution even after simulation over a spring-neap cycle as shown in Figure A6.2 when compare with MF 1.

In principle, the run with MF 10 must have produced the morphological changes 10 times of that as over a spring-neap cycle with MF 1. But, the changes are even less than the one with MF 1. This clearly shows the morphological factor in the model did not work effectively. This behaviour makes the model uncertain when using the morphological factor.

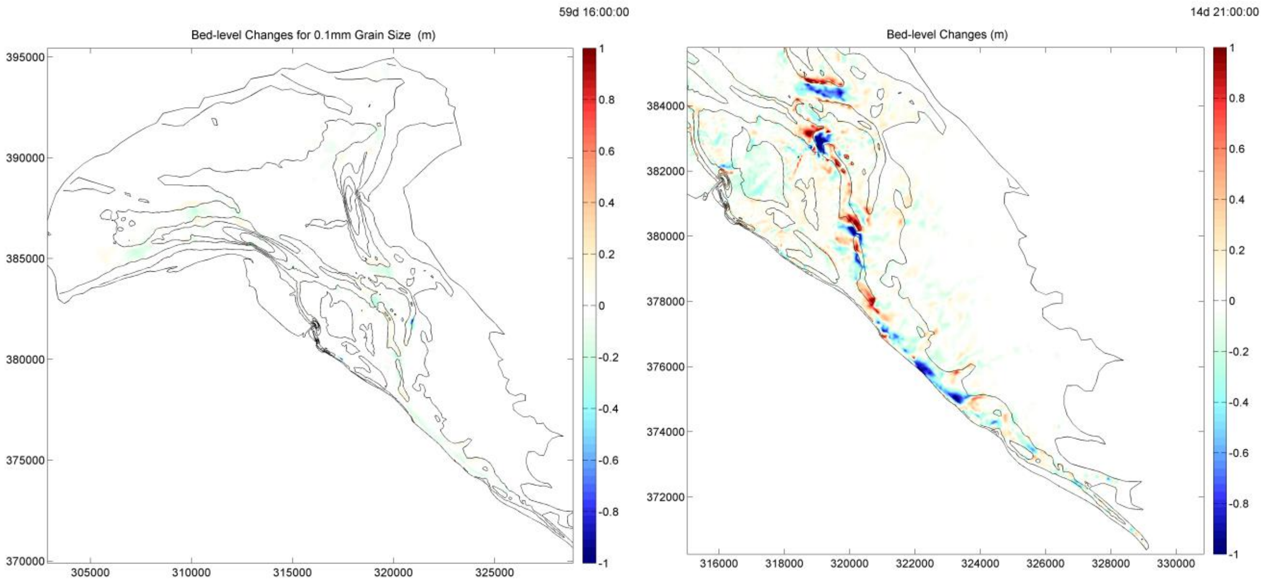

MF 10, 1 hr time step

MF 1, 1 hr time step

Figure A6.2 Comparison of morphological changes obtained for MF 10 and MF 1

Negative water depths and huge concentration of sediments:

At certain locations of the model output shows sudden increase in the sediment concentration, this causes for depositing huge amount of sediments. This was encountered even running the model with MF 1 as shown in Figure A6.3. By checking the flow results, it was identified that the model gets negative water depths at those locations that caused for the higher concentration. The reason for why the concentration has got sudden increase in the model is not clear yet. More investigation is required to identify this issue.

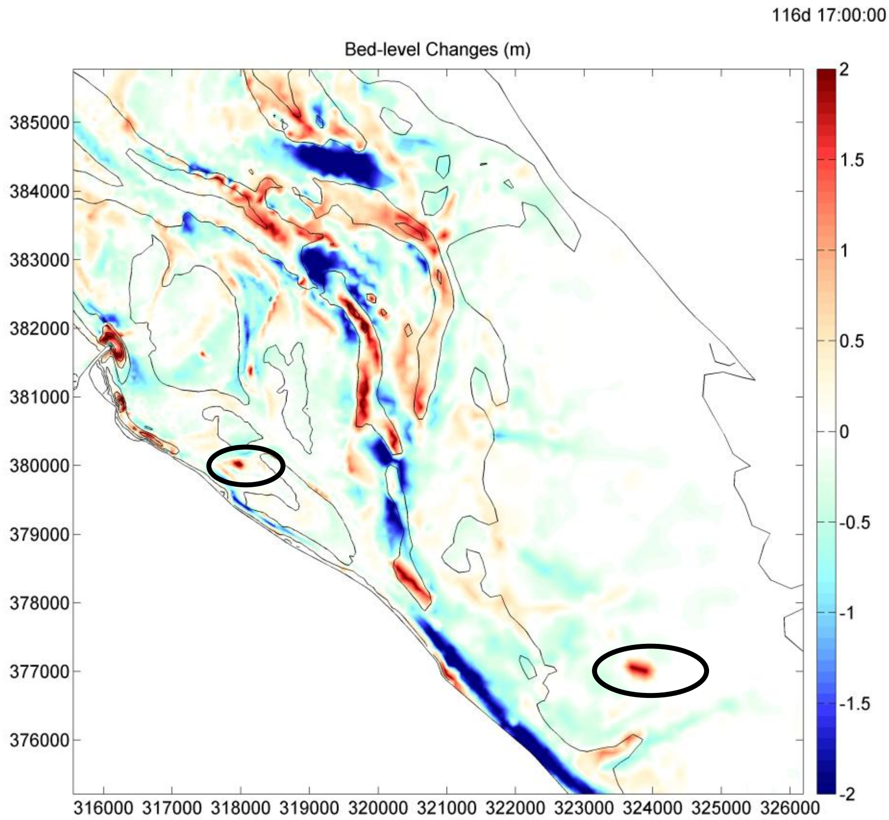

Figure A6.3 Huge deposition patched observed in the mod results

Appendix. A8 Points of data extraction from the model

Figure A7.1 shows number of points in each region of the estuary that have been used to extract the model results for various analyses and also used for Brier Skill Score calculations. Note, the area near the Port of Mostyn and Mostyn Channel have not been included for the analysis because, dredging of the port access channel during the period (2003-2006) might alter the natural morphological changes that have occurred during the study period.

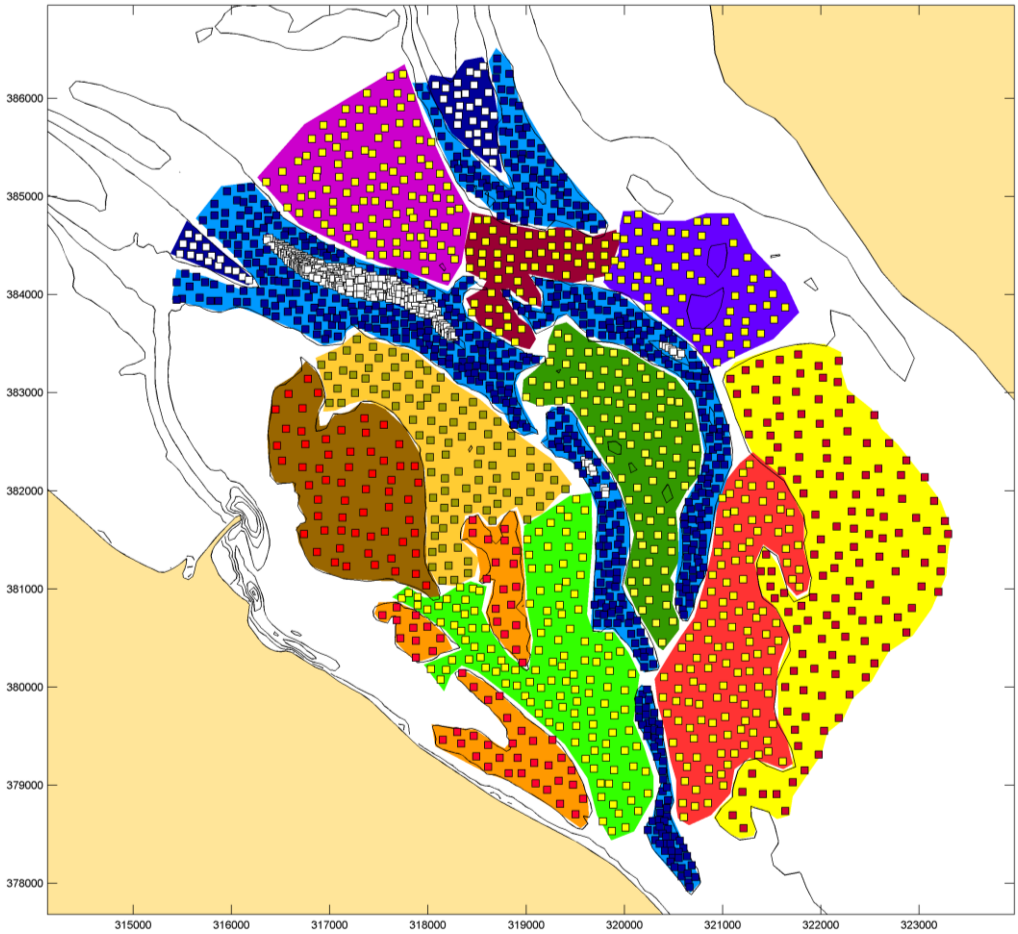

Figure A7.1 Points of data extraction

Appendix. A9 Scatter plots – Comparison of morphological changes between modelled and observed

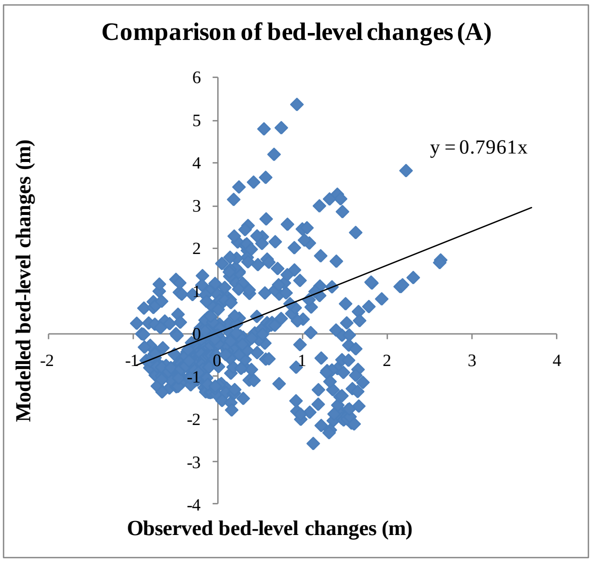

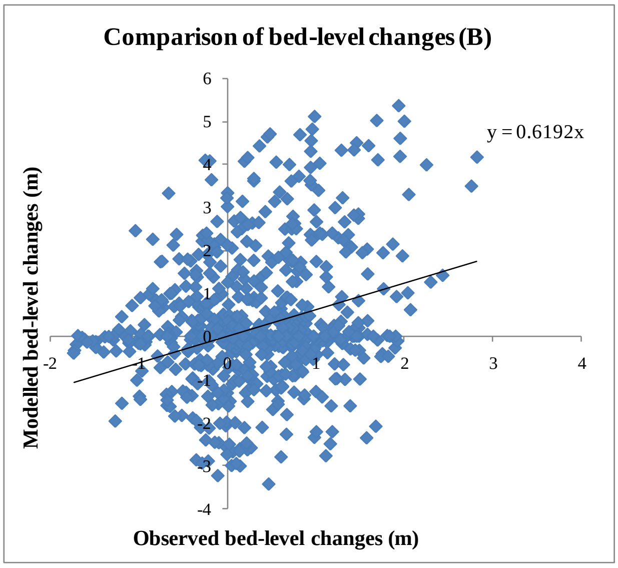

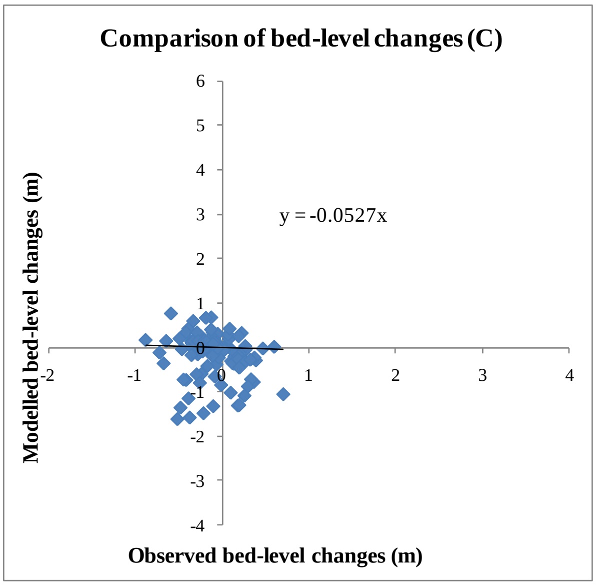

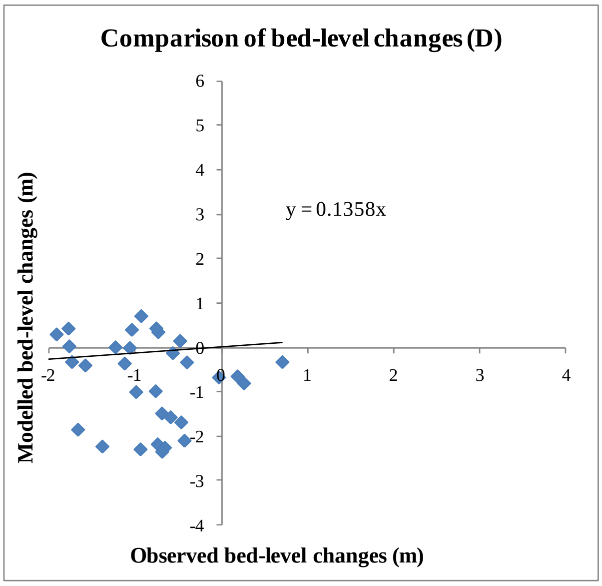

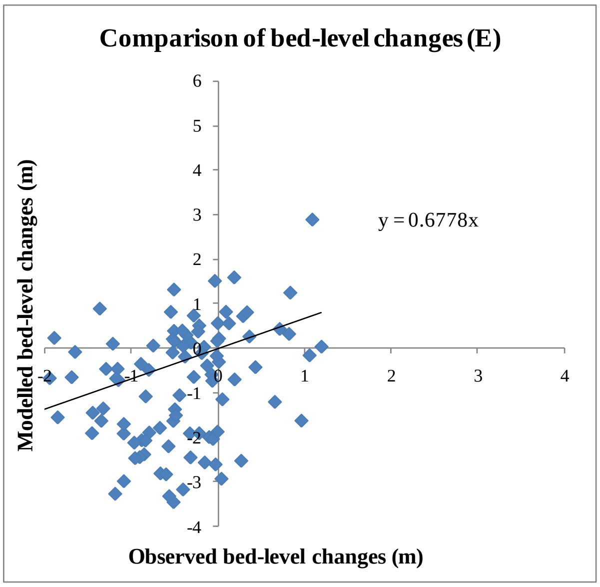
Comparison of bed-level changes (E)
y = 0.6778x
Modelled bed-level changes (m)
Observed bed-level changes (m)

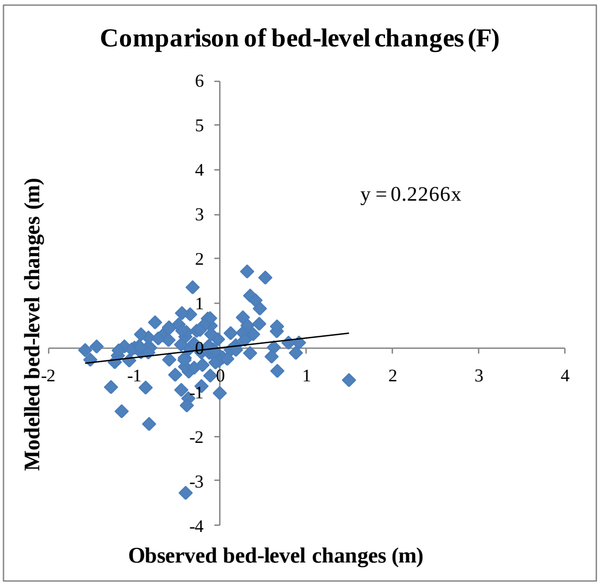
Comparison of bed-level changes (F)
y = 0.2266x
Modelled bed-level changes (m)
Observed bed-level changes (m)

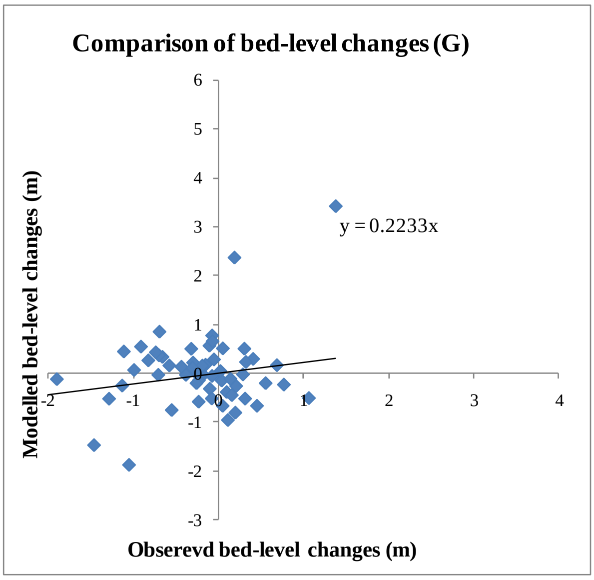
Comparison of bed-level changes (G)
y = 0.2233x
Modelled bed-level changes (m)
Obserevd bed-level changes (m)

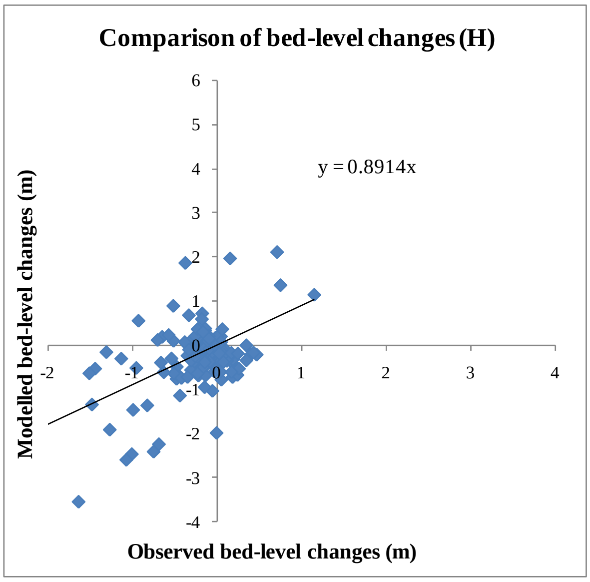
Comparison of bed-level changes (H)
y = 0.8914x
Modelled bed-level changes (m)
Observed bed-level changes (m)

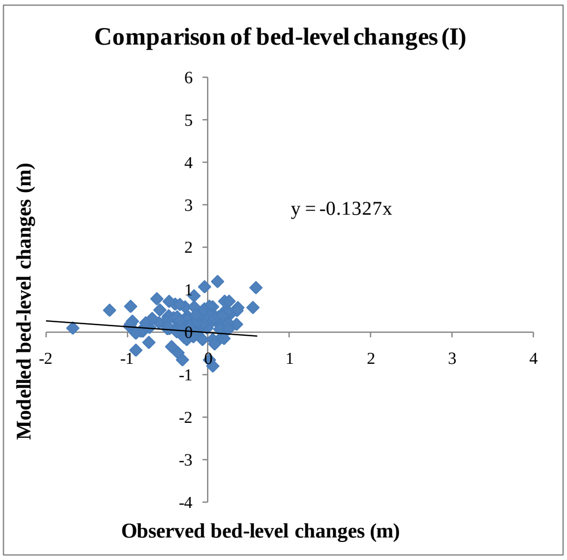
Comparison of bed-level changes (I)
y = -0.1327x
Modelled bed-level changes (m)
Observed bed-level changes (m)

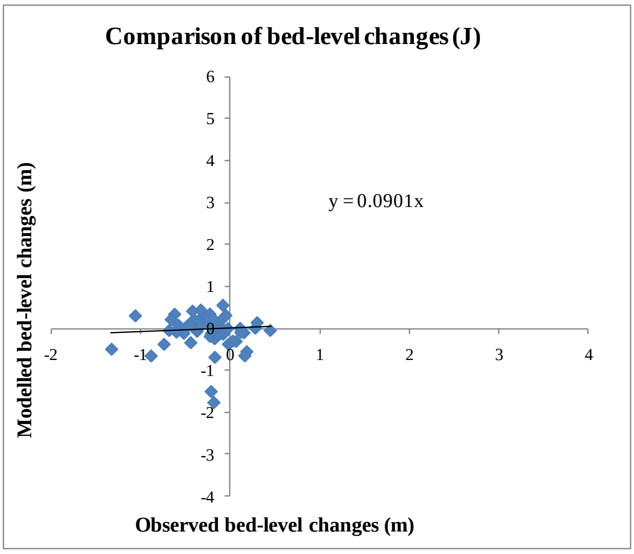
Comparison of bed-level changes (J)
y = 0.0901x
Modelled bed-level changes (m)
Observed bed-level changes (m)

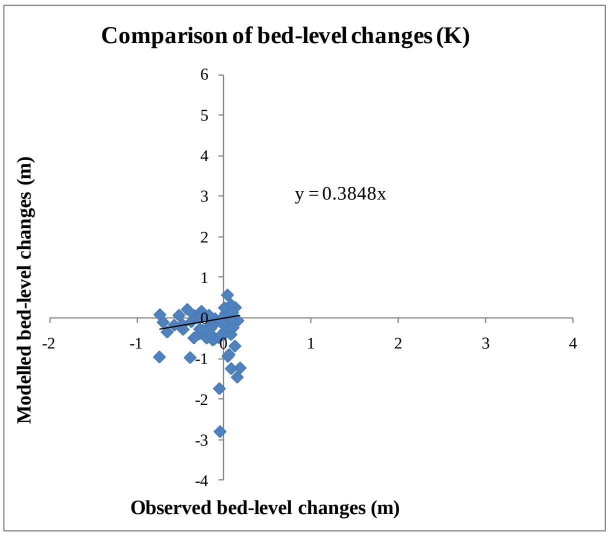

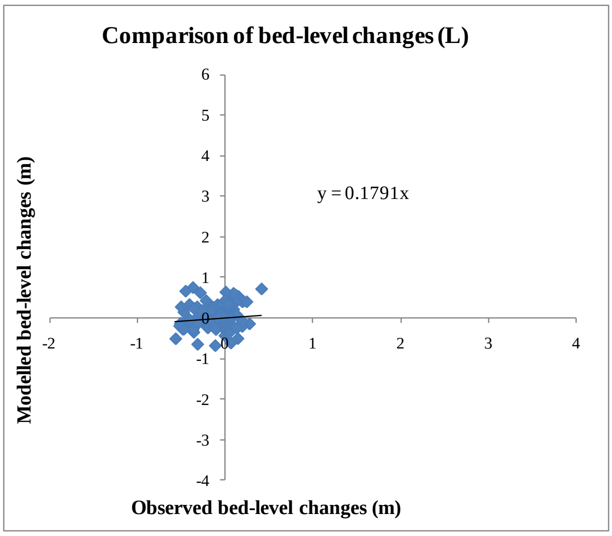

Figure A8.1 Comparison between modelled and observed bed-level changes